



저작자표시-비영리-변경금지 2.0 대한민국

이용자는 아래의 조건을 따르는 경우에 한하여 자유롭게

- 이 저작물을 복제, 배포, 전송, 전시, 공연 및 방송할 수 있습니다.

다음과 같은 조건을 따라야 합니다:



저작자표시. 귀하는 원저작자를 표시하여야 합니다.



비영리. 귀하는 이 저작물을 영리 목적으로 이용할 수 없습니다.



변경금지. 귀하는 이 저작물을 개작, 변형 또는 가공할 수 없습니다.

- 귀하는, 이 저작물의 재이용이나 배포의 경우, 이 저작물에 적용된 이용허락조건을 명확하게 나타내어야 합니다.
- 저작권자로부터 별도의 허가를 받으면 이러한 조건들은 적용되지 않습니다.

저작권법에 따른 이용자의 권리는 위의 내용에 의하여 영향을 받지 않습니다.

이것은 [이용허락규약\(Legal Code\)](#)을 이해하기 쉽게 요약한 것입니다.

[Disclaimer](#)

Doctoral Thesis

**LAB-ON-A-DISCS FOR QUANTIFICATION OF  
MICROALGAL LIPIDS AND NATURAL  
ANTIOXIDANTS OF BEVERAGE SAMPLES**

Yubin Kim

Department of Chemical Engineering

Graduate School of UNIST

2019

# LAB-ON-A-DISCS FOR QUANTIFICATION OF MICROALGAL LIPIDS AND NATURAL ANTIOXIDANTS OF BEVERAGE SAMPLES

Yubin Kim

Department of Chemical Engineering

Graduate School of UNIST

# Lab-on-a-discs for quantification of microalgal lipids and natural antioxidants of beverage samples

A thesis/dissertation  
submitted to the Graduate School of UNIST  
in partial fulfillment of the  
requirements for the degree of  
Doctor of Philosophy

Yubin Kim

06. 14. 2019

Approved by



Advisor

Yoon-Kyoung Cho

# Lab-on-a-discs for quantification of microalgal lipids and natural antioxidants of beverage samples

Yubin Kim

This certifies that the thesis/dissertation of Yubin Kim is approved.

06. 14. 2019



Advisor: Yoon-Kyoung Cho

Thesis Committee: Dong-Pyo Kim



Thesis Committee: Cheol-Min Ghim

Thesis Committee: Hyun-Wook Kang



Thesis Committee: Kyung Hwa Cho



## Abstract

Since the first introduction in 1960s, lab-on-a-disc platform has gained much attention due to its great advantages such as simple operation, rapid reaction, low cost, full integration and automation. Lab-on-a-disc has been applied for various research fields such as biomedical, environmental, energy and food agricultural field. In this thesis, fully integrated lab-on-a-disc platform was demonstrated for quantification of microalgal lipid and natural antioxidants from beverage samples, and disc analyzer was introduced to operate the on-disc optical detection.

For microalgae lipid quantification, fully automated lab-on-a-disc platform was developed for rapid on-site quantification of lipids from microalgal samples. The whole serial process for microalgal lipid quantification was integrated on lab-on-a-disc platform. Lab-on-a-disc operation time was 13 min. To integrate liquid-solvent extraction of microalgal lipid on a disc, the organic solvent compatible (for ethanol and n-hexane) lab-on-a-disc was newly fabricated. Fabrication technique was developed by combining thermal fusion bonding and laser printed carbon dot based valving. For natural antioxidant determination from beverage samples, lab-on-a-disc platform was developed to integrate the complicated determination steps of antioxidant activity (AA) and the total phenolic content (TPC) from beverage sample. Different beverage samples including wine, beer, various fruit juices and tea were analyzed using our lab-on-a-disc platform. For disc analyzer, on-disc optical signal detecting instrument was developed. It can detect on-disc signal of absorbance and chemiluminescence from result solution. The trials and errors to develop the disc analyzer for following researchers was demonstrated.

From both lab-on-a-disc quantification methods, it is proved that lab-on-a-disc can be effectively used for quantification of microalgal biofuel and food antioxidants. It is expected that our lab-on-a-disc based microalgal lipid quantification works give considerable contribution to the commercial production of microalgal-based biofuels by providing rapid, cost-effective, user-friendly on-site quantification of microalgal lipids. Also, our on-disc natural antioxidant detection works would also contribute to functional beverage industry as providing fast, simple determination of natural antioxidants from beverage sample. Both lab-on-a-disc was fabricated by the organic solvent compatible (for ethanol and n-hexane) manner, and it can be used for chemical engineering fields for quality control.

## Table of Contents

<b>Abstract</b> .....	i
<b>Table of Contents</b> .....	ii
<b>List of Figures</b> .....	iv
<b>List of Tables</b> .....	xi
<b>CHAPTER 1. Introduction</b> .....	1
<b>1.1 Microfluidics</b> .....	1
<b>1.1.1 Microfluidics in biofuel quantification</b> .....	3
<b>1.1.2 Microfluidics in food antioxidants determination</b> .....	10
<b>1.1.3 Absorbance detection in microfluidics</b> .....	14
<b>1.2 Lab-on-a-disc</b> .....	19
<b>1.2.1 Basic principle of lab-on-a-disc system</b> .....	22
<b>1.2.2 Lab-on-a-disc functions</b> .....	24
<b>1.2.3 Lab-on-a-disc application in biomedical field</b> .....	29
<b>1.2.4 Lab-on-a-disc application in other fields</b> .....	32
<b>1.3 Research motivations</b> .....	35
<b>1.4 Research aims</b> .....	36
<b>CHAPTER 2. Microalgal lipid quantification using lab-on-a-disc</b> .....	37
<b>2.1 Introduction</b> .....	37
<b>2.2 Previous studies of microalgal lipid quantification on microfluidics</b> .....	37
<b>2.3 Development of essential techniques</b> .....	38
<b>2.3.1 n-Hexane solvent resistive lab-on-a-disc platform</b> .....	38
<b>2.4 A fully integrated lab-on-a-disc for microalgal lipid quantification</b> .....	39
<b>2.4.1 Experimental details</b> .....	39
<b>2.4.2 Result and discussion</b> .....	51
<b>2.4.3 Conclusions</b> .....	60
<b>CHAPTER 3. Fully integrated lab-on-a-disc for determination of natural antioxidants from beverage samples</b> .....	61
<b>3.1 Introduction</b> .....	61
<b>3.1.1 Total phenolic contents and antioxidant activity</b> .....	61



3.1.2	Importance of total phenolic content analysis and antioxidant activity evaluation in beverage samples .....	62
3.2	Available methods for total phenolic content and antioxidant activity.....	63
3.3	Simultaneous determination of total phenolic contents and antioxidant activity of beverage sample using lab-on-a-disc.....	66
3.3.1	Experimental details .....	66
3.3.2	Results and discussion .....	75
3.3.3	Conclusions .....	85
CHAPTER 4.	Absorbance and luminescence detection on a disc .....	87
4.1	History of on-disc absorbance and luminescence detection .....	87
4.2	On-disc absorbance detection .....	93
4.3	On-disc luminescence detection set-up.....	99
4.4	Conclusions.....	107
4.4.1	On-going portable disc analyzer .....	108
CHAPTER 5.	General conclusions and future perspectives .....	110
5.1	General conclusions .....	110
5.2	Future perspective .....	112
5.2.1	Microfluidic in biofuel production.....	112
5.2.2	Microfluidics in food nutrient determination .....	115
References.....		118

## List of Figures

**Figure 1.1.** (A) Lab-on-a-chip platform for determination of total phenolic content in honey<sup>3</sup> and (B) Microfluidic device that minimizes the dynamic of liver metabolism and the subsequent antioxidant activity of food components.<sup>6</sup> ..... 11

**Figure 1.2.** (A) First Lab-on-a-disc platform by Oak Ridge National Laboratories (ORNL)<sup>1</sup> and (B) First lab-on-a-disc platform can be used as an advanced sample-to-answer system by Madou's group.<sup>4,21</sup>

**Figure 1.3.** (A) Lab-on-a-disc picture and (B) schematic diagram showing a geometry and forces acting on a liquid plug in a channel of a rotating disc. This picture was obtained from reference.<sup>11</sup> ..... 23

**Figure 1.4.** Various valving techniques, metering, mixing on centrifugal microfluidic system: (A) capillary valve,<sup>12</sup> (B) hydrophobic valve; The region illustrated with red line zone represents hydrophobic surface,<sup>12</sup> (C) laser irradiated ferrowax microvalves (LIFM); Both normally-closed and normally-open LIFM were demonstrated.<sup>13</sup> (D) Schematic illustration of laser irradiated carbon dot valves.<sup>14</sup> (E) Schematic illustration of individually addressable diaphragm valves (ID valves).<sup>15</sup> (F) Schematic diagram showing the principle of the metering; The fluid fills the pre-defined volume first and excess liquid are removed to the waste chamber.<sup>12</sup> (G) Enhanced mixing on a disc by periodically alternating the rotation sense.<sup>16</sup> ..... 28

**Figure 1.5.** (A) Design of a disc for multiplexed immunoassay from Gyros, Miniaturized unit can perform maximum 112 targets detection.<sup>17</sup> (B) Disc layout of fully automated immunoassay from Samsung, utilization of sacrificial valve facilitates integration from whole blood separation to detection.<sup>18</sup> (C) Image of disc for secondary PCR, pre-amplification and secondary PCR was implemented sequentially without contamination from handling.<sup>19</sup> (D) Photograph (left) of the LabDisk for sample-to-answer nucleic acid based detection of respiratory pathogens with complete reagent prestorage. .... 31

**Figure 1.6.** (A) Representative image of pathogen detection on a disc.<sup>2</sup> (B) Disc design for water analysis, six nutrients were detected within 5 min.<sup>5</sup> (C) Operation images for caffeine detection disc, solid phase extraction was integrated for extraction caffeine from real sample and amount of caffeine was quantified by fluorescence dye.<sup>7</sup> (D) Representative image for facile, rapid, and sensitive isolation

and analysis of EVs from raw biological samples using lab-on-a-disc.<sup>8</sup> (E) Arrangement of designed functional units and schematic procedure for crystallization of colloidal particles in a lab-on-a-disc platform.<sup>9</sup> (F) Lab-on-a-disc image and design of chip cartridge for analysis of nuclear spent fuels.<sup>10</sup> 34

**Figure 2.1.** Schematic illustration of (A) a lab-on-a-disc for microalgal lipid quantification, and (B) the thermal fusion assembly technique and laser-irradiated carbon-dot valves. .... 40

**Figure 2.2.** The layout of the four layers of a lab-on-a-disc. (A) Top layer containing sample inlet holes, vent holes, and flow channels. (B) Polycarbonate (PC) film (0.125 mm thick) containing carbon dot patterns, inlets, vent hole, and open holes for optical detection. (C) Middle layer (5 mm thick) containing sample and reagent chambers. (D) Bottom layer (1 mm thick). The diameter of the disc is 120 mm. . 41

**Figure 2.3.** Experimental set-up for microalgal lipid detection on a disc. The motor for rotating the disc, the laser to irradiate the carbon dot, the portable spectrometer, the optical fiber, and the light sources are integrated into our experimental set-up. .... 44

**Figure 2.4.** Calibration curve for the amount of lipid standards with the resulting quinoneimine absorbance at 540 nm. Each data point derives from three repeated experiments (n = 3). .... 46

**Figure 2.5.** (A) A bright field image of wild-type microalgal cells (cc125). The effects of lysis time (B) and volume of lysis buffer (C) on microalgal lipid extraction efficiency. The number of microalgal cells (cc125 in 500  $\mu$ L) used to study the effects of lysis time and buffer volume were  $1.43 \times 10^6$  cells and  $1.22 \times 10^6$  cells, respectively. The extraction efficiency of microalgal lipids at different solvent ratios (D), solvent volumes (E), and numbers of extraction steps (F) were compared. Microalgae cells (cc125;  $0.91 \times 10^6$  cells in 500  $\mu$ L) were used for the experiments reported in (D)–(F). For experiments reported in (B), (C), and (F), 300  $\mu$ L of 1:1 (n-hexane: ethanol) solvent was used. Data point represents the average of three repeated experiments (n = 3). .... 48

**Figure 2.6.** Correlation curve of microalgae densities (strain cc125) and optical densities at 750 nm. 50

**Figure 2.7.** Illustration of the processes used to quantify microalgal lipids on a disc. (A) Microalgal sample (strain cc125) was loaded onto the disc, the excess sample was transferred to the metering chamber, and 500  $\mu$ L of microalgal sample was metered. (B) After spinning at 6,000 rpm to sediment the microalgal cells, (C) valve #1 was opened to discard the supernatant into the waste chamber. Then, valve #2 was opened to add 100  $\mu$ L of lysis buffer to the microalgae sediments. Subsequently, valve #3

was opened to transfer the microalgae lysate into an extraction chamber containing 300  $\mu$ L of solvent to extract the lipid. (D) The disc was shaken for liquid-liquid extraction, and the microalgal lipids were extracted. (E) The lipid-containing solution was transferred to the lipid collection chamber after valve #4 had been opened. A phase separation between the solvent and microalgal lysate occurred owing to the different densities. The position of the valve was designed so that the solvent could selectively transfer into the collection chamber. (F) One more step of lipid extraction and (G) collection was repeated by opening valves #5 and #6. (H) Finally, the solvent was evaporated and the lipid dye was transferred to the lipid collection chamber by opening valve #7. The absorbance at 540 nm was measured using an optical fiber-coupled spectrometer (MAYA2000 Pro, Ocean Optics, FL, USA) to quantify the microalgal lipids. .... 53

**Figure 2.8.** (A) Calibration curve between different microalgal (strain cc125) concentrations and microalgal lipid levels measured using the lab-on-a-disc. (B) Lipid accumulation in microalgae (strain cc125) cultured in different media. Control, complete media; -N, nitrogen-deficient media; -A, acetate-deficient media; -Fe, iron-deficient media. (C) Microalgal lipid accumulation in  $10^6$  cells (strain cc125) was monitored for 3 days under two different conditions of stress: -N by changing the media to that lacking nitrogen, and -L by blocking light. Control cultures were grown under normal culture conditions. Stress conditions were applied immediately after seeding or (D) after 24 hours of growth. Each point derives from three repeated experiments ( $n = 3$ ). .... 54

**Figure 2.9.** (A) Calibration curve between different microalgal (strain cc503) densities and microalgal lipid levels measured using the lab-on-a-disc. (B) Lipid accumulation in microalgae (strain cc503) cultured in different media. Control, complete medium; -N, nitrogen-deficient medium; -A, acetate-deficient medium; -Fe, iron-deficient medium. .... 56

**Figure 2.10.** Correlation curves (A) to compare the microalgal lipid (strain cc125) extracted by lab-on-a-disc and by a manual process, and (B) to demonstrate the correlation of the microalgal lipid amounts measured by colorimetric assay and by gas chromatography - mass spectrometer (GC-MS) analysis. Each point derives from three repeated experiments ( $n = 3$ ). .... 58

**Figure 2.11.** Comparison of the microalgal lipid amount measured by absorbance detection and GC-MS (microalgae strain: cc125). Data represent mean  $\pm$  standard deviation of three independent experiments. R.E represents relative errors between two methods.  $*P > 0.05$  and  $**P < 0.05$ . .... 59

**Figure 3.1.** (A) Colorimetric reactions of FC, DPPH and FRAP methods and (B) overview of disc

design. .... 68

**Figure 3.2.** The lab-on-a-disc is composed of 4 layers of polycarbonate (PC). (A) Top layer containing sample inlet holes, vent holes, and flow channels. (B) Polycarbonate (PC) film (0.125 mm thick) containing carbon dot patterns, inlets, vent hole, and open holes for optical detection. (C) Middle layer disc (5 mm thick) containing sample and reagent chambers. (D) Bottom layer (1 mm thick). The diameter of the disc is 120 mm. .... 69

**Figure 3.3.** The disc layout with detailed information about the chamber design. (A) the design of the microfluidic layout, and (B) the volume of metering chambers. .... 70

**Figure 3.4.** Experimental design for the simultaneous determination of total phenolic content and antioxidant activity using three colorimetric reactions on lab-on-a-disc device. The motor for rotating the disc, the laser to irradiate the carbon dot, the portable spectrometer, the optical fiber, and the light sources are integrated into our experimental set-up. .... 72

**Figure 3.5.** Investigations of reduced volume of reagent by manual method. Correlation curves to compare the results conducted by using original volume of reagent and reduced volume of reagent for (A) FC (B) DPPH and (C) FRAP reactions, respectively. .... 77

**Figure 3.6.** The investigation of reduced mixing time of (A) FC, (B) DPPH and (C) FRAP methods on a disc. Mixing condition on a disc was  $\pm 3,000$  rpm clockwise and counterclockwise with acceleration time to reach the target speed (0.2 sec) and deceleration time to stop the rotation (0.2 sec). The volume of reagents was reduced to from the 200  $\mu\text{L}$  of final detection volume for each method. Note that the mixing time of first reaction of FC method was fixed to 40 sec. .... 79

**Figure 3.7.** Illustration of the processes used to total phenolic content and antioxidant activity detection on a disc. (A) Beverage sample was loaded onto the disc, the excess sample was transferred to the metering chamber, and 15  $\mu\text{L}$  of beverage sample was metered. (B) After spinning at 3,000 rpm to sediment the colloidal particle, (C) valve #1 was opened to transfer the supernatant into dilution chamber and the disc was shaken for mixing. Then, (D) valve #2 was opened to transfer the diluted beverage sample to metering chamber for each reaction. Subsequently, (E) valve #3 was opened to transfer the diluted beverage sample to  $\text{H}_2\text{O}_2$  containing chamber to remove the interference in FC method. (F) Valve #4 was opened to transfer  $\text{H}_2\text{O}_2$  treated diluted beverage sample to 1<sup>st</sup> FC reaction chamber. Then, (G) valve #5 was opened to transfer the 1<sup>st</sup> FC reacted solution to 2<sup>nd</sup> FC reaction

chamber. Simultaneously, valve #6 and #7 were opened to transfer metered beverage sample to DPPH reaction chamber and FRAP reaction chamber respectively. Then, (H) disc was shaken for mixing and precipitated white particles in 2<sup>nd</sup> FC reaction chamber were sediment. Finally, the absorbance was measured using an optical fiber-coupled spectrometer (QE65000, Ocean Optics, FL, USA) to detect the total phenolic content and antioxidant activity (750 nm for FC method, 490 nm for DPPH method and 593 nm for FRAP method). ..... 81

**Figure 3.8.** Total phenolic content and antioxidant analysis results by using manual (conventional) assay and on-disc assay from 8 different beverage samples. (A) FC method, (B) DPPH method and (C) FRAP method. .... 84

**Figure 3.9.** Correlation curves of on-disc real sample evaluation results between (A) FC and DPPH method, (B) FC and DPPH method, and (C) DPPH and FRAP method. .... 86

**Figure 4.1.** Schematic illustration of absorbance detection where  $I_0$  = Initial light intensity,  $I$  = light intensity after transmitting target solution,  $T$  = Transmittance,  $\epsilon$  = the molar attenuation coefficient of that material,  $l$  = optical pathlength. .... 89

**Figure 4.2.** Schematic illustration of (A) absorbance detection set-up for lab-on-a-disc,<sup>20</sup> (B) the total internal reflection for absorbance measurements in lab-on-a-disc,<sup>21</sup> (C) paired emitter detector diode (PEDD) device for absorbance detection in lab-on-a-disc.<sup>22</sup> ..... 90

**Figure 4.3.** (A) Schematic image of versatile concept for the automated protocols and high-speed (< 1s) read of parallel chemiluminescent ELISAs,<sup>23</sup> (B) illustration of LabDisk player which integrate detector to measure chemiluminescent signal by immunoassay for human C-reactive protein.<sup>24</sup> ..... 92

**Figure 4.4.** (A) Schematic image of optical analyzer for absorbance detector (B) Side view and optical elements; 1. Optical fiber (60 um optical diameter), 2. collimating lens, 3. iris, 4. motor, 5. lab-on-a-disc (C) Image of customized software to operate the optical analyzer for absorbance. .... 94

**Figure 4.5.** Absorbance data by radial position of chamber (A) chamber with clear surface (B) chamber with scratched surface. .... 96

**Figure 4.6.** Absorbance data of our disc analyzer. Absorbance from (A) whole concentration (log scale) (B)  $1/2^5$  to 0 concentration (C) comparison with conventional spectrometer (Tecan, Infinite® 200 PRO).

For conventional spectrometer, 96 well plated was used. .... 97

**Figure 4.7.** Comparison with commercial spectrometer (Tecan, Infinite® 200 PRO) in small absorbance range (under 0.1 OD). For conventional spectrometer, 10 mm pathlength cuvette was used. .... 98

**Figure 4.8.** (A) Image of disc analyzer for absorbance and chemiluminescence detection. (B) Light blocking black box for containing disc analyzer. .... 100

**Figure 4.9.** Effect of ferrofluid chemiluminescence barrier. CRP solution was used as chemiluminescence sample of center chamber. 2.9 % of chemiluminescence signal in center chamber affected to next detection chamber without ferrofluid barrier (left bar graph) and 0.63 % of chemiluminescence signal was transfer to next detection chamber with ferrofluid barrier (right bar graph). .... 102

**Figure 4.10.** Effect of ferrofluid chemiluminescence barrier in whole disc. CRP solution was used as chemiluminescence sample of center chamber (C1). .... 103

**Figure 4.11.** Chemiluminescence data using our disc analyzer. Chemiluminescence from (A) whole concentration range (B) 0.0001 to 0 concentration. C-Reactive protein (CRP) was used as chemiluminescence sample solution. .... 105

**Figure 4.12.** Chemiluminescence comparison data between conventional spectrometer (PerkinElmer, EnVision 2105 Multimode Plate Reader) (A) whole CRP concentration range and (B) in low concentration range. .... 106

**Figure 4.13.** Schematic illustration presenting (A) functional module (B) top-view of board (C) detection module (D) expected image of device. (E) Scheme of side view of sensing part, overall pathlength for absorbance detection is 5.14 mm. Dynamic range is 0 – 2 OD, and limit of detection is 0.03 OD with 0.67 % CV. .... 109

**Figure 5.1.** Schematic illustration presenting (A) symbiotic metabolic pathway between microalgae cell and symbiotic bacteria.<sup>25</sup> (B) possible application to study the symbiosis of microalgae and bacteria; high-throughput combinatorial cell co-culture using microfluidics.<sup>26</sup> .... 136

## List of Tables

<b>Table 1.1.</b> Microfluidic approaches to check the microalgal lipid. ....	7
<b>Table 1.2</b> Research list of food antioxidant analysis using microfluidics. ....	13
<b>Table 1.3</b> Various approaches to increase the optical pathlength in microfluidics. ....	17
<b>Table 2.1.</b> Spin program used for microalgal lipid quantification on a disc. ....	43
<b>Table 3.1.</b> Analytical methods for determination of total phenolic content and antioxidant evaluation in different types of sample with analysis time required. ....	64
<b>Table 3.2.</b> Spin program used for total phenolic content and antioxidant activity detection in our lab-on-a-disc. ....	73
<b>Table 3.3.</b> Applied condition in manual procedure for FC, DPPH and FRAP methods (original volume from batch method and reduced volume for disc method) and mixing time. ....	76
<b>Table 3.4.</b> Analytical characteristic of lab-on-a-disc method for determination of total phenolic content (FC method) and antioxidant activity (DPPH and FRAP). ....	83
<b>Table 5.1.</b> Research lists of food nutrient analysis using microfluidics. ....	116



## CHAPTER 1. Introduction

### 1.1 Microfluidics

Micro total analysis system ( $\mu$ TAS), also known as lab-on-a-chip, has been studied by many researchers to miniaturize and integrate several laboratory functions on microfluidic platforms.<sup>27-31</sup> One of the lab-on-a-chip purpose is to integrated the all complicated laboratory process on single chip to realize the sample to answer platform; user would simply add sample then the chip would automatically process sequential steps of the assay and return the results. The unique characteristics of microfluidic devices such as laminar flow, large surface-to-volume ratios, and surface tension and capillary effects at the micrometer scale enable more efficient methods for processing and analyzing complex samples. Moreover, compared to conventional fluidic systems, microfluidic devices require lower fabrication cost, power budget and chemical consumption, but improved analytical performance and biocompatibility.

In early 1950s, the first microfluidic technology was reported when researchers trying to disperse sub-nanoliter volume of liquids for ink-jet application.<sup>32</sup> In 1979, a miniaturized gas chromatograph was developed by Terry which lead to a realization of fluidic propulsion in microchannels.<sup>33</sup> In addition, first high-pressure liquid chromatography (HPLC) device using Si based microfluidic chip was published by Manz *et al.*<sup>34</sup> Several microfluidic structure enabling valving and pumping have been developed in the early 1990s and the integration of each microfluidic function on a single chip facilitated the integration and automation of laborious steps for biological assays.<sup>35-37</sup>

Compared to conventional laboratory assays, lab-on-chip platform provides great advantages. In usual, lab-on-chip deals with extremely small amount of sample as small as sub-micro liters. Thus, the required reagents volume as well as the dead volume was low amount. In addition, assay time can be significantly reduced due to the faster reaction because of short diffusion distances, high surface to volume ratios, and faster heating originated from low heat capacities. Lab-on-chip system is advantageous not only due to reduced size, but also because of its high productivity and low cost. Disposable chip material and the miniaturized features on small scale allow mass production of chips with the low-cost fabrication processes.

Despite the great advantages explained above, there are also several limitations in lab-on-a-chip. First, the scale down effects does not always give positive ways. In a small scale, physical and chemical effects such as capillary forces, surface roughness, surface properties of construction materials on reaction processes become more major and governing equation in bulky scale is not valid anymore.

Thus, a small scale can sometimes make processes in lab-on-chips more complex than those in conventional lab equipment.

However, the fact that lab-on-chip is not fully developed demonstrates the lab-on-chip's huge potential for all kinds of assay and has been being applied to many fields. Therefore, lab-on-chip would be the powerful tool in research field as well as in industrial application.

### 1.1.1 Microfluidics in biofuel quantification

Biofuel is one of the most promising eco-friendly energy resource, and there is demand for research to deliver high-efficiency, low-cost, and low-environmental-impact biofuels. To this end, researchers have been focusing on developing new technologies to generate biofuels from microalgae. To address this engineering and scientific challenges in the biofuel industry, innovation is needed for new processes, products and tools.  $\mu$ TAS is considered one of the top emerging technologies that lead the efficient and environmental-friendly biofuel productions.<sup>38-40</sup>

Among many biofuel sources, microalgae has been considered as bio-based cell factories, able to rapidly colonize a liquid medium and produce a large variety of chemicals synthesized from their environment.<sup>41</sup> Many efforts have been paid for finding good strains, enhancing biofuel production, and controlling metabolic pathways to increase the efficiency of biofuel products.<sup>42</sup> Bioreactor designs,<sup>43</sup> microalgae harvest techniques,<sup>44</sup> downstream chemical/physical treatments,<sup>45</sup> and metabolite extraction methods<sup>46</sup> are also intensively investigated to reduce the production costs. Regardless of these efforts, the commercial production of microalgal biofuel still face the challenges because of high production costs and low efficiency due to the low throughput and the high cost of using laboratory-scale or pilot-scale processes to optimize the biofuel production. Microfluidics approaches have proven their high throughput and cost efficiency in a number of microbial applications such as screening and directed evolution of prolific yeast strains,<sup>47, 48</sup> detection of pathogen,<sup>49</sup> and miniaturized microbial fuel cells.<sup>50</sup> As taking advantages of microfluidic techniques, the expediting of enhancement of microalgal fuel and the biorefinery industry is anticipated.

#### **High-throughput single cell level detection of microalgal lipid without extraction using microfluidics**

In a biofuel industry, main concerning is to reach a high productivity in a specific high value product, one should select the most proper microalgae species with good culture conditions to maximize the production of biofuels. To obtain the optimal strains and culture conditions, the first studies of microfluidic techniques for microalgae was to identify the characteristics of different microalgae strains and establish microscale bioreactors. Various microfluidic-based screening platforms have been fabricated to cultivate microalgae and study their growth rate at microscale.<sup>51</sup> Miniaturized culture systems are extremely convenient to monitor in-situ single cell impacts of culture conditions on microalgae viability, morphology, and accumulation of lipids for biofuels. Future more, microalgae culture conditions can be precisely controlled regarding nutrient supply, and light diffusion. As taking these advantages, following microfluidic studies were able to study growth kinetics and heterogeneity

of single cells as well as optimize the production of lipids from multiples microalgae strains with high throughputs. However, in situ analysis of microalgal biofuels still requires the development of novel miniaturized detection technologies.<sup>52</sup> The feasibility of microfluidic approaches for optimizing bigger scales of microalgae cultivation and commodity production is the focal point of future applications

The microfluidic approaches to check the biofuels can be classified into three categories based on their designs: (1) mechanical traps; (2) droplets; (3) Cytometric; and (4) microchambers (Table 1). Mechanical traps are composed of microstructures designed in flow channels to retain cells; droplet systems trap cells in small (~ nL) water droplets surrounded by hydrophobic solvents; and microchambers are small bioreactors where cell population are free in an enclosed environment.

In general, mechanical traps enable to study single cells, immobilized in a small environment, while a medium could flow. Such microtraps allow continuous cell monitoring via microscopy. (Table 1.1 2<sup>nd</sup>, 3<sup>rd</sup>, 4<sup>th</sup> row)

One of representative works is done by Kim *et al.* They developed a high-throughput microfluidic microalgae photobioreactor array to investigate growth and lipid production of microalgae under 64 different light conditions with single-colony resolution, in parallel (Table 1.1 2<sup>nd</sup> row)<sup>53</sup> In this report, *B. braunii* colonies were successfully characterized using the developed platform and resulted in identifying light conditions that showed maximum oil production that differed from conditions typically used in conventional cultures. This screening was achieved at 250 times higher throughput and 850 times less reagent consumption. We expect that this platform will serve as a powerful tool to investigate how algal growth and oil production are influenced by light conditions as well as screening through various growth conditions against algal strains of interest, all at significantly lower cost and shorter time, which can dramatically accelerate the development of renewable algal energy systems.

The use of microfluidic droplets enables to trap single or multiple cells in an independent environment, and therefore it can mimic the batch culture conditions in high-throughput manner. (Table 1.1 5<sup>th</sup>, 6<sup>th</sup>, 7<sup>th</sup> row) In addition, droplets allow easy cell sorting. Microfluidic droplets fabrication have been widely applied to research in multiple areas, such as cell culture (microbial and mammalian), protein crystallization, and chemical reactions.<sup>54</sup> However, the study for microalgae in microfluidic droplets applications were started late in 2011

Lee *et al.*, encapsulated microalgal cells within alginate hydrogel-based microcapsules in a microfluidic device that incorporated a microbridge structure. (Table 1.1 7<sup>th</sup> row)<sup>55</sup> Their works is the first report that live algae cells could be encapsulated and their lipid contents determined in an online, real-time manner. By utilizing the fast migration of the additional control flow, which includes a

calcified oil phase, via a microbridge structure, we could fabricate stable alginate hydrogel microcapsules with suitable spacing; moreover, no aggregation of microcapsules was identified. The fabricated microcapsules showed characteristics of monodispersity, enough robustness in handling, stability for long-term manipulation, and maintenance of cell viability.

Erickson *et al*, developed a microfluidic cytometer that measures photosynthetic efficiency and lipid accumulation (as NR fluorescence) on single algal cells in real time (**Table 1.1** 8<sup>th</sup> row).<sup>38</sup> To demonstrate instrument performance, They tested unstressed (nutrient-replete) and stressed (nutrient-limited) cultures of the marine diatom *Phaeodactylum tricornutum* and are correlated to values obtained in bulk samples using traditional pulse-amplitude-modulating fluorometry. Their approaches were the first time that both photosynthetic efficiency and lipid accumulation have been simultaneously evaluated at the single cell level, and that in doing so, the diversity within these populations was revealed.

#### **Non-high-throughput and relatively bulk level (> 1 mL) detection of microalgal lipid with extraction using microfluidics**

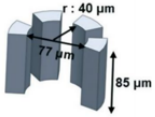
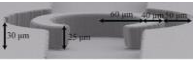
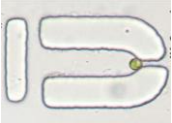
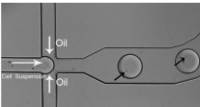
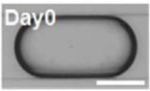
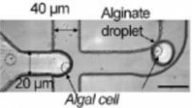
Microchambers for microalgae can be considered as downscaled photobioreactors, where a cell population are cultivated. The culture scale is generally bigger than the existing microfluidic devices and enables to conduct analysis based on biomass and for getting closer results to bulk culture conditions.

Lim *et al*, showed a simple microchannel with a micropillar array integrated to connect the cell chamber and output reservoir, which act like a filtration unit that enables change of medium and solvent extraction by using fluid injection by a syringe pump (**Table 1.1** 9<sup>th</sup> row).<sup>40</sup> Multiple processes such as cell culture, lipid accumulation, and lipid extraction were conducted using a single microfluidic device without labor-intensive steps. Various extraction conditions of solvent volume and temperature were tested to optimize lipid extraction efficiency in the microfluidic device. Compared to bulk system, their microfluidic system showed higher lipid extraction efficiency under same solvent. The lipid extraction efficiency using less toxic isopropanol on the integrated device was 113.6% when it compared with the conventional Bligh–Dyer method.

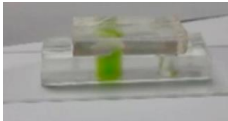
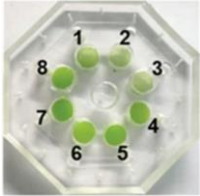
From same group, Kwak *et al*, developed a PDMS-based multiplex microfluidic system with 8 chambers and micropillar arrays to expedite multiple steps for lipid sample preparation from different microalgal strains (**Table 1.1** 10<sup>th</sup> row).<sup>56</sup> They used same microchamber dimension with Lim's works but they advanced it to show lipid extraction of 8 different microalgal strains simultaneously on a single device without purification steps and harvesting, which is labor-intensive and energy-intensive.

Both approaches focused on relatively bulk level (~ 500  $\mu$ L) microalgae cell culture and extraction of lipid from cultured microalgae. They used TLC for lipid quantification and GC-MS for lipid qualification & quantification. It has great meaning that microfluidic device can provide the integrated microalgae culture and lipid extraction steps before using GC-MS for lipid component analysis (qualification). However, it required additional complicated steps to modify microalgal lipid to fatty acid methyl ester (FAME) for GC-MS analysis and GC-MS required several hours to analysis the lipid. Thus, it also not suitable for on-site quantification of microalgal lipid.

**Table 1.1.** Microfluidic approaches to check the microalgal lipid.

Methods	Author	Single cell Level?	On-chip culture	Image	Culture size	Culture condition	Throughput for analysis	Analysis method	On-site detection	Additional apparatus or method
Microtraps	Kim et al <sup>53</sup>	Yes	Yes, 8 days		77 μm width, 80 μm height	TAP media, Light control	64	No lipid extraction, Fluorescence	<i>Difficult</i>	
	Bae et al <sup>39</sup>	No, ~200 cells in a trap	Yes, 18 hours		60 μm radius, 30 μm height	TAP media, Acetate control	40	No lipid extraction, Fluorescence	<i>Difficult</i>	Syringe pumps, Microscope, Sample dilution
	Kim et al <sup>57</sup>	Yes	Yes, 32 hours		15 μm opening width, 62.5 μm length, and 16 μm height	TAP media	1,204	No lipid extraction, Fluorescence	<i>Difficult</i>	
Droplets	Pan et al <sup>58</sup>	Yes	Yes, 10 days		~80 μm diameter	TAP media	1,500	No lipid extraction, Fluorescence	<i>Difficult</i>	
	Kim et al <sup>59</sup>	Yes	Yes, 3~5 days		~200 μm diameter	TAP media, Nitrogen control	100	No lipid extraction, Fluorescence	<i>Difficult</i>	Syringe pumps, Microscope, Sample dilution
	Lee et al <sup>55</sup>	Yes	No, 3hr viability test only		~26 μm diameter	BG 11 medium	110,000	No lipid extraction, Fluorescence	<i>Difficult</i>	

**Table 1.1.** Microfluidic approaches to check the microalgal lipid. (*continued*)

Methods	Author	Single cell Level?	On-chip culture	Image	Culture size	Culture condition	Throughput for analysis	Analysis method	On-site detection	Additional apparatus or method
Microfluidic Cytometer	Erickson et al <sup>38</sup>	Yes	No	N/A	180 $\mu\text{m}$ width, 90 $\mu\text{m}$ in height channel	TAP media, Nitrogen control	~2,000	No lipid extraction, Fluorescence	<i>Not easy but have potential to be portable</i>	Optical set-up for flow cytometer, Sample dilution
Micro Chamber	Lim et al <sup>40</sup>	No	Yes, 9 days		500 $\mu\text{L}$ culture chamber (8 mm in diameter and 15 mm in height)	TAP media, Nitrogen control	1	Lipid extraction, TLC, GC-MS (Lipid composition study)	<i>Very difficult</i>	Syringe pumps, GC, TLC Lipid transesterification to FAME for GC analysis
	Kwak et al <sup>56</sup>	No	Yes, 8 days		500 $\mu\text{L}$ culture chamber (8 mm in diameter and 15 mm in height)	TAP media, Light, temperature, nutrient stress	8	Lipid extraction, TLC, GC-MS (Lipid composition study)	<i>Very difficult</i>	



### **Needs of new platform for on-site determination of microalgal lipid**

Above previous study has great meaning that microfluidic based biofuel research can contribute to microalgal lipid industry. However, most of the their studies have focused mainly on biofuel production screening at the single-cell level and high-throughput manner or based on culture in the confined space of microchambers under controlled light<sup>53</sup> and stress<sup>60</sup> conditions with expensive analysis steps such as fluorescence requiring microscope and qualification requiring GC-MS. Thus, a practical approach is required for a rapid, automated method for quantification of lipids from microalgae grown in larger scales under moist conditions, which does not require drying or heating steps and sample dilutions.

## 1.1.2 Microfluidics in food antioxidants determination

With a rapidly growing global population, food and agriculture researches are getting important for safe and nutrient dietary life and have been performed to improve food quality, quantity and safety. For food research, precise detection and analysis are significantly important. Especially, food nutrients determination with high-performing analysis technique can guarantee reliable results even with low-content nutrients.

The presence of natural antioxidants in food and beverages, as reflected in their total phenolic content (TPC) and antioxidant activity (AA) values, has attracted considerable interest because of their potential therapeutic effects. These compounds are known to protect against harmful oxygen radicals or highly reactive oxygen species (ROS) by scavenging or neutralizing free radicals.<sup>61</sup> In particular, ROS is known to be closely associated with accelerated aging and the occurrence of such diseases as arteriosclerosis and cancer.<sup>62</sup> Thus, there is great interest in reducing the effects of these species on human health.

In academic research, flow injection analysis (FIA)<sup>63</sup> and sequential injection analysis (SIA)<sup>64</sup> have been developed for determination of total phenolic content of wine and beer samples. These methods have novelty in reducing the time, labor and handling errors from manual experiment. However, it required complicated pumping and tubing in FIA, and it required large sample and reagent volume in SIA. Also, both methods did not measure both total phenolic content and antioxidant activity.

Recently, lab-on-a-chip system has been employed for a food component detections.<sup>65, 66</sup> Among them, simple one-step reaction and detection of total phenolic content and antioxidant activity in microfluidic channels have been researched. It has been developed for determination of total phenolic content in honey<sup>3</sup> (**Figure 1.1A**) and a lab-on-a-chip device has also been developed a two-compartment microfluidic device that minimizes the dynamic of liver metabolism and the subsequent antioxidant activity of food components by Lee *et al* (**Figure 1.1B**).<sup>6</sup> They used 2,2-diphenyl-1-picrylhydrazyl radical (DPPH) method for antioxidant activity detection. Both lab-on-a-chip based total phenolic content and antioxidant activity detection have novelty in automating the complicated steps and reducing the sample and reagent volume. However, this technique requires external syringe pumps and external interconnects to induce fluid movement. In addition, both studies cannot detect total phenolic content and antioxidant activity simultaneously, and in Lee's work, they only used DPPH method for antioxidant activity detection.

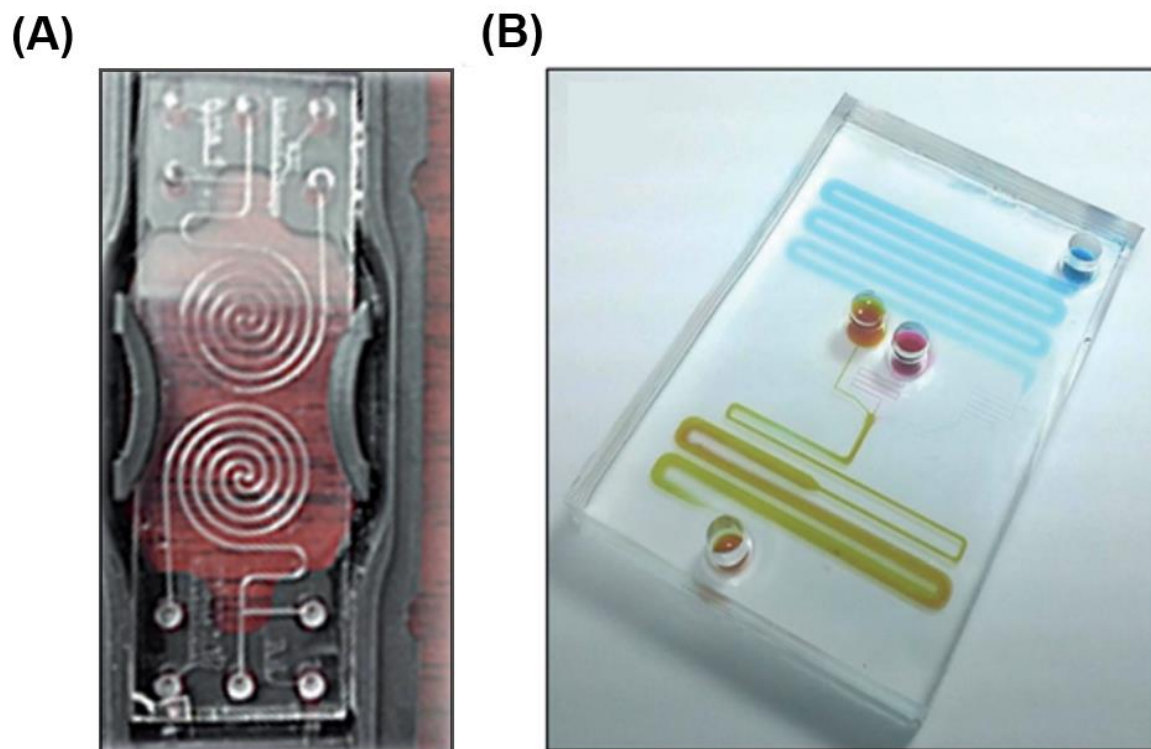


**Figure 1.1.** (A) Lab-on-a-chip platform for determination of total phenolic content in honey<sup>3</sup> and (B) Microfluidic device that minimizes the dynamic of liver metabolism and the subsequent antioxidant activity of food components.<sup>6</sup>

### **Needs of new platform for antioxidant detection from food.**

Not only micro-structure chip-based antioxidant detection but also capillary electrophoretic (CE) microchip has been used for determination of antioxidants from alcoholic beverage (wine, sakes, beers), fruits (apple, pears) and tea (**Table 1.2**). It has advantages because it can isolate the antioxidants and it can determinate each species of antioxidants in one sample. However, all CE chip requires additional off-chip sample preparation such as off-chip dilution, filtration and extraction of antioxidants. Thus, it is relatively time-consuming, and it required skilled researcher for sample pretreatment.

To address all the problems of microfluidic approach, special platform which can integrate more than 2 antioxidant methods for accurate analysis and can accomplish full integration and automation of whole processes; from sample pretreatment to determination is required.

**Table 1.2.** Research list of food antioxidant analysis using microfluidics.

	<b>Nutrients</b>	<b>Sample</b>	<b>Microchip</b>	<b>Sample preparation</b>	<b>Device for detection</b>
1 <sup>67</sup>	Antioxidants (rutin, etc.), vitamins (ascorbic acid, etc.)	Apples and natural vanilla beans	Glass CE microchip	Off-chip extraction, pulverization, macerated, dilution and filtration	Glass CE microchip using CNTs as electrode
2 <sup>68</sup>	Antioxidants (catechin, rutin, etc.)	Apples, pears, wines, green tea	CE microchip	Off-chip extraction, dilution, and filtration	Adaption of traditional analytical methods on MCE with electrochemical detection
3 <sup>69</sup>	Total isoflavones, antioxidant (arbutin, rutin, etc.)	Apples, pears	Glass CE microchip	Off-chip extraction and filtration	Glass CE microchip with MWCNTs based electrode as a flow injection system for analysis of total isoflavones and as a separation system for antioxidants detection
4 <sup>70</sup>	Antioxidant (chlorogenic)	Red wine	Glass CE microchip	Dilution and filtration, off-chip	Electrochemical detection (SPE electrode)
5 <sup>71</sup>	Antioxidants (catechins)	Green tea extract (nutraceutical)	PDMS CE, microchip	Solid-liquid extraction and filtration, off-chip	Electrochemical detection
6 <sup>72</sup>	Antioxidant (arbutin, ascorbic acid)	Pear pulps and commercial juices	Glass CE microchip	Juice filtration or solid-liquid extraction and filtration, off-chip	Electrochemical detection

\*CNTs : carbon nanotubes, CE: capillary electrophoresis, MWCNTs : Multi-walled carbon nanotubes, CZE : capillary zone electrophoresis, SPE : screen printed electrode.

### 1.1.3 Absorbance detection in microfluidics

UV/Vis absorption spectroscopy (absorbance detection) is the most straightforward and popular detection method in microfluidics applications due to its generality, simplicity, and adequate detection limit.<sup>73</sup> Absorption spectrums are related to the structure of the target analyte, concentration of the analyte in solution and are based on the capability of samples to absorb the incident light at various wavelengths.

In absorbance detection, sensitivity is mainly caused by optical path length which is the length of analyte solution that incident light path through. Unfortunately, the channel depths in microfluidic device is relatively shallow compared to their width because of the character of the fabrication method. If incident light is designed to pass through the channel only perpendicular direction to the chip plane, the optical path length through the sample is very limited by the depth of the channel, where path length was shortened from millimeters in conventional analysis to few micrometers in microfluidic chip, seriously impacting the sensitivity. To solve the issue from the low sensitivity caused by a short optical path length, various approaches were introduced to increase the optical path length.

Collins *et al.*, introduce the straightforward optical pathlength increasing method.<sup>74</sup> They fabricate the three-dimensional U-type flow cell on a thick glass microdevice which can increase the optical pathlength. A small hole (75  $\mu\text{m}$  diameter) was laser etched in a glass substrate having thickness (100  $\mu\text{m}$ ) defined most of the pathlength of the cell. Projecting out of the plane of the separation device was a 126  $\mu\text{m}$  optical pathlength flow cell as defined by the laser etched hole with the attached microchannels. (**Table 1.3** 2<sup>nd</sup> row)

Despite that, these methods suffer from the limited improvement of optical length because the changes of channel geometry are detrimental to maintaining separation efficiency and to blocking stray light. Salimi-Moosavi *et al.*, developed significant increase of optical path length by using multireflection cells in microfluidics chip.<sup>75</sup> In their approach, multireflection cell was made lithographically using a three-mask process to make patterns of aluminum mirrors below and above flow channel in a microfluidics device, which having 30 mm diameter optical entrance or exit apertures (one in each mirror) positioned 200 mm apart. Optical path length increases by 5 to 10-fold over single-pass chip. And Billot *et al.*, showed a similar idea on a glass–PDMS–glass microchip by patterning the mirrors on the inside of the microfluidics channel.<sup>76</sup> (**Table 1.3** 3<sup>rd</sup> row)

Besides generating light reflection multiple times inside the channel, using axially light passing along the microfluidics channel in a straight line is another way of increasing the optical path length.<sup>77-</sup>

<sup>79</sup> This approach is implemented by fabricating two parallel 45° mirrors at each end of the microchannel therefore light could be reflected into the channel and pass out to the detector by the mirrors. Thus, in this method, optical pathlength is defined by channel length of microfluidic device. For example, Noda *et al*, showed long optical path length (5 mm) is realized on the microfluidic device for highly sensitive absorption photometry.<sup>77</sup> Two 45° mirrors are made in ‘Multi-layered smart-MEMS structure’ to make a long optical path. 10 times increasing of optical pathlength has been achieved using this method. And when comparing using food color solution, effects of optical path extension are clearly shown as detectable lower limit improvement. Furthermore, no adverse effects due to utilization of 45° mirrors were observed. Their method proved that optical path extension with 45° mirrors can be effective to realize highly sensitive measurement in the microchip. (**Table 1.3** 4<sup>th</sup> row)

In lab-on-a-disc platform, there also approach to increase the optical pathlength for absorbance detection. Grumann *et al*, introduced the total internal reflection for absorbance measurements. A light beam directed onto the disc plane was deflected by a disc-integrated V-groove and passed through a microfluidic chamber in the azimuthal direction. A following V-groove deflected the light beam out of the disc plane to the optical detector. Therefore, the overall path length for the absorption measurement (and the sensitivity) was increased from 1 mm to 10 mm.

However, with increasing optical pathlength, optical losses have been observed because of stray light and light dispersion, leading to a reduction in incident light and loss of pathed light which containing absorbance results of target analyte.<sup>80, 81</sup>

Accordingly, reduce the loss of light from stray light and light dispersion, additional collimating system has been used.<sup>82-84</sup> Llobera *et al*, developed the absorbance detection system which integrated optical fibers, air mirrors, and collimation microlenses on a chip.<sup>82</sup> Using collimating microlenses, incident light has been focused before pass the target solution. And then, the passed light can be focused again using collimating microlense before going to detecting optical fiber. Thus, light dispersion can be decrease and so the result light intensity can be increased. (**Table 1.3** 5<sup>th</sup> row)

From the summary of absorbance detection techniques in microfluidics, we found that there have been researches to increase the optical pathlength. But it requires light collimating due to the loss of light from light dispersion and stray light. In lab-on-a-disc platform, there also have been research to increase the optical pathlength. But recent works adapted light collimating when detecting absorbance and optical pathlength is same with disc thickness which means detecting absorbance in perpendicular direction of disc. We believed that this is because disc thickness (optical pathlength) is around ~ few mm (for lab-on-a-chip, ~ hundred μm), and this optical pathlength satisfy the limit of detection (LOD)

and dynamic range for their applications. Thus, to set the optical pathlength, researcher should confirm the dynamic range and LOD of their application using batch test (with conventional absorbance detector). Then, if LOD and dynamic range is satisfied when the optical pathlength is ~few mm level, we can just consider light collimating to prevent light loss in absorbance detection. Otherwise, if it requires sensitive detection (low LOD), increasing optical pathlength should be considered additionally.

For examples in lab-on-a-disc platform to use the collimating light for absorbance detection, Kong *et al*, developed collimating lens couple fiber optics for absorbance detection in lab-on-a-disc.<sup>20</sup> All spectral measurements were made using an absorbance instrumental configuration with components. However, they didn't develop customized software for absorbance detection. Thus, to detect the absorbance of each chamber, they required labors to control the motion of motor, to measure light intensity before and after passing chamber, and calculating absorbance based on measured light intensity. Thus, it is time-consuming if number of detection chamber increase. To be honest, it is not mandatory to make the customized software. However, it is clear that software which can control all modules; motor and spectrometer can reduce the labors and time in on-disc analyzing.

Ding *et al*, showed an in-line, miniature, low-cost spectrophotometric detection system can be used for rapid protein determination and calibration in lab-on-a-disc platform.<sup>85</sup> Their detection analyzer is configured with paired emitter and detector diodes, which is the light beam between both paired LEDs is collimated having enhanced system tolerance. They built their own software and data communication hardware which detected data can be transport toward smartphone using wireless (Bluetooth) data transmission. This approach can be benefit for low-cost and efficient set-up for absorbance detection, and it have big potential to be used in portable device. However, it can detect only one wavelength for detection, and if user want to change the wavelength, LED should be changed, and collimation set-up should be tested again for optimization. Thus, it has some disadvantages if used for universals uses as a bench top on-disc analyzer.

#### **Needs of new disc analyzer for absorbance detection.**

To address the problems above, development of new on-disc analyzer for absorbance detection will be benefit. New disc analyzer may contain light collimating set-up to prevent the light loss from light dispersion and stray light, customized software to help to reduce the labor and time, and all spectral measurements (300 nm to 1000 nm) for universal applications.



**Table 1.3** Various approaches to increase the optical pathlength in microfluidics.

Studies	Representative image	Characteristics
<p><sup>174</sup> Increasing chip thickness; Bonding additional chip inside the chip layer to increase the optical pathlength.</p>		<ul style="list-style-type: none"> <li>✓ Simple increasing of optical path length. (100 μm increasing)</li> <li>➤ Limited improvement of optical length because of affect to separation efficiency and stray light</li> </ul>
<p><sup>275, 76</sup> Using multiple reflection; Mirror patterning above and bottom channel</p>		<ul style="list-style-type: none"> <li>✓ Almost infinite increasing of optical pathlength.</li> <li>✓ 5 – 10 times increasing of optical pathlength</li> <li>➤ Can lose the light because of light straying.</li> </ul>
<p><sup>377-79</sup> Using light reflection; channel pass through; Integrating 45° mirrors in microfluidic device</p>		<ul style="list-style-type: none"> <li>✓ Relatively simple compared to multiple reflection.</li> <li>✓ ~ 10 times increasing of optical pathlength</li> <li>➤ Limited to channel or chamber length</li> </ul>

**Table 1.3** Various approaches to increase the optical pathlength in microfluidics. (*continued*)

Studies	Representative image	Characteristics
<p>4<sup>82-85</sup> Increasing chip thickness;                      Bonding additional chip                      inside the chip layer to                      increase the optical                      pathlength.</p>		<ul style="list-style-type: none"> <li>✓ Simple increasing of optical path length.</li> <li>➤ Limited improvement of optical length because of affect to separation efficiency and stray light.</li> </ul>

## 1.2 Lab-on-a-disc

Lab-on-a-disc or lab-on-a-CD was also known to as centrifugal microfluidic technology. Lab-on-a-disc platform was commercially available in the market as analytical tool such as immunoassay analysis, exosome isolation and RT-PCR.<sup>86</sup> Lab-on-a-disc system has advantages in the term of integration, automation, parallel analysis and miniaturization. All of process of sample filtering, metering, mixing, reaction, and detection was performed on a disc device employing a single motor to control multiple fluidic transports which can be applied in a wide range of scientific applications for example, clinical diagnostics,<sup>87</sup> biological analysis,<sup>88</sup> chemical analysis<sup>5</sup> and food analysis.<sup>2</sup> The lab-on-a-disc system provides many advantages over conventional batch method in terms of reducing analysis time, and consumption of sample and reagents, and complete automation (reduce error due to handling). lab-on-a-disc does not require complex interconnections with external equipment, and whole system size as well as the product cost can be reduced.<sup>89</sup>

The history of lab-on-a-disc was started from the late 1960s. In the late 1960s, N. Anderson from Oak Ridge National Labs (ORNL) developed a clinical analyzer by using a rotating disc, cuvette and computer connected optical detector for detection (**Figure 1.2A**).<sup>90</sup> This work was the pioneer of the field of lab-on-a-disc. In consequence, miniaturized analytical system was introduced and the detection platform was modified to read out optical signal from reaction mixture such as light transmittance, absorbance, fluorescence and chemiluminescence. After Anderson's publication, several companies wanted to commercialize the centrifugal analyzer. For the first time, Electro-Nucleonics developed commercial centrifugal analyzer system. Other companies such as GEMSAEC and GEMINI, Centri Union Carbide- American Instruments-Rotochem, CentrifChem, Instrumentation Laboratories, Inc.- Multistat, and Roche-Cobas-Bio were also started to supply related products. In 1989, Abaxis, Inc was established and shifted the utilization of the lab-on-a-disc from a research tool toward the diagnostic purposes. Abaxis took the patents from ORNL and invented a new type of blood analysis platform, known as Piccolo rotor system in 1995. All reagents were integrated on a disc and Piccolo system integrated the whole process for the analysis. As a result, the Piccolo became a representative platform for commercially available blood analysis.

In 1998, M. Madou and G. Kellogg from Gamera introduced the possibility of more advanced lab-on-a-disc as a sample to answer system for the first time by presenting "The LabCD: A centrifuge-based microfluidic platform for diagnostics"(**Figure 1.2B**).<sup>4</sup> They reviewed basic fluidic elements on centrifugal microfluidics such as pumping, valving, mixing, metering and sample introduction. They also proposed a new strategy to expand application area of lab-on-a-disc by employing micro-fabrication techniques capable of miniaturization of microchannel network and integration of

microsensors. Previous centrifugal analyzers often required trained person to perform the assays, however LabCD platform overcame such limitation by successfully employing automation and micro fabricated fluidic functions on a disc.

Since M. Madou and G. Kellogg suggested a new possibility to a “next generation disc”, academic researches and commercial efforts have been continuously made to integrate new assays on a disc. In academia, Kido *et al.* first developed immunoassay system on a disc for environmental analysis<sup>91</sup> and many other groups have been reported different types of miniaturized immunoassay.<sup>17, 18, 92-94</sup> Micro-fabrication technique facilitated the design of multiple chambers on a single disc and thus multiplex assays could be integrated to detect several biomarkers simultaneously.<sup>17, 87, 92</sup> Besides immunoassay, several kinds of bioassays or sample preparation including blood separation, blood chemistry, DNA extraction and amplification are actively being developed.<sup>19, 95-97</sup> The application area were expanded beyond bioassays encompassing environmental and food examinations.<sup>5, 7</sup> In terms of commercial product, Abaxis and Gyros AB commercialized disc-based blood chemistry and immunoassays, respectively.<sup>94</sup> There are many follow up companies for automated immunoassay such as Quadraspec, Burstein Technologies, Advanced Array Technology and Samsung. In particular, Samsung team suggested the breakthrough for the integration of various assay on a disc and it was attributed to the utilization of a sacrificial valve.<sup>98</sup>

As reviewed in this section, lab-on-a-disc has been a strong candidate for sample-to-answer system due to its capability for integration and automation. Thus, it has been commercialized in various fields, and it is expected that the field of application will be even more enlarged in the future.

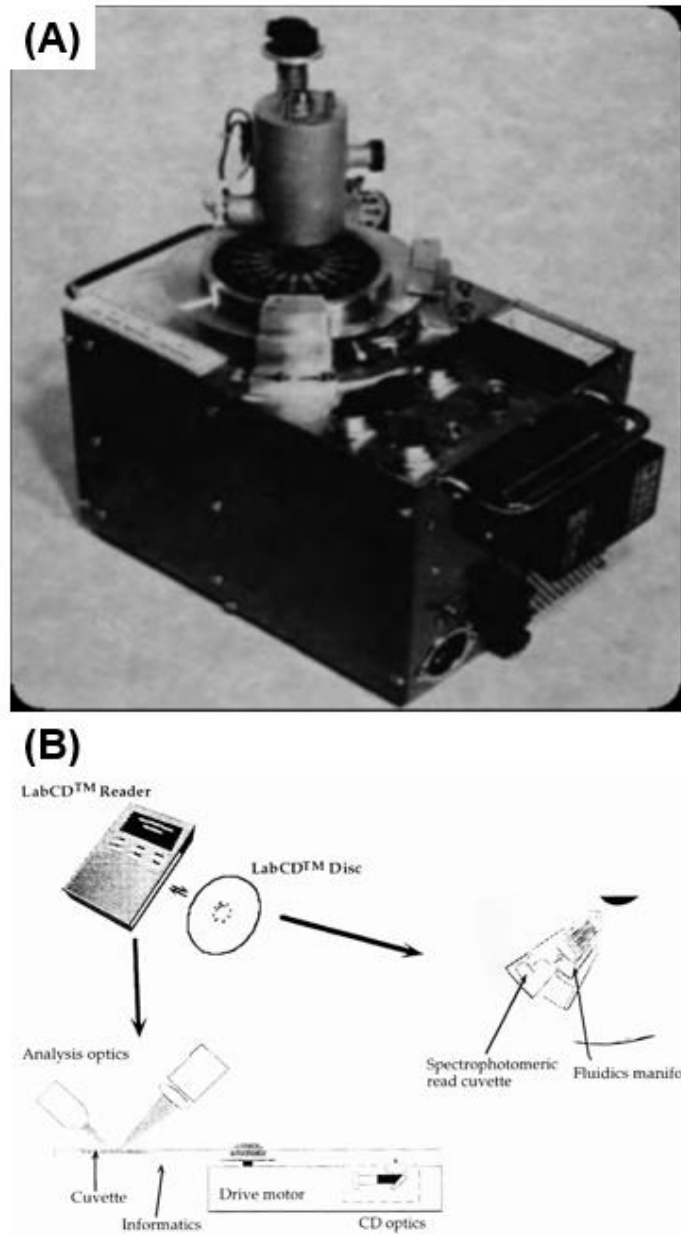


**Figure 1.2.** (A) First Lab-on-a-disc platform by Oak Ridge National Laboratories (ORNL)<sup>1</sup> and (B) First lab-on-a-disc platform can be used as an advanced sample-to-answer system by Madou's group.<sup>4</sup>

### 1.2.1 Basic principle of lab-on-a-disc system

As shown in **Figure 1.3**, the forces experienced by a liquid plug on a rotating disc.<sup>99</sup> The fluidic control in lab-on-a-disc system relied on the centrifugal force ( $F_c$ ), Coriolis force ( $F_{co}$ ), Euler force ( $F_E$ ). Three force are based on a single rotation process.

#### *Centrifugal force ( $F_c$ )*

Centrifugal force is the driving force for fluid transport in lab-on-a-disc systems and causes fluid to flow radially outward from the center of the disc to the outer circumference. The centrifugal force can be described by the equation<sup>11</sup>

$$F_c = -\rho\omega^2r \quad (1-1)$$

when  $\rho$  is the mass density of fluid in the channel,  $\omega$  is the angular rotational frequency and  $r$  is the position on the disc device, and. The centrifugal force not only used for facilitating fluid flow through a system but also can be applied for sedimentation or separation of a sample (centrifugation) and for compression of fluid.

#### *The Coriolis force ( $F_{co}$ )*

Coriolis force is the force moving perpendicular to the centrifugal force. It can be utilized for of samples in a lab-on-a-disc system, as well as for flow switching, or moving of a sample into a specific channel path. The Coriolis force is described by the equation<sup>11</sup>

$$F_{co} = -\rho\omega v \quad (1-2)$$

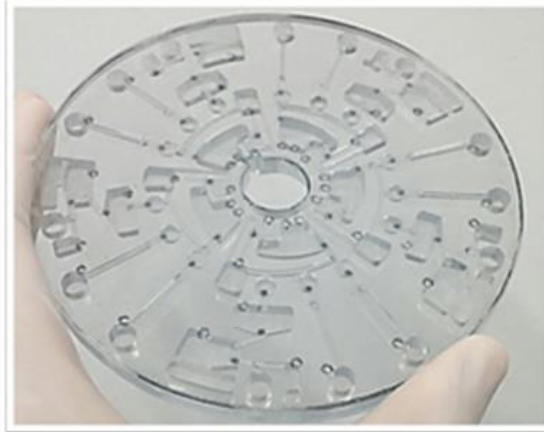
when  $\rho$  is the mass density of fluid in the channel,  $\omega$  is the angular rotational frequency and  $v$  is the vector of flow velocity.

#### *The Euler force ( $F_E$ )*

Euler force is proportional to the angular acceleration and it exists only when the rotation acceleration is not zero. The Euler force ( $F_E$ ) equation is given in the equation<sup>11</sup>

$$F_E = -\rho d\omega/dt (r). \quad (1-3)$$

(A)



(B)

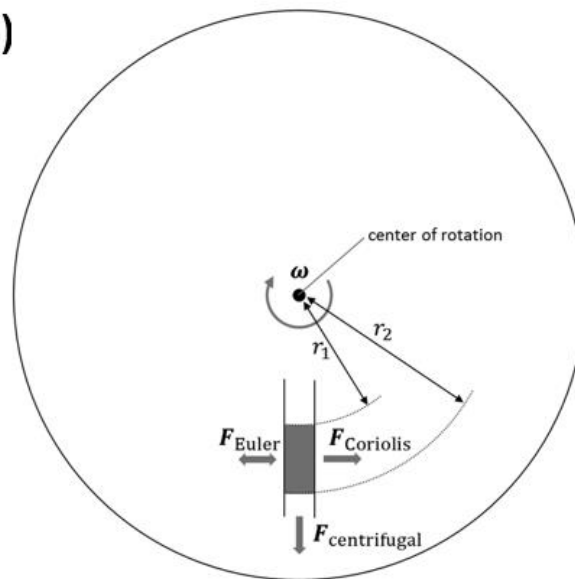


**Figure 1.3.** (A) Lab-on-a-disc picture and (B) schematic diagram showing a geometry and forces acting on a liquid plug in a channel of a rotating disc. This picture was obtained from reference.<sup>11</sup>

### 1.2.2 Lab-on-a-disc functions

The basic of lab-on-a-disc function platform is composed of the (1) centrifugal pumping, (2) valving, (3) metering, (4) mixing and (5) detection.

*Centrifugal pumping for lab-on-a-disc:*

The centrifugal pumping is referred to the liquid transportation obtained from a disc spin which induced the sample fluids drive liquids radially outwards from the center toward the edge of the disc. The flow rate of fluids in lab-on-a-disc system depends on rotation rate, channel geometry and location of channels and reservoirs, and fluid properties. The average velocity of the liquid ( $U$ ) from centrifugal theory is given as<sup>86</sup> :

$$U = \frac{D_h^2 \rho \omega^2 \bar{r} \Delta r}{32\mu L} \quad (1-4)$$

when  $D_h$  is the hydraulic diameter of the channel,  $\rho$  is the density of the liquid,  $\omega$  is the angular velocity of the disc,  $\bar{r}$  is the average distance of the liquid in the channels from the center of the disc,  $\Delta r$  is the radial extent of the fluid,  $\mu$  the viscosity of the fluid, and  $L$  the length of the liquid in the microchannel.

*Valving*

Valving is used for the control of fluidic flow movement in lab-on-a-disc system. Valves for lab-on-a-disc system have been reported into passive valves and active valves. Passive valves are controlled simply by changing the rotation speed of the disc device and require the channel geometry designs or surface modifications. The opening of a normally closed passive valves is carried out by centrifugal pressure and capillary forces. The most commonly used passive valves in lab-on-a-disc system are capillary valves, hydrophobic valves, and siphoning valves.<sup>11</sup> The physics of capillary valves can be explained like below.

When a fluid passes through a microchannel, a fluid experiences capillary pressure ( $P_s$ ), also known as surface tension induced pressure;

$$P_s = \frac{4\gamma \cos\theta}{D_h} \quad (1-5)$$



where  $\gamma$  is the surface energy of the fluid-air interface and  $\theta$  is the contact angle between sample fluid and channel surface. Generated centrifugal pressure by rotation has to be stronger than capillary pressure for a sample fluid to flow through the microchannel. Therefore, burst frequency ( $\omega_c$ ) at which centrifugal pressure overcome the capillary pressure can be defined as:

$$\omega_c = \left( \frac{4\gamma \cos\theta}{\pi^2 \rho \bar{r} \Delta r D_h} \right)^{\frac{1}{2}} \quad (1-6)$$

Thus, burst frequency can be controlled by adjusting channel geometry, radial position and surface energy. Generally, a sample fluid at inner radial position or channel smaller hydraulic diameter gets burst later. This can be utilized for valving mechanism for centrifugal microfluidics (**Figure 1.4A**). It does not require an external energy source to operate valve. Madou *et al.* has calculated burst frequency and compared with experimental result showing that both values are consistent.<sup>100</sup> The capillary valve were utilized to implement multiple assays by increasing rotational speed sequentially

Hydrophobic valve is presented in **Figure 1.4B**. Similar to capillary valves, Gyros AB coated hydrophobic patches at entrances of microchannel to impede fluidic movement.<sup>94</sup> A sample fluid can flow through the functionalized hydrophobic area in microchannels as a rotational frequency higher than the threshold value.

Capillary valves and hydrophobic valves, which do not require external energy source for actuation, are also called passive type valves and they have advantages because valvings can be achieved by modifying channel dimension and surfaces properties. However, valving is valid only for liquids, not for vapors. Also, local actuation of a valve is difficult to achieve. Thus, the need for development of new type of valve has emerged.

In active valves, it is controlled by external means and require additional interfaces to the processing device. The active valves can be switched on or off by external means during an experiment. There are three examples in active valve system to be used in lab-on-a-disc platform.

Park *et al.* developed a sacrificial valve actuated by a laser irradiation. Paraffin wax was mixed with ferro-fluid containing magnetic particle that can absorb the heat from laser activation and melt wax rapidly. This was utilized as a sacrificial material for valving as described in **Figure 1.4C**. With neighboring plug structures in the channel, melting and re-solidification of wax by laser activation made microchannels open and close on demand.<sup>13</sup> Unlike passive valves, operation of valve was independent

to rotational rate of a disc, and valving of vapor was also possible. Therefore, it was possible to integrate more complicated biological assays on a disc.<sup>18,96</sup>

Kim *et al.*, developed the laser printed carbon dot valve for lab-on-a-disc platform.<sup>14</sup> (**Figure 1.4D**). A thin thermoplastic film with laser printed carbon dots were inserted and bonded between top and bottom discs. The carbon dots absorb the laser energy and melt the underline thermoplastic film substrate, thereby open the fluidic passage. The similar valving technique was previously demonstrated in microfluidics in 2010 by Jose L. Garcia-Cordero *et al.*, and they used it for milk quality monitoring in lab-on-a-disc.<sup>101, 102</sup> Laser printed carbon dot on centrifugal microfluidics has also been used for hydrophobic valving by Thompson *et al.* They deposit a ‘patch’ of laser printed carbon dot toner that creates a dramatically different surface hydrophobicity relative to the native transparency film.<sup>103</sup>

Kim *et al.*, developed an individually addressable diaphragm valves (ID valves) that enable the reversible and thermally stable actuation of multiple valves with unprecedented ease and robustness.<sup>15</sup> These ID valves are configured from an elastic epoxy diaphragm embedded on a 3D printed push-and-twist valve, which can be easily actuated by a simple automatic driver unit (**Figure 1.4E**).

### *Metering*

Metering of liquid volume on a disc is often achieved based on a disc design. A liquid is filled a metering chambers with a defined volume. The excess is gated into a waste chamber. The metered liquid volume can be transferred into the microfluidic network via the valves (**Figure 1.4F**). Sample and reagent volume metering play an important role in lab-on-a-disc system to achieve proper reagent volume for analytical analysis and it also ensure reproducible valving processes on a disc.<sup>104</sup>

### *Mixing*

A mixing of liquids in lab-on-a-disc system is based on the centrifugal force, Coriolis force and Euler force (**Figure 1.4G**). The mixing on a disc are performed by the changing the rotation speed of the disc periodically and by rapid oscillations of the disc to achieve rapid mixing in low-Reynolds number regimes.<sup>86</sup>

### *Detection*

The most common detection method of lab-on-a-disc system are based on optical for example, colorimetric detection,<sup>105</sup> fluorescence detection,<sup>92</sup> and imaging detection.<sup>106</sup> Other alternative methods used in lab-on-a-disc system are an electrochemical detection and mechanical sensors.<sup>107</sup> Many research groups focus on the development of lab-on-a-disc system for improving the unit operation such as disc

design and fabrication, valve for fluid control and detection system. Lab-on-a-disc is a mature technology that can be applied as an alternative method for microfluidic analysis systems.

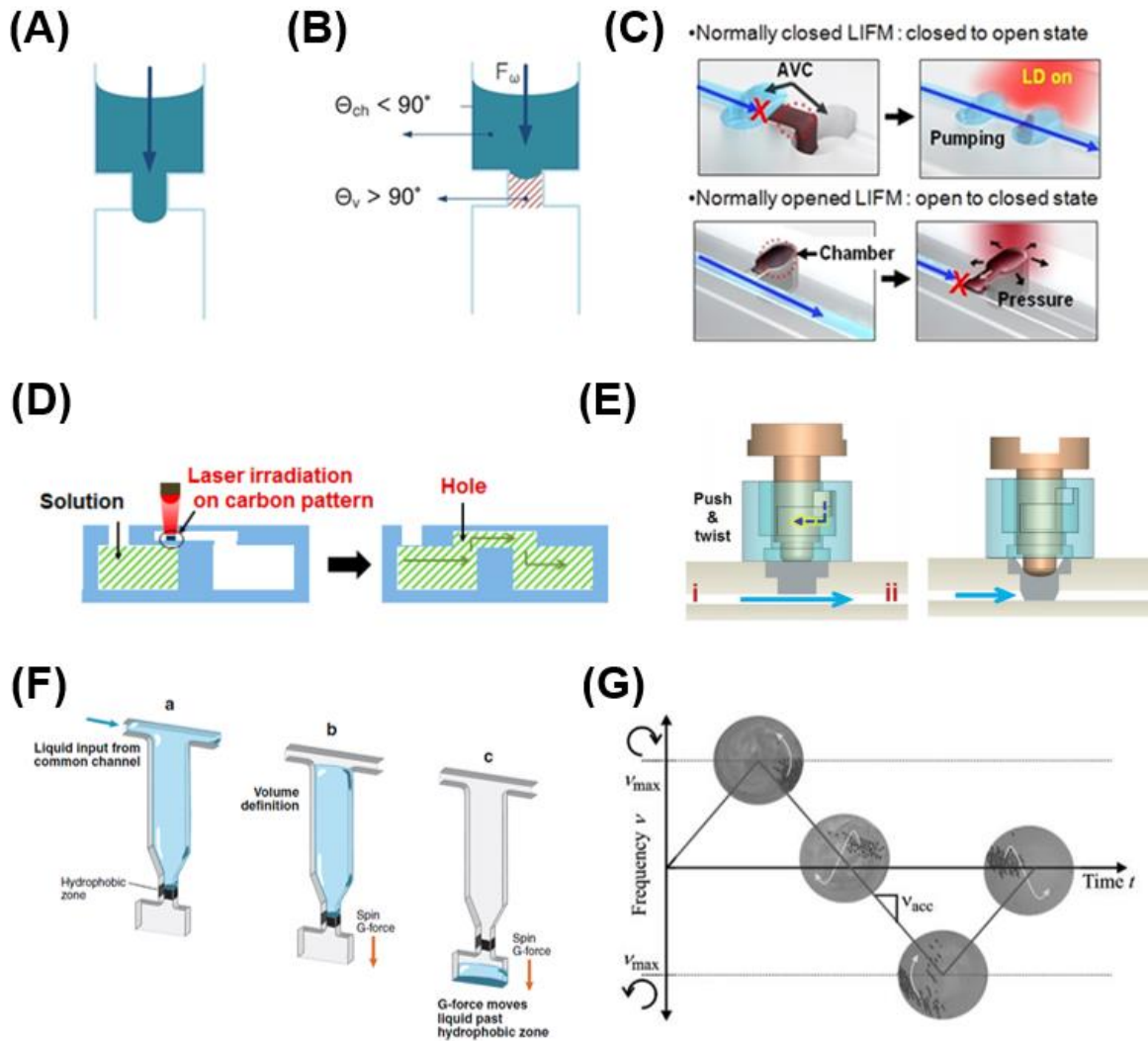


**Figure 1.4.** Various valving techniques, metering, mixing on centrifugal microfluidic system: (A) capillary valve,<sup>12</sup> (B) hydrophobic valve; The region illustrated with red line zone represents hydrophobic surface,<sup>12</sup> (C) laser irradiated ferrowax microvalves (LIFM); Both normally-closed and normally-open LIFM were demonstrated.<sup>13</sup> (D) Schematic illustration of laser irradiated carbon dot valves.<sup>14</sup> (E) Schematic illustration of individually addressable diaphragm valves (ID valves).<sup>15</sup> (F) Schematic diagram showing the principle of the metering; The fluid fills the pre-defined volume first and excess liquid are removed to the waste chamber.<sup>12</sup> (G) Enhanced mixing on a disc by periodically alternating the rotation sense.<sup>16</sup>

### 1.2.3 Lab-on-a-disc application in biomedical field

Cho *et al.* reported laser induced thermal lysis method to extract DNA from pathogens in whole blood.<sup>97</sup> Target cells in whole blood were captured by magnetic beads modified with antibodies specific to the target. Then, magnetic beads were collected in small chamber and laser was activated to heat bead. Thermal shock was provided to the cell causing faster and more efficient cell lysis as compared to a commercially available lysis method.

Honda *et al.* and Gyros also demonstrated a multiplexed immunoassay with fluorescent detection (**Figure 1.5A**).<sup>17, 94</sup> A disc named Bioaffy was operated in automated robotic handling system, GyroLab workstation. Robotic liquid handler introduced prepared sample from well plate to CD and spinning of disc automated bead-based immunoassay. Finally, signal detection was carried out by laser induced fluorescence detector. Maximum 112 targets could be test on a disc for multiplex assays; however, it still requires expensive and precise liquid handling machine to run the assays. Therefore, it is more preferred to be used in pharmaceutical industry where many parallel tests are desired rather than point-of-care test settings.

Lee *et al.* from Samsung developed a fully automated and integrated immunoassay on a lab-on-a-disc (**Figure 1.5B**).<sup>18</sup> Target antigens, blood plasma driven hepatitis B virus were separated first by disc spinning and transferred to incubate with secondary antibody. Then, target-antibody complex was moved toward detection chamber containing capture antibodies immobilized on polystyrene beads to increase the effective surface area. After few washings, substrate solution was introduced, and optical signal was measured. Local fluidic controls on demand for sequential assays were possible by wax based sacrificial valve actuated by laser irradiation. As a result, whole processes were integrated from blood separation to final detection on a disc. Recently, Park *et al.* further demonstrated automated multiplex immunoassay using same sample solution.<sup>87</sup> Several biomarkers for cardiovascular disease such as C-reactive protein, cardiac troponin I, and N-terminal pro-B were detected from biological fluids (saliva and whole blood) and the process time was approximately 20 min.

Stetten *et al.* demonstrated disc based real-time quantitative PCR system for a two-step PCR.<sup>19, 108, 109</sup> They pre-loaded reagents for pre-amplification of specific DNA sequences and the automated aliquoting of amplicons was perform for real-time secondary PCR without contamination that may result from the handling of DNA samples (**Figure 1.5C**).

F. Stumpf *et al.* showed the fully integrated sample-to-answer protocol including chemical lysis, RNA extraction and real-time RT-PCR was introduced in the lab-on-a-disc platform (**Figure 1.5D**).<sup>110</sup> Reduction to one initial manual handling step (sample supply) was realized by pre-storage of all required liquid and solid reagents. The use of frequency dependent on-demand release of liquid buffers

out of stick-packs facilitates handling and post-lysis addition of highly wetting binding buffer. Lab-on-a-disc verification was performed with RNA bacteriophage MS2 as sample (75 pfu per ml) and additionally the influenza A H3N2 virus was detected with clinical relevant sensitivity. The space efficient microfluidic design leaves room for an advanced lab-on-a-disc design taking more reaction cavities enabling the integration of more pathogen panels and therefore, increases the degree of multiplexity.

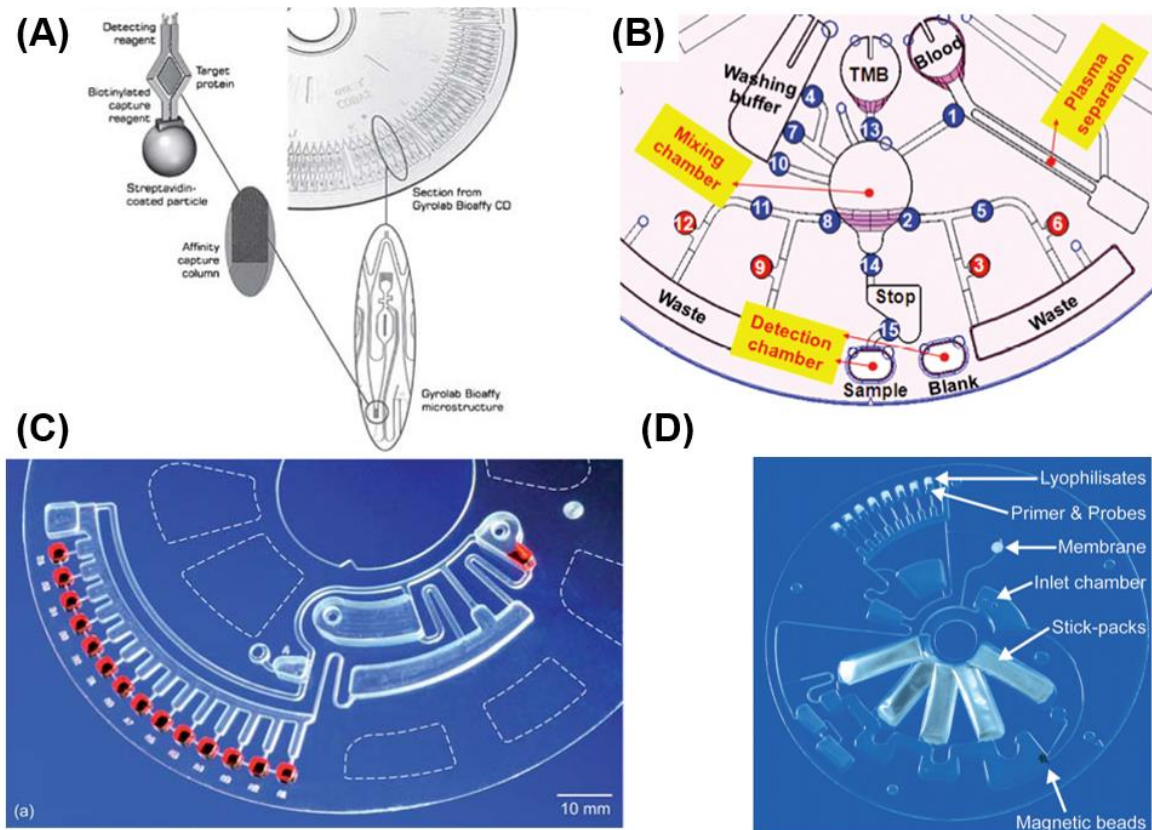


**Figure 1.5.** (A) Design of a disc for multiplexed immunoassay from Gyros, Miniaturized unit can perform maximum 112 targets detection.<sup>17</sup> (B) Disc layout of fully automated immunoassay from Samsung, utilization of sacrificial valve facilitates integration from whole blood separation to detection.<sup>18</sup> (C) Image of disc for secondary PCR, pre-amplification and secondary PCR was implemented sequentially without contamination from handling.<sup>19</sup> (D) Photograph (left) of the LabDisk for sample-to-answer nucleic acid based detection of respiratory pathogens with complete reagent prestorage.

### 1.2.4 Lab-on-a-disc application in other fields

Beyond diagnostic applications based on centrifugal microfluidic platform, various research fields have been adapted in centrifugal devices for their applications.

Kim *et al.* reported a fully integrated lab on a disc for molecular diagnostics of Salmonella, a major food pathogen.<sup>2</sup> They developed a lab-on-a-disc platform, which integrating the three major steps of pathogen detection, DNA extraction from pathogen, isothermal recombinase polymerase amplification (RPA) of DNA, and final detection, onto a single spinning disc. A laser diode was used for wireless control of active valve actuation, lysis of cell, and contact free heating in the isothermal amplification step, therefore it showed a compact and miniaturized system. For achieving high detection sensitivity, pre-enrichment of rare cells in large volumes of phosphate-buffered saline (PBS) and milk samples were done before loading into the disc using antibody-coated magnetic beads. The whole processes, from DNA extraction through to detection, was finished within 30 min in a fully automated manner. The final detection was done by using strip sensor by naked eye observation; limit of detection was 10 cfu/mL and 10<sup>2</sup> cfu/mL in PBS and milk, respectively. Their device allowed rapid molecular analysis. And it does not need trained researcher or expensive equipment. (**Figure 1.6A**).

Hwang *et al.* introduced application of lab-on-a-disc for environmental analysis by examining water quality.<sup>5</sup> Water analysis disc as shown in **Figure 1.6B** enabled simultaneous determination of nitrite, nitrate and nitrite, ammonium, orthophosphate, and silicate in real water samples. All detection procedures were automated on a disc platform and only 500  $\mu$ L of sample was required. Concentration of nutrients could be determined using calibration curve, total analysis time was 7 min 40 s and it is about 40 times faster than the conventional method.

Xu *et al.* developed a microfluidic disc for a caffeine detection as well as a microfluidic disc for monitoring chemotherapy compounds (**Figure 1.6C**).<sup>7</sup> Solid phase extraction (SPE) was successfully integrated on a disc by installing a chamber containing absorbent materials in parallel direction with respect to radial direction and whole procedures were automated. The developed microfluidic disc platform provided sample-to-answer system for a caffeine detection from real samples such as coke, milk tea, coffee and so on and quantified analysis.

Woo *et al.* introduce a s a lab-on-a-disc platform for facile, rapid, and sensitive isolation and analysis of EVs from raw biological samples, such as CCS and urine (**Figure 1.6D**).<sup>8</sup> One of the main advantages of their device is that intact EVs captured on the filter can be easily retrieved for downstream molecular analysis and/or be directly analyzed for surface-protein markers using on-disc ELISA, which can be easily adapted for clinical settings. Their method exhibited enhanced nanoscale-filtration efficiency through the incorporation of highly porous membranes on the centrifugal microfluidic platform.



S.-K. Lee *et al.* presented a centrifugal cartridge for the fabrication of photonic crystals. The cartridge was used to centrifuge suspensions of polystyrene latex spheres or monodisperse silica into dead-end channels, which is the nanoparticles formed closely packed columns with predefined shapes. By subsequently rotating different bead-solutions, they were able to make hybrid colloidal crystals (**Figure 1.6E**).<sup>9</sup>

Bruchet *et al.* demonstrated the use of a lab-on-a-disc platform for the analysis of nuclear spent fuels. In existing setting, nuclear spent fuels are dissolved in nitric acid and experimented in a specially shielded hot cell. They showed a 1000-fold reduction in the required sample volume using lab-on-a-disc, which allowed the analysis to be performed in a glove box. For the first proof of concept, Bruchet *et al.* showed that a lab-on-a-disc platform with an integrated monolithic anion exchange stationary phase was capable of extracting europium at a yield of ~ 97% (**Figure 1.6F**).<sup>10</sup>

We have reviewed fundamental principle of microfluidic functions on centrifugal devices and application fields. All microfluidic functions could be performed by simple rotation of a disc and micro-size fluidic network facilitates automation and integration of complex assays. Thus, centrifugal microfluidic platform utilized in research field and industry has been the strongest candidate for sample-to-answer system. Beyond the application for diagnostics, versatility of the centrifugal device has been demonstrated by applying it to food & beverage analysis, environmental analysis, nano-size EV filtration. Therefore, the centrifugal microfluidic platform can serve as a valuable research tool in a wide variety of area in near future.

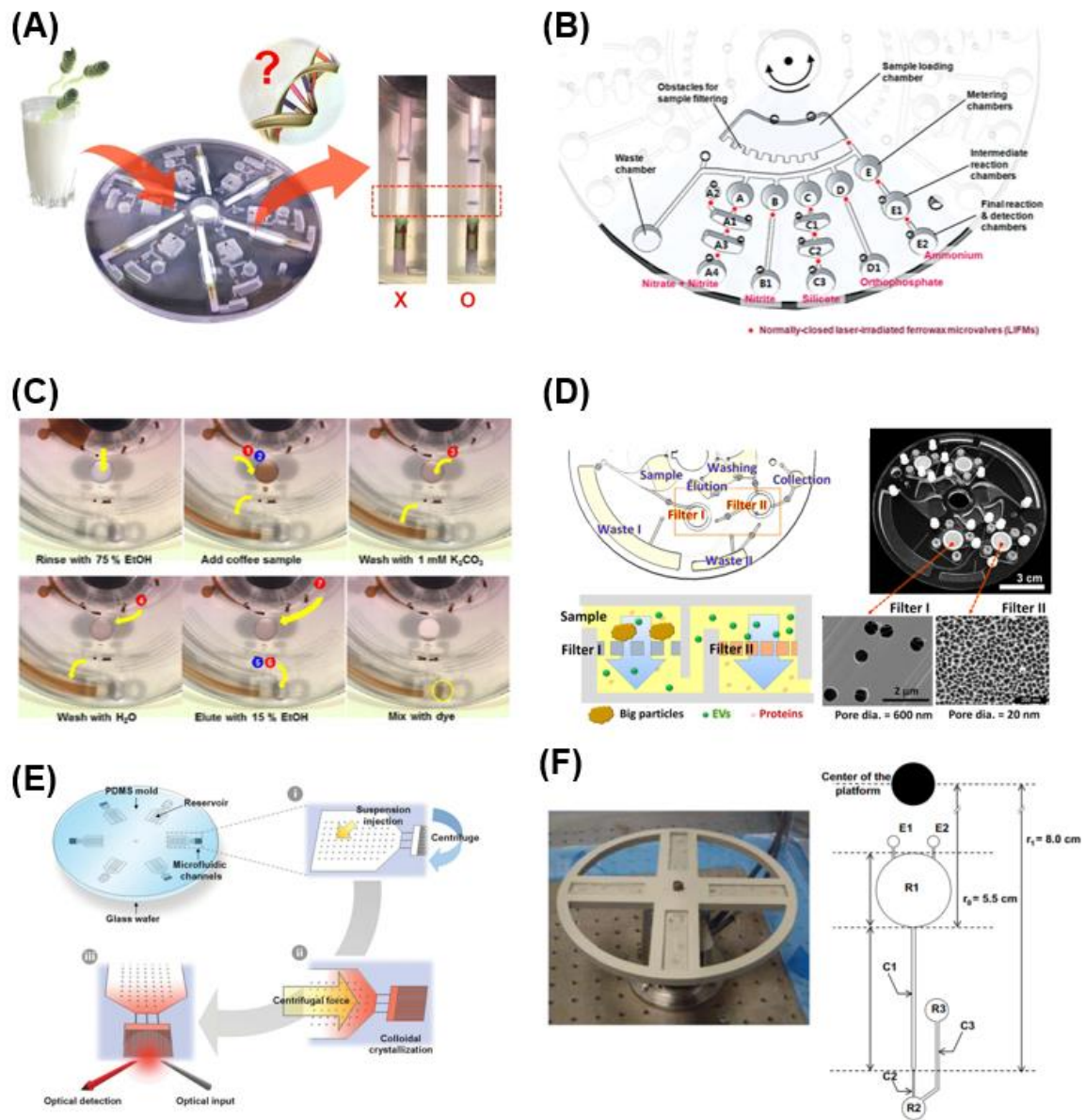


**Figure 1.6.** (A) Representative image of pathogen detection on a disc.<sup>2</sup> (B) Disc design for water analysis, six nutrients were detected within 5 min.<sup>5</sup> (C) Operation images for caffeine detection disc, solid phase extraction was integrated for extraction caffeine from real sample and amount of caffeine was quantified by fluorescence dye.<sup>7</sup> (D) Representative image for facile, rapid, and sensitive isolation and analysis of EVs from raw biological samples using lab-on-a-disc.<sup>8</sup> (E) Arrangement of designed functional units and schematic procedure for crystallization of colloidal particles in a lab-on-a-disc platform.<sup>9</sup> (F) Lab-on-a-disc image and design of chip cartridge for analysis of nuclear spent fuels.<sup>10</sup>

### 1.3 Research motivations

In past few decades, the lab-on-a-chip system, which for integrating complicated laboratory work into a simple chip platform, has attracted a great deal of attention. The miniaturization of the lab-on-a-chip system allows bioassays to be implemented with decreased reagent use, a decreased total operation time, and increased abilities for parallel processing. In addition, the automation of lab-on-a-chip devices requires no skilled worker, and the absence of human error in laboratory protocols makes the result of these assays consistent.

Current research on the lab-on-a-disc platforms has been mainly focused on biomedical applications. As taking advantage of fully automated operation and powerful mixing, lab-on-a-disc platform has been applied for various biomedical applications such as handling and analysis of cell or bioparticles molecular diagnostics, immunoassay like ELSIA.

We believe, not only for biomedical applications but also for biofuel and food chemistry fields, the use of lab-on-a-disc platform can be huge benefits because it can reduce the complicated steps and enhance the reaction efficiency by providing full automation and powerful mixing in complex chemical reaction. Also, lab-on-a-disc platform can reduce the human handling errors in manual steps. Step with increasing of industry of biofuel and food chemistry, we expect that there will be huge need of simple and user-friendly analysis device which can quantify the biofuel amount from next generation energy source for biofuel industry and can detect the food ingredient for customer and functional food like polyphenol containing beverage.

## 1.4 Research aims

The research aim in this thesis is the development of fully integrated lab-on-a-disc systems for biofuel quantification and food chemistry. Here, we demonstrate a sample-to-answer system facilitating the integration and automation of the entire process for complicated biofuel quantification and food chemistry in lab-on-a-disc

### **Microalgal lipid quantification**

In this thesis, a fully integrated centrifugal microfluidic device for rapid on-site quantification of lipids from microalgal samples. The fully automated serial process involving cell sedimentation and lysis, liquid–liquid extraction, and colorimetric detection of lipid contents was accomplished within 13 min using a lab-on-a-disc. The presented organic solvent tolerable (for n-hexane, ethanol) microfluidic disc was newly fabricated by combining thermal fusion bonding and carbon dot based valving techniques. It is expected that this novel platform will possibly contribute toward sustainable biofuel applications by providing a practical solution for on-site monitoring of lipid accumulation in microalgal samples, thus providing imperative contribution toward energy and environmental purposes of centrifugal microfluidic technology.

### **Determination of natural antioxidants in beverage samples**

In second, fully integrated and automated lab-on-a-disc for the rapid determination of the total phenolic content (TPC) and antioxidant activity (AA) of beverage samples are demonstrated. The simultaneous measurements of TPC and AA on a spinning disc was achieved by integrating three independent analytical techniques: TPC measured using the Folin–Ciocalteu method, AA measured using the 2,2-diphenyl-1-picrylhydrazyl radical (DPPH) and the ferric reducing antioxidant power methods. The TPC and AA of 8 different beverage samples, including various fruit juices, tea, wine and beer, were analyzed. Unlike conventional labor-intensive processes for measuring TPC and AA, our fully automated platform offers one-step operation and rapid analysis.

### **Portable device for the future works**

Finally, for future applications of all above, we introduce the portable lab-on-a-disc spinning device. In this device, five wavelength LED & Photodiode for absorbance detection, BLDC motor with encode driver for motion control, rechargeable battery pack for portability, laser actuation for valving and camera module for disc imaging will be integrated.

## CHAPTER 2. Microalgal lipid quantification using lab-on-a-disc

### 2.1 Introduction

Biofuels are considered as an alternative to fossil fuels, as they are renewable and carbon-neutral energy sources. Among other potential resources for biofuel production, microalgae have gained particular attention owing to their inherent advantages such as short growth cycles, high lipid contents, and relatively small cultivation area requirements. For example, microalgae proliferate rapidly and can double their population within 12 hours, producing as much as 800-times more oil than other crops from the same cultivation area. In addition, they can produce oil even on unfavorable land and in saline water, which resolves the issue of competing food and fuel production requirements.<sup>111</sup>

Despite these advantages, many challenges remain.<sup>112</sup> Microalgal lipid contents usually depend on various culture conditions such as temperature, light intensity, pH, culture time, and the nature of the culture medium. Therefore, there is a demand for research that identifies optimal microalgal culture conditions to achieve maximum oil production. On-site monitoring tools would be useful for determining the best harvest time and optimizing mass production of microalgal oil by quantifying lipid contents in a real-time manner. However, conventional lipid quantification is complicated and time consuming (> 5 hours per sample), and involves a series of processes such as pre-concentration from the cell medium, drying, cell lysis, lipid extraction, and quantification. Moreover, the process also requires a large sample volume (~200 mL per sample), expensive equipment, and energy- and labor-consuming liquid extraction steps.<sup>113</sup>

### 2.2 Previous studies of microalgal lipid quantification on microfluidics

Recently, microfluidic platforms have been actively used in biofuel applications.<sup>38-40</sup> However, most of the previous studies have focused mainly on biofuel production at the single-cell level, based on culture in the confined space of microchambers under controlled light<sup>53</sup> and stress<sup>60</sup> conditions. Previously, lipid contents in single microalgal cell in alginate droplets was analysed by fluorescent staining, which only verified comparative heterogeneity under viable conditions.<sup>55</sup> Thus, a practical approach is required for a rapid, automated method for quantification of lipids from microalgae grown in larger scales under moist conditions, which does not require drying or heating steps and performs well at room temperature and under ambient pressure.

Centrifugal microfluidic platform was first introduced by Oak Ridge National Labs (ORNL) in 1960s and further developed by Gamera<sup>12, 114</sup> as an advanced sample-to-answer system. As shown in the recent comprehensive reviews,<sup>11, 86</sup> the lab-on-a-disc have been actively utilized for various biomedical purposes such as automated blood analysis, immunoassays, and disease diagnostics.<sup>2, 87, 115</sup> In our previous examples of studies, the employed format utilizes centrifugal pumping force and valves controlled by remote laser activation.<sup>13</sup> In principle, the centrifugal microfluidic technology may be extended to energy and environmental studies<sup>5</sup> for rapid on-site monitoring of microalgal lipid production by facilitating serial lipid extraction in organic solvents and quantification processes.<sup>116</sup>

Here, we have developed a rapid and fully automated on-site method for quantifying microalgal lipids. The method is an intensified process involving pre-concentration and lysis of wet cells, extraction, and optical detection of lipids using a lab-on-a-disc device that is tolerant of organic solvents (n-hexane and ethanol). In this study, repeated lipid extractions employed a mixture of n-hexane and ethanol, followed by on-chip quantification of lipid accumulation in microalgae using colorimetric detection. Intriguingly, the entire process was completed within 13 min with 500  $\mu$ L of microalgae sample cultivated under various conditions.

## 2.3 Development of essential techniques

### 2.3.1 n-Hexane solvent resistive lab-on-a-disc platform

Despite the great advantages of lab-on-a-disc including fast, cost-effective and simple operation in biological and environmental application, the use of lab-on-a-disc has been limited to aqueous solution because of the poor organic solvent compatibility. Most of prototype lab-on-a-disc was assembled using organic solvent incompatible adhesives, and some of them use the organic solvent incompatible ferrowax as a sacrificial valve. Here, we present a hexane compatible lab-on-a-disc composed of solvent resistive bonding and valving technique to expand the application of lab-on-a-disc to organic solvent based chemical engineering problems such as microalgal lipid extraction. For solvent resistive bonding, adhesive-free thermal fusion assembling (TFA) was used for assembling the disc components. TFA is a process which fuses more than one material via hot embossing. For solvent resistive valving technique, a thin thermoplastic film with laser printed carbon dots were inserted and bonded between top and bottom discs. The carbon dots absorb the laser energy and melt the underline thermoplastic film substrate, thereby open the fluidic passage. The similar valving technique was previously demonstrated but it was not compatible with organic solvents because it used the solvent incompatible adhesives to assemble the microfluidic device.<sup>1</sup> To the best of our knowledge, this is the first report of n-hexane

compatible lab-on-a-disc by using TFA and laser printed carbon dots valves together. We expect that our new lab-on-a-disc platform can be applied for more applications required organic solvent compatibility.

## 2.4 A fully integrated lab-on-a-disc for microalgal lipid quantification

### 2.4.1 Experimental details

#### Disc design and fabrication method

As shown in **Figure 2.1A**, each disc has five identical units for microalgal lipid extraction, each starting from a 500  $\mu\text{L}$  minimum microalgal sample. Each unit is composed of chambers for sample injection, metering, detergent storage, lipid extraction, lipid collection, lipid dye, and waste storage. The disc is fabricated by bonding four layers, as shown in **Figure 2.2**. The top layer (1 mm thick) contains a sample flow channel, inlets, and vent holes. The middle polycarbonate (PC) film (0.125 mm thick) has a carbon pattern for valving purposes. Upon laser irradiation, the carbon dot areas are punctured, allowing liquid to flow through. The middle plate (5 mm thick) contains chambers to store samples and reagents. The chambers, channels, inlets, and vent holes were cut into the PC plate using a computer numerical control (CNC) milling machine (3D Modeling Machine; M&I CNC Lab, Korea). Finally, the bottom layer (1 mm thick) was bonded to the middle layer to provide an optically clear surface for colorimetric quantification. The optical path length was fixed at 5.125 mm, equal to the thickness of the middle layer and the PC film.

#### Disc layout

A detailed layout of the disc components is shown in **Figure 2.2**. The disc is fabricated by bonding four different polycarbonate (PC) layers: a top layer, a middle film, a middle layer, and a bottom layer. There are inlet and vent holes in the top layer (1 mm thick), and carbon dots for valving are printed on the middle film (0.125 mm thick). Sample and reagent chambers are prepared in the 5-mm thick middle layer. The bottom layer (1 mm thick) supports the middle layer and provides a transparent window for colorimetric detection of the microalgal lipids.

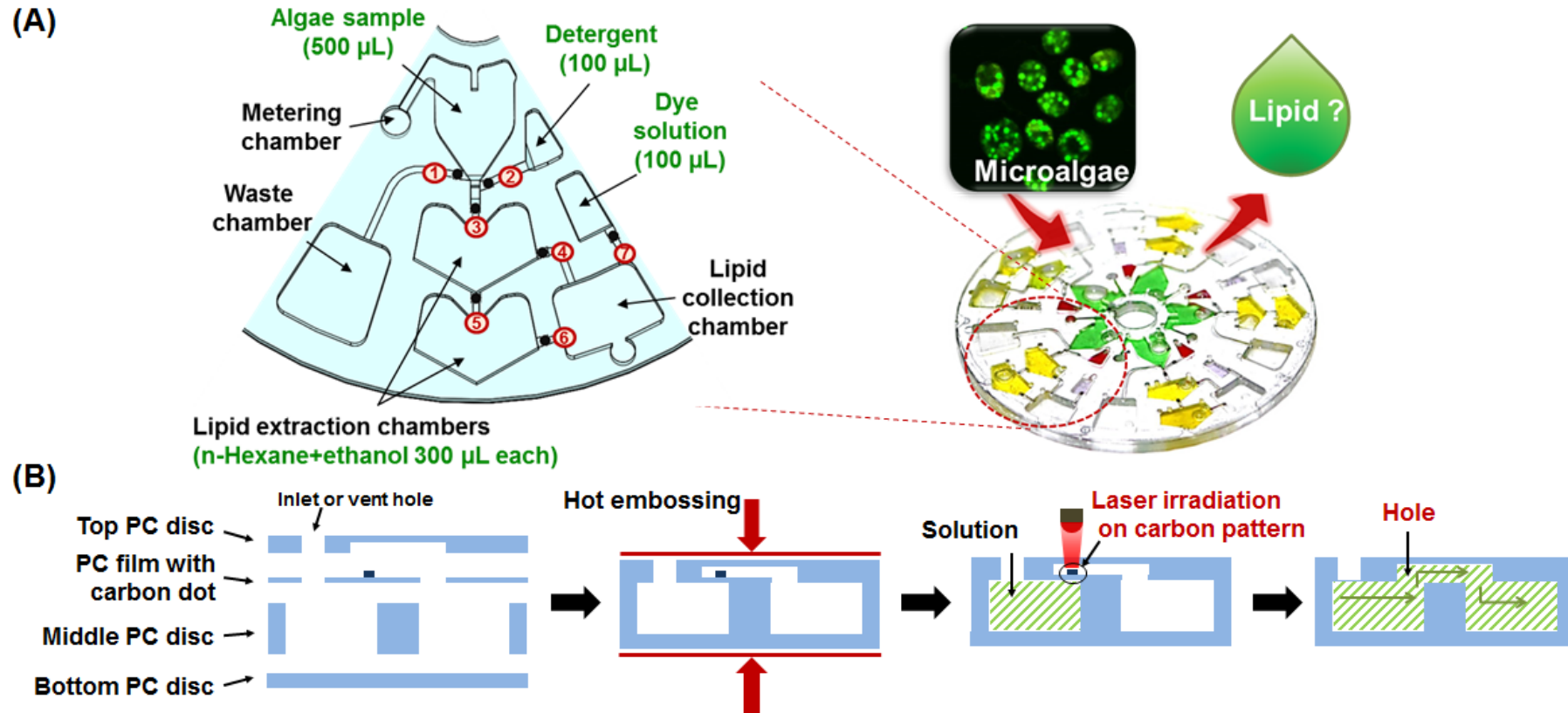


**Figure 2.1.** Schematic illustration of (A) a lab-on-a-disc for microalgal lipid quantification, and (B) the thermal fusion assembly technique and laser-irradiated carbon-dot valves.



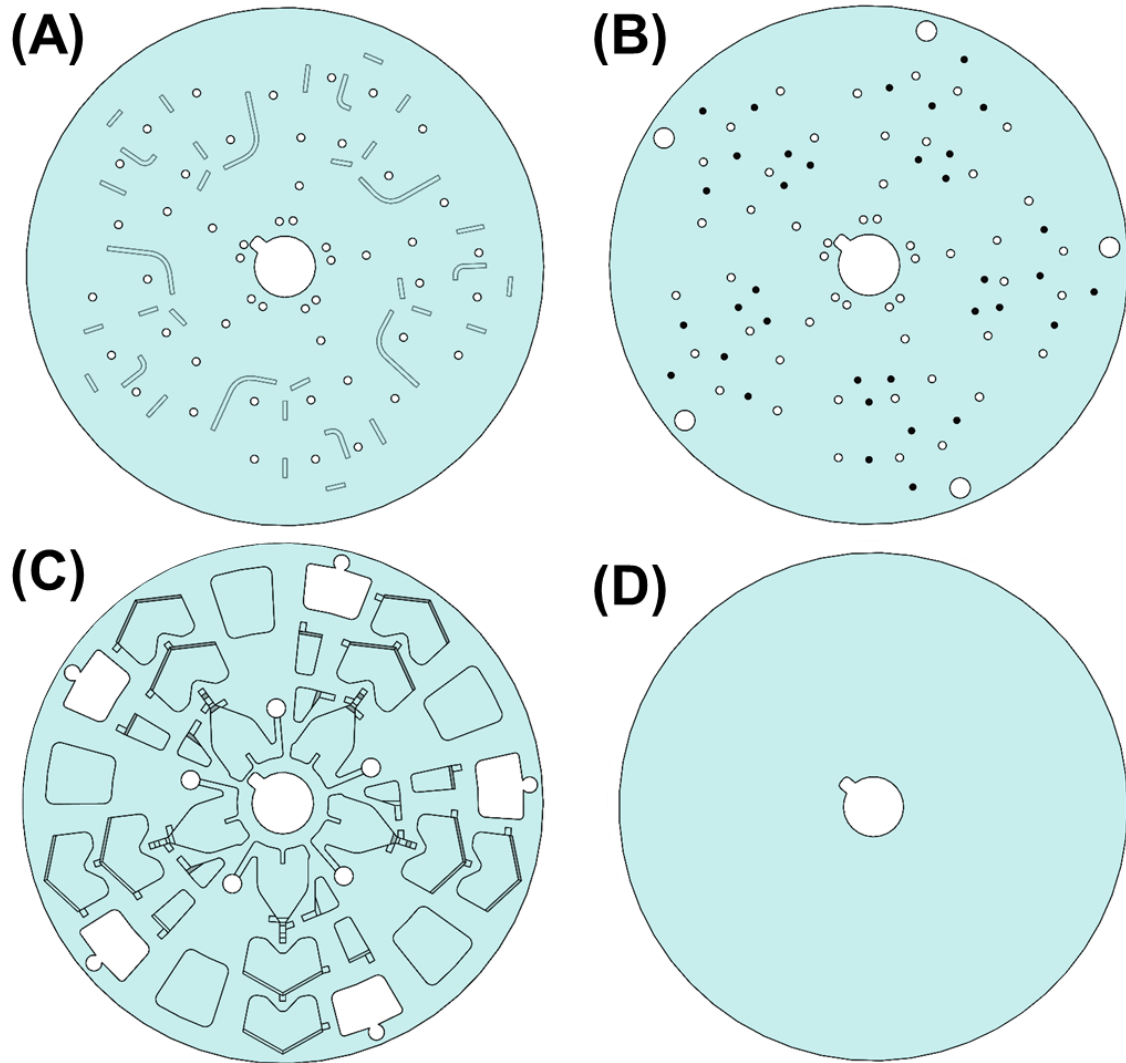


**Figure 2.2.** The layout of the four layers of a lab-on-a-disc. (A) Top layer containing sample inlet holes, vent holes, and flow channels. (B) Polycarbonate (PC) film (0.125 mm thick) containing carbon dot patterns, inlets, vent hole, and open holes for optical detection. (C) Middle layer (5 mm thick) containing sample and reagent chambers. (D) Bottom layer (1 mm thick). The diameter of the disc is 120 mm.

All layers were assembled using the thermal fusion assembly technique shown in **Figure 2.1B**. No leakage was observed even when the discs were operated at spin speeds as high as 6,000 rpm. Laser-irradiated carbon dot valves were employed because the previously used ferrowax valves<sup>13</sup> are not solvent-tolerant. Carbon dots were prepared on the surface of the PC film using a laser printer (DocuCentre-IV C2263, Fuji Xerox Co. Ltd., Japan) and were irradiated using a BS808T2000C-MOUNT laser diode (Best-Sources Industry (HK) Co. Ltd., China).

### **Disc operation procedure**

The detailed procedure of the disc operation is summarized in **Table 2.1**. First, 500  $\mu\text{L}$  of the microalgae sample was measured, the excess sample was discarded, and the microalgae cells were allowed to form a sediment. The supernatant was then removed to the waste chamber. The lysis buffer was added to the microalgae sediment and subsequently transferred to the extraction chamber. For lipid extraction, the disc was operated in shaking mode at 6 Hz with a  $\pm 5^\circ$  angle. The lipid-containing solution was transferred to the collection chamber and the remaining microalgae residue was transferred to the next extraction chamber. The extraction step was repeated once more and the lipid-containing solution was transferred to the lipid collection chamber. After evaporating the solvent in vacuum, the lipid dye solution was added to the collection chamber. Finally, the absorbance was measured using a fiber-coupled spectrometer. A detailed description of the experimental set-up is provided in **Figure 2.3**.

**Table 2.1.** Spin program used for microalgal lipid quantification on a disc.

Step	Spin speed (rpm)	Time	Operation
1	6,000	2 min	The microalgal sample is measured and the cells form a sediment in the bottom of the channel.
2	3,000	10 sec	Valve #1 is opened to remove the supernatant to the waste chamber.
3	3,000	15 sec	Valves #2 and #3 are opened to transfer the lysis buffer to the microalgae sediments and the microalgae lysate into an extraction chamber, respectively.
4	shaking	2 min	The disc is shaken for liquid-liquid extraction.
5	3,000	10 sec	Valve #4 is opened to transfer the lipid-containing solution to the collection chamber.
6	3,000	5 sec	Valve #5 is opened to transfer the lysate residues to the 2nd extraction chamber.
7	Shaking	2 min	The disc is shaken for liquid-liquid extraction.
8	3,000	5 sec	Valve #6 is opened to transfer the lipid-containing solution to the collection chamber.
9	1200	3 min	Solvent is evaporated under vacuum.
10	3,000	10 sec	Valve #7 is opened to transfer the lipid dye to the lipid collection chamber.
11	± 3,000	3 min	The absorbance is measured.
<b>Total Time</b>		<b>~ 13 min</b>	

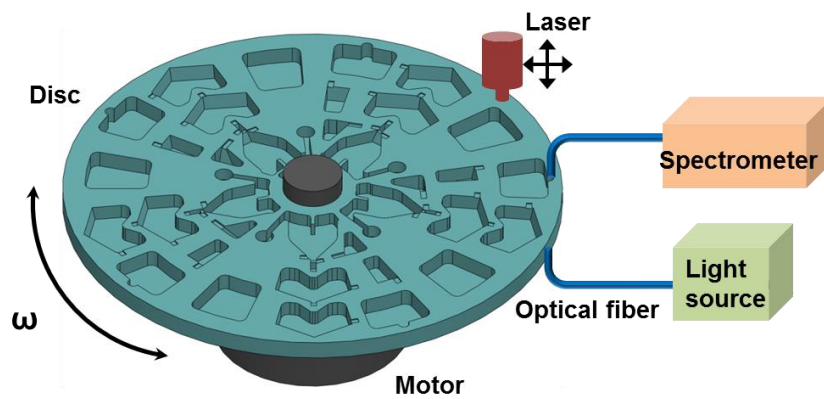
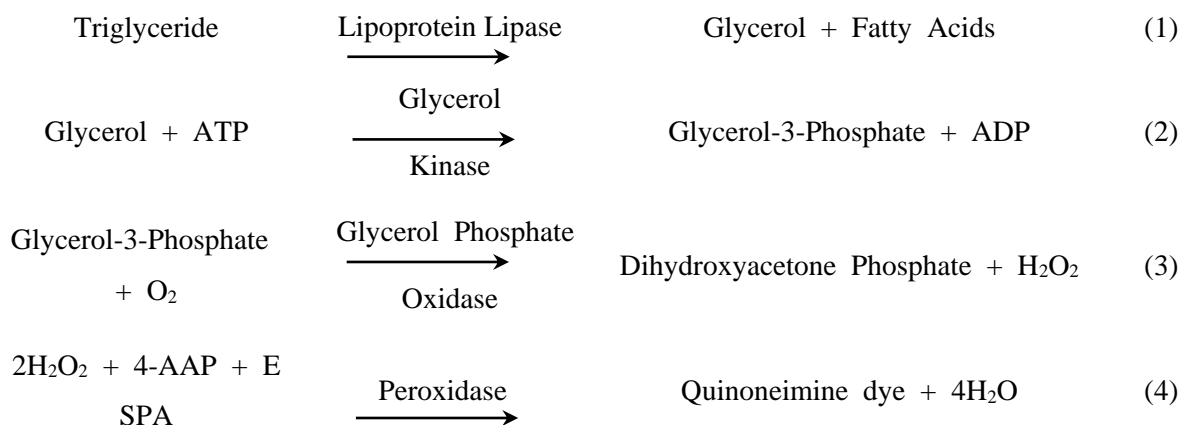


**Figure 2.3.** Experimental set-up for microalgal lipid detection on a disc. The motor for rotating the disc, the laser to irradiate the carbon dot, the portable spectrometer, the optical fiber, and the light sources are integrated into our experimental set-up.

### Quantification of lipid concentrations by measurement of absorbance

Extracted microalgal lipids (triglycerides) were quantified using a triglyceride colorimetric assay kit (Cayman Chemical Company, USA). The enzymatic hydrolysis of lipids by a lipase generates glycerol and free fatty acids. The released glycerol was measured using a three-step enzymatic reaction as follows. The glycerol formed in reaction (1) was phosphorylated to glycerol-3-phosphate by glycerol kinase catalysis in reaction (2). The glycerol-3-phosphate was then oxidized by glycerol phosphate oxidase to produce dihydroxyacetone phosphate and hydrogen peroxide ( $H_2O_2$ ) in reaction (3). Peroxidase in turn catalyzed the redox-coupled reaction of  $H_2O_2$  with 4-aminoantipyrine (4-AAP) and N-ethyl-N-(3-sulfopropyl)-m-anisidine (ESPA), producing a brilliant purple color in solution (4).



The absorbance of the produced quinoneimine dye was measured at 540 nm using an optical fiber-coupled MAYA2000 Pro spectrophotometer (Ocean Optics, Inc., USA). The results of the colorimetric assays were used to quantitate lipid production by interpolation with a calibration curve generated using triglyceride lipid standards (Cayman Chemical Company), as shown in **Figure 2.4**.

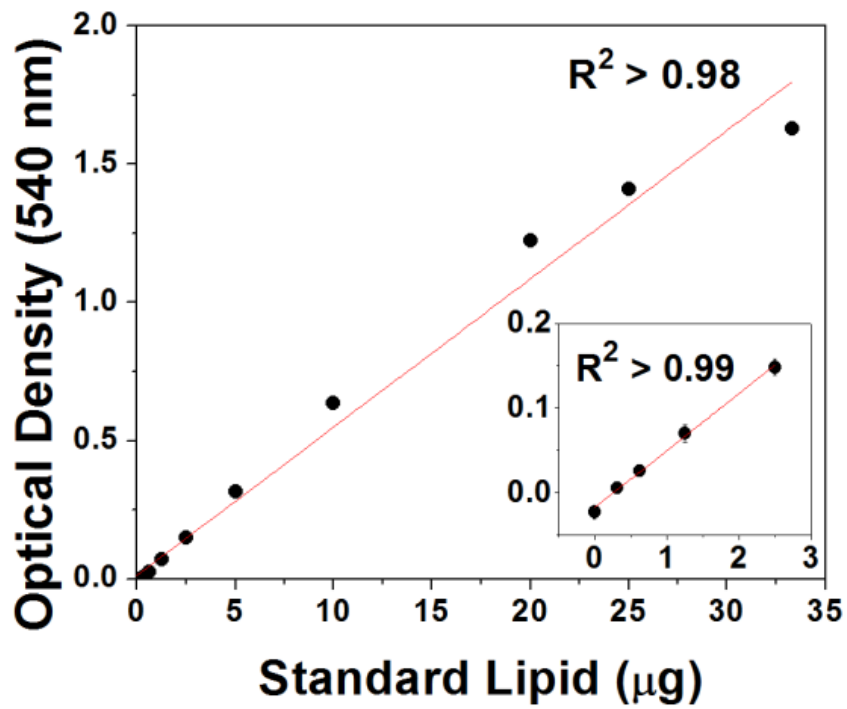


**Figure 2.4.** Calibration curve for the amount of lipid standards with the resulting quinoneimine absorbance at 540 nm. Each data point derives from three repeated experiments ( $n = 3$ ).

### Cell culture and optimization of microalgal lipid extraction protocol

In this works, *Chlamydomonas reinhardtii* which mostly used in microalgae research was used.<sup>117</sup> *Chlamydomonas reinhardtii* strains cc125 (wild-type mt+) and cc503 (mutation-type cw92 mt+) were grown photoheterotrophically at 25°C in T75 flasks containing 50 mL of standard Tris/acetate/phosphate (TAP) medium<sup>118</sup>, as shown in **Figure 2.5A** (the image was taken using a Nikon Eclipse 80i, Japan).

Cells were harvested by centrifugation at 97.24 relative centrifugal force (RCF) (1,200 rpm, rotor GAM-1.5-12) for 3 min. For lipid accumulation and lipid monitoring experiments, microalgal cells (cc125 and cc503) were cultured under different nutrient-depletion conditions, such as nitrogen<sup>119</sup>, acetic acid<sup>120</sup>, or iron depletion.<sup>121</sup> After harvesting, the microalgae were lysed in 100 µL 10% 3-[(3-cholamidopropyl)dimethylammonio]-1-propanesulfonate (CHAPS) lysis buffer (Amresco, USA), without additional mixing. N-hexane and ethanol for solvent extractions were purchased from Samchun Pure Chemical Co., Ltd. (Korea).

Microalgal cell culture growth was measured by hemocytometry (Marienfeld Superior, Germany) and absorbance measurement at 750 nm. **Figure 2.3** shows a correlation curve plotting optical densities versus microalgae populations. Using the correlation curve, microalgae populations were calculated from the optical density measurements and used for the normalization of lipid amount per cell population.

### Gas chromatography - mass spectrometer analysis (GC-MS) for lipid quantification

The extracted microalgal lipid was converted to fatty acid methyl esters (FAMES) by adding methanol and sulfuric acid as a catalyst at 95°C for 1 hour (transesterification). Commercial mixture of fatty acid methyl ester (18917-1AMP, Sigma Aldrich, USA) was used as an internal standard for lipid analysis. After transesterification, deionized water with n-hexane (1:1 ratio) was added to the FAME-containing flask, and the FAME-containing organic phase (n-hexane) was separated from the deionized water by centrifuging at 3,000 rpm for 10 min. The separated FAMES in n-hexane were analyzed by gas chromatography and mass spectrometer (7890A for GC and 5976C for MS, Agilent, USA)

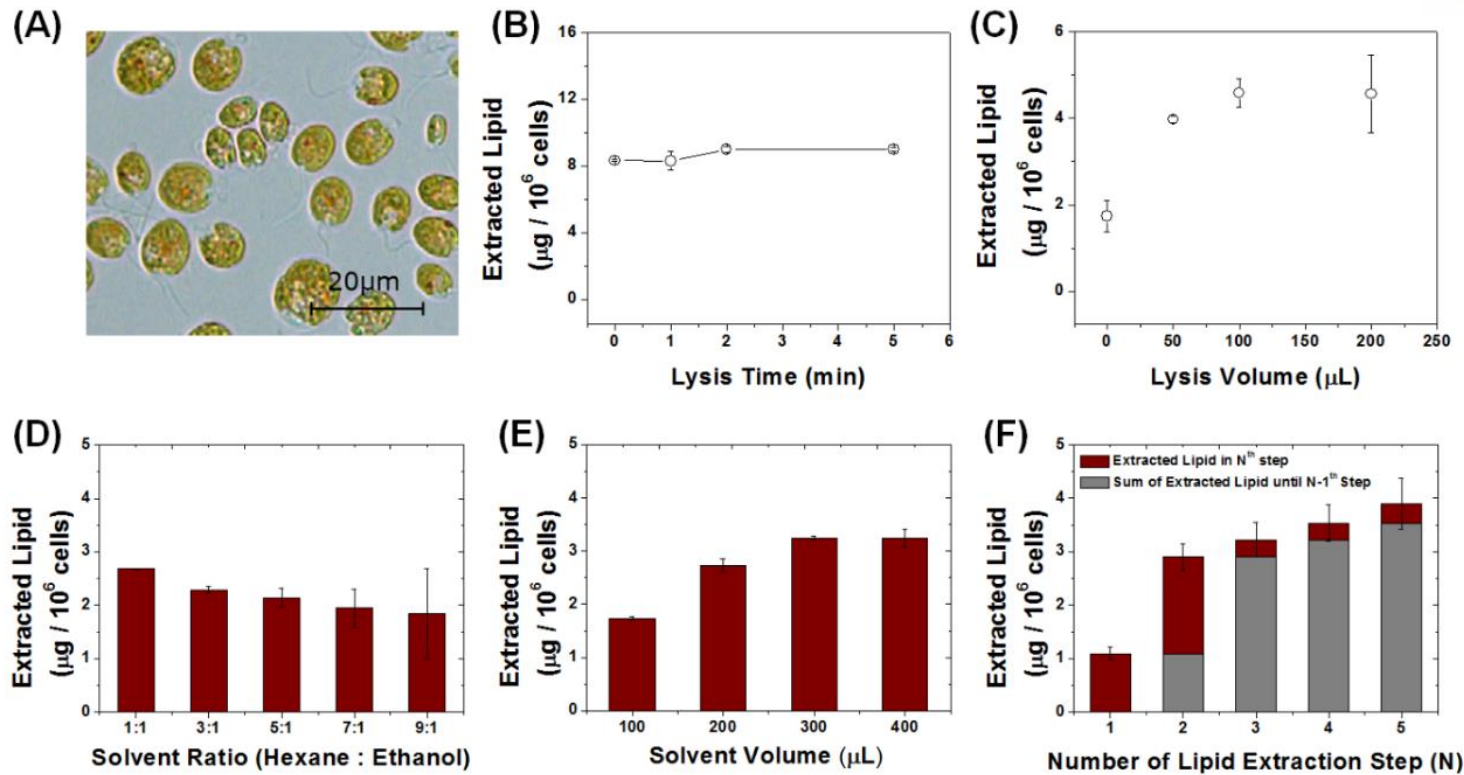


**Figure 2.5.** (A) A bright field image of wild-type microalgal cells (cc125). The effects of lysis time (B) and volume of lysis buffer (C) on microalgal lipid extraction efficiency. The number of microalgal cells (cc125 in 500 µL) used to study the effects of lysis time and buffer volume were  $1.43 \times 10^6$  cells and  $1.22 \times 10^6$  cells, respectively. The extraction efficiency of microalgal lipids at different solvent ratios (D), solvent volumes (E), and numbers of extraction steps (F) were compared. Microalgae cells (cc125;  $0.91 \times 10^6$  cells in 500 µL) were used for the experiments reported in (D)–(F). For experiments reported in (B), (C), and (F), 300 µL of 1:1 (n-hexane: ethanol) solvent was used. Data point represents the average of three repeated experiments ( $n = 3$ ).



### **Measurement of microalgal populations by determining their optical densities**

Microalgae populations were measured by determining their optical densities at 750 nm using an optical fiber-coupled MAYA2000 Pro spectrophotometer (Ocean Optics, Inc., USA). First, by diluting the microalgal sample (1/2 serial dilution), microalgal suspensions of various densities were prepared, and the population of each sample was measured using a hemocytometer (Marienfeld Superior, Germany). The optical density of each sample was also measured simultaneously with a spectrophotometer. **Figure 2.6** shows an example of a correlation curve plotting optical densities versus microalgal populations. Using the correlation curve, microalgae populations were measured directly on a disc and the amount of extracted lipid was normalized to the cell population ( $10^6$  cells).

### **Experimental set-up**

The experimental set-up is shown in **Figure 2.3**. The lab-on-a-disc device was mounted on a programmable spinning motor. The laser-irradiated carbon dot valves could be selectively melted and opened by a laser diode (Best-Sources Industry (HK) Co. Ltd., China). Colorimetric detection of target analytes was conducted using an optical fiber-coupled spectrometer (MAYA2000 Pro, Ocean Optics, FL, USA)

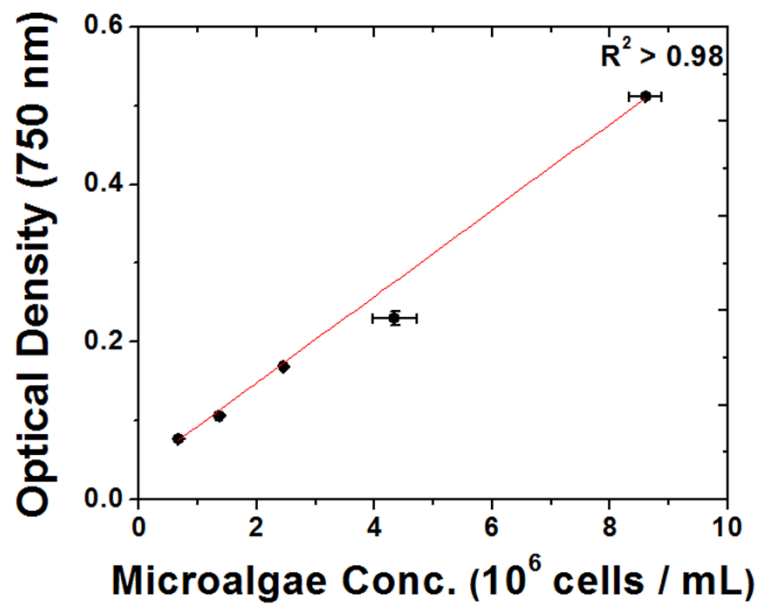


**Figure 2.6.** Correlation curve of microalgae densities (strain cc125) and optical densities at 750 nm.

## 2.4.2 Results and discussion

### Optimization of lipid extraction condition

The experimental conditions for lipid extraction were optimized prior to the development of lab-on-a-disc. The effect of the lysis time on the amount of extracted lipid obtained was marginal (**Figure 2.5B**), indicating that an initial lysis for 1 min was sufficient to release internal lipids by cell wall disruption. The amount of extracted microalgal lipid increased as the volume of lysis buffer used increased. One hundred microliters of 10% CHAPS lysis buffer was selected as the optimal volume (**Figure 2.5C**).

The mixing ratio of the n-hexane/ethanol solvent, the extraction volumes, and the number of lipid extraction steps were investigated to optimize the lipid extraction protocol from cc125 cells (**Figure 2.5D–2.5F**). Note that a mixture of n-hexane and ethanol was chosen because it has low toxicity and a similar lipid extraction efficiency to other solvent mixtures, such as chloroform and methanol.<sup>122</sup> The 1:1 mixture of n-hexane and ethanol was found to maximize the efficiency and reproducibility of lipid extraction compared with the extraction efficiencies of other ratios tested on the microalgal strain (cc125). As shown in **Figure 2.5D**, a solvent mixture with a higher ethanol content can extract more polar lipids and can more easily penetrate cell walls, making neutral lipids such as triglycerides more available for n-hexane, which is a non-polar solvent. Note that the mixed solvent with low ethanol fraction caused the reduced extraction efficiency, resulting in the less reproducible extraction yields with high experimental error. Moreover, during optimization experiments, twice-sequential repeated extractions using each 300  $\mu\text{L}$  of solvent showed optimum lipid extraction rates with minimal waste of chemicals and time (**Figure 2.5E** and **2.5F**). All the experiments in **Figure 2.5** were carried out manually.

### Disc operation procedure

Schematic illustrations of sequential cell pelleting and direct lysis of the wet cell pellet for extraction of microalgal lipids are shown in **Figure 2.7**, with corresponding images captured from a movie recorded using a charge-coupled device (CCD) camera. First, an excess amount of microalgae sample (cell population:  $\sim 10^6$  cells) was introduced into the lab-on-a-disc and transferred into the metering chamber to measure 500  $\mu\text{L}$  of the sample (**Figure 2.7A**). Subsequently, microalgal cells were quickly subjected to sedimentation by spinning at 6,000 rpm for 2 min to minimize the water content of the cell residue (total volume was reduced to 24  $\mu\text{L}$ ) (**Figure 2.7B**), and the supernatant medium was removed to the waste chamber by opening valve #1. The transfer of the lysate towards the extraction chamber containing 300  $\mu\text{L}$  of the

organic solvent mixture was then performed by controlling valves #2 and #3 and spinning the disc at 3,000 rpm (**Figure 2.7C**).

Liquid-liquid extraction was conducted by shaking the disc at 6 Hz at a 10° tilting angle for 2 min (**Figure 2.7D**). The lysate showed phase separation due to density difference and the extracted lipid solution was collected in the neighbor chamber through valve #4, which was designed so that the supernatant could be selectively transferred into the collection chamber (**Figure 2.7E**). The second extraction was performed in the next chamber by repeating the afore-mentioned process (**Figure 2.7F** and **Figure 2.7G**). After collecting the extracted lipid solution, solvent evaporation was achieved by applying a vacuum for 3 min at 1,200 rpm to obtain solvent-free lipid contents. Finally, microalgal lipids in the form of triglycerides were quantified by *in situ* measurement of absorbance at 540 nm after treatment using a colorimetric assay kit, which was accomplished within 3 min (**Figure 2.7H**).

### Quantification of microalgae population

Quantification of microalgae population ( $\sim 10^6$  cells) was carried out using a correlation curve between the microalgae population and the optical density at 750 nm (obtained at high linearity ( $R^2 > 0.98$ )), as shown in **Figure 2.6**. It is noteworthy that the entire process from sample loading to lipid quantification took only 13 min, which demonstrates a significant reduction compared with conventional manual chromatography-based processes that take approximately 5 hours. The spin program for continuous procedure of microalgal lipid quantification is summarized in **Table 2.1**

### Calibration curves

As shown in **Figure 2.8A**, the fidelity of the integrated microalgal lipid quantification using our lab-on-a-disc had a highly linear relationship ( $R^2 > 0.98$ ) when microalgal lipids were measured as a function of microalgae cell concentration. Note that there was no pre-treatment of the microalgae samples used in our device. In **Figure 2.8A**, our device shows a broad dynamic range (0–30  $\mu\text{g}$ ) of quantified microalgal lipid accumulation from the unprocessed microalgae sample. Extraction efficiency was not significantly affected by microalgae population within  $1.4 \times 10^6$  cells/mL to  $8.0 \times 10^6$  cells/mL. Additionally, the alternative microalgae strain (cc503, wall-less) revealed a similar result (**Figure 2.9A**) suggesting that the presence of cell wall does not have significant impact on the microalgal lipid extraction efficiency.

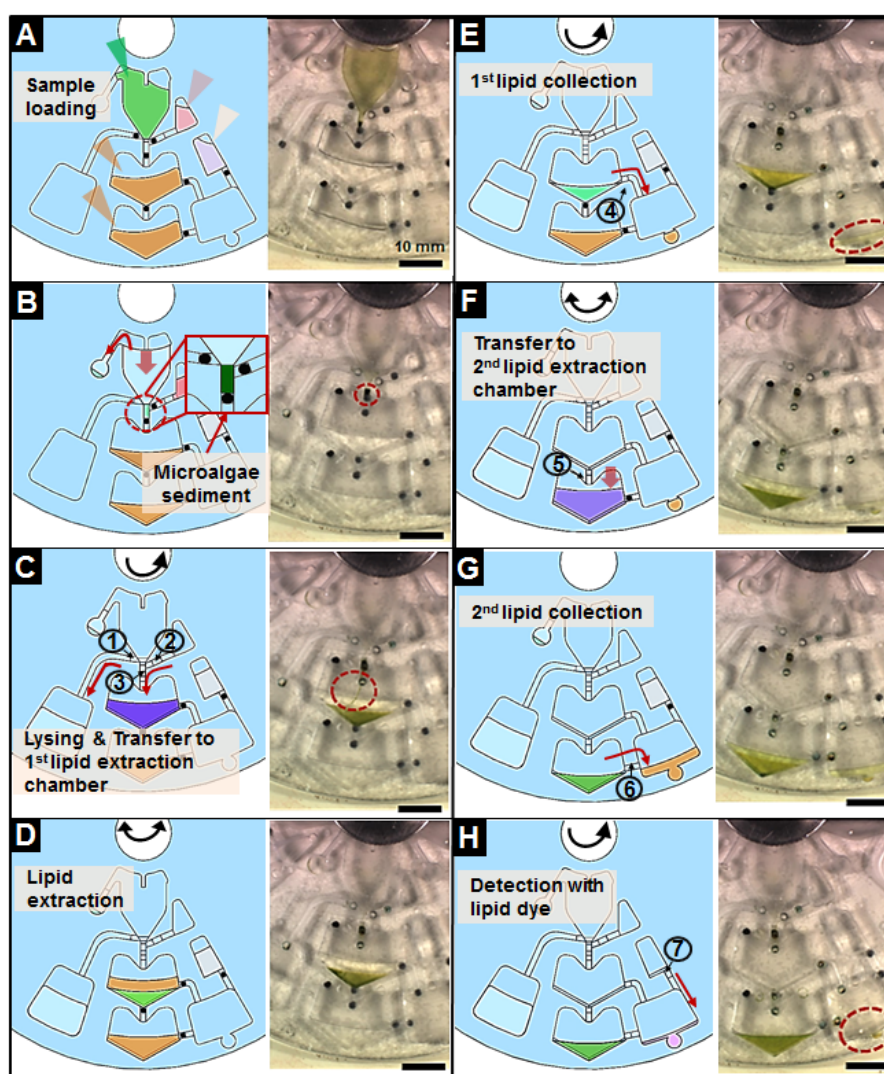


**Figure 2.7.** Illustration of the processes used to quantify microalgal lipids on a disc. (A) Microalgal sample (strain cc125) was loaded onto the disc, the excess sample was transferred to the metering chamber, and 500  $\mu\text{L}$  of microalgal sample was metered. (B) After spinning at 6,000 rpm to sediment the microalgal cells, (C) valve #1 was opened to discard the supernatant into the waste chamber. Then, valve #2 was opened to add 100  $\mu\text{L}$  of lysis buffer to the microalgae sediments. Subsequently, valve #3 was opened to transfer the microalgae lysate into an extraction chamber containing 300  $\mu\text{L}$  of solvent to extract the lipid. (D) The disc was shaken for liquid-liquid extraction, and the microalgal lipids were extracted. (E) The lipid-containing solution was transferred to the lipid collection chamber after valve #4 had been opened. A phase separation between the solvent and microalgal lysate occurred owing to the different densities. The position of the valve was designed so that the solvent could selectively transfer into the collection chamber. (F) One more step of lipid extraction and (G) collection was repeated by opening valves #5 and #6. (H) Finally, the solvent was evaporated and the lipid dye was transferred to the lipid collection chamber by opening valve #7. The absorbance at 540 nm was measured using an optical fiber-coupled spectrometer (MAYA2000 Pro, Ocean Optics, FL, USA) to quantify the microalgal lipids.

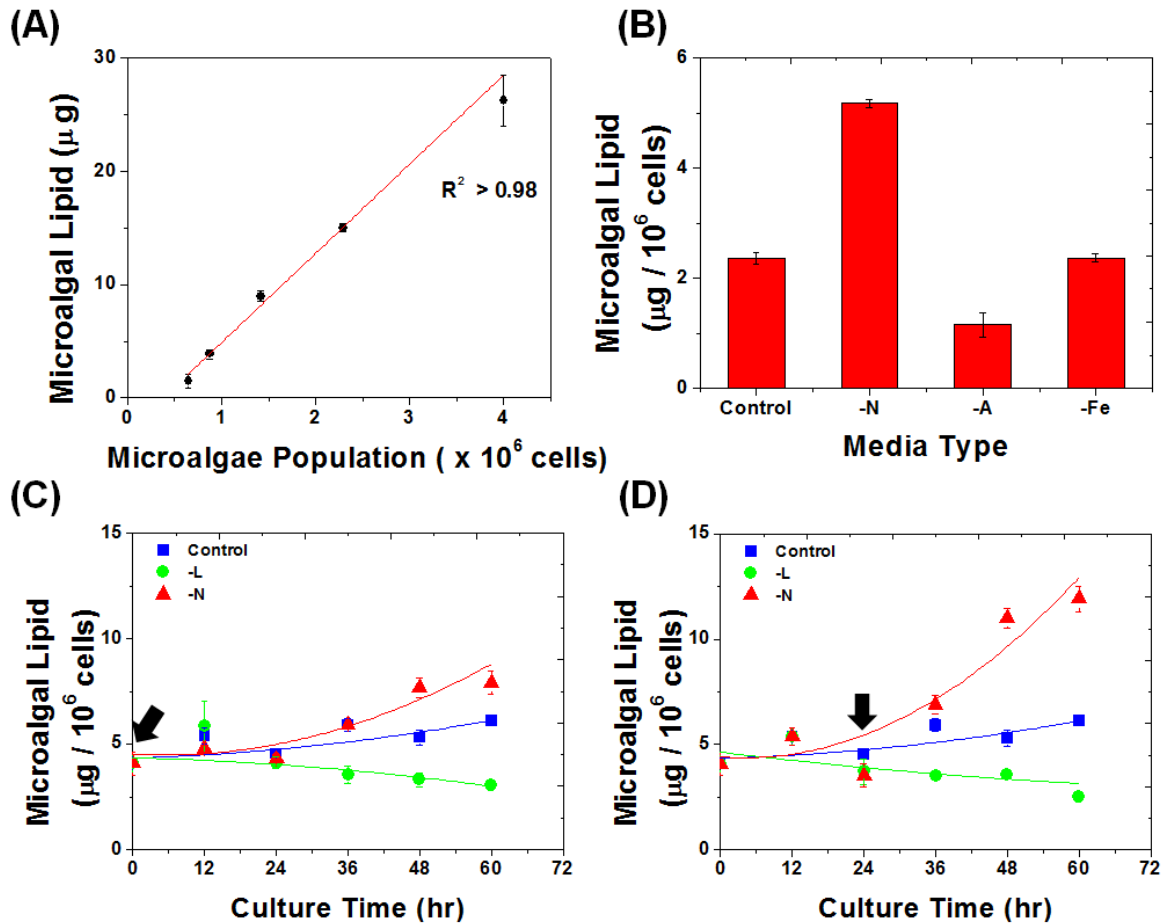


**Figure 2.8.** (A) Calibration curve between different microalgal (strain cc125) concentrations and microalgal lipid levels measured using the lab-on-a-disc. (B) Lipid accumulation in microalgae (strain cc125) cultured in different media. Control, complete media; -N, nitrogen-deficient media; -A, acetate-deficient media; -Fe, iron-deficient media. (C) Microalgal lipid accumulation in  $10^6$  cells (strain cc125) was monitored for 3 days under two different conditions of stress: -N by changing the media to that lacking nitrogen, and -L by blocking light. Control cultures were grown under normal culture conditions. Stress conditions were applied immediately after seeding or (D) after 24 hours of growth. Each point derives from three repeated experiments ( $n = 3$ ).

### Microalgal lipid quantification using lab-on-a-disc for various culture conditions

It is known that several microalgae species show enhanced lipid production under certain nutritional deficiencies to attain higher bio-oil productivity.<sup>123</sup> Here, three kinds of nutrient stress condition, nitrogen-deficient medium (-N), acetate-deficient medium (-A), and iron-deficient medium (-Fe), were tested to ascertain their effects on lipid accumulation. As shown in **Figure 2.8B**, microalgae (cc125, wild-type) cultured in -N showed higher lipid accumulation compared with microalgae cultured in -A, -Fe, or a control medium. Compared with the control, the subsection of microalgae to -N, -A, or -Fe media showed differences in lipid production of 119, -51, and -0.2%, respectively, which is consistent with previous results.<sup>112</sup> In addition, the alternative microalgae strain (cc503, wall-less) revealed a similar trend under the three different nutrient stress conditions (**Figure 2.9B**).

Moreover, the rapid lipid quantification method was utilized for on-site monitoring of lipid accumulation as a function of stress onset time during 3 days of culture. Lipid amount was quantified after the exposure of microalgae to either nutrient- (-N) or light- (-L) deficient stress. As shown in **Figure 2.8D**, the microalgae in -N showed dramatically increased lipid accumulation with 3.2 times higher lipid contents compared with the control when the stress was applied after 24 hours of culture. A similar observation was made when -N stress was applied at the beginning of the 3-day culture period (**Figure 2.8C**). However, the amount of lipid accumulated was considerably reduced owing to the retarded growth. These results indicate that high lipid production induced by stress is accompanied by slow growth rates and low cell counts, which ultimately affect the total biomass and lipid productivity. In the case of microalgae in the -L condition, blocking light either after 24 hours of growth or immediately after seeding resulted in a lowering of lipid accumulation in both the cases and the controls (**Figure 2.8C & Figure 2.8D**). These results are consistent with the previous observation that light-deficient stress induces formation of polar lipids (unsaturated fatty acids) in the cell membrane, whereas light-abundant stress increases levels of neutral storage lipids, mainly triglyceride, with a simultaneous decrease in polar lipid contents.<sup>124</sup>

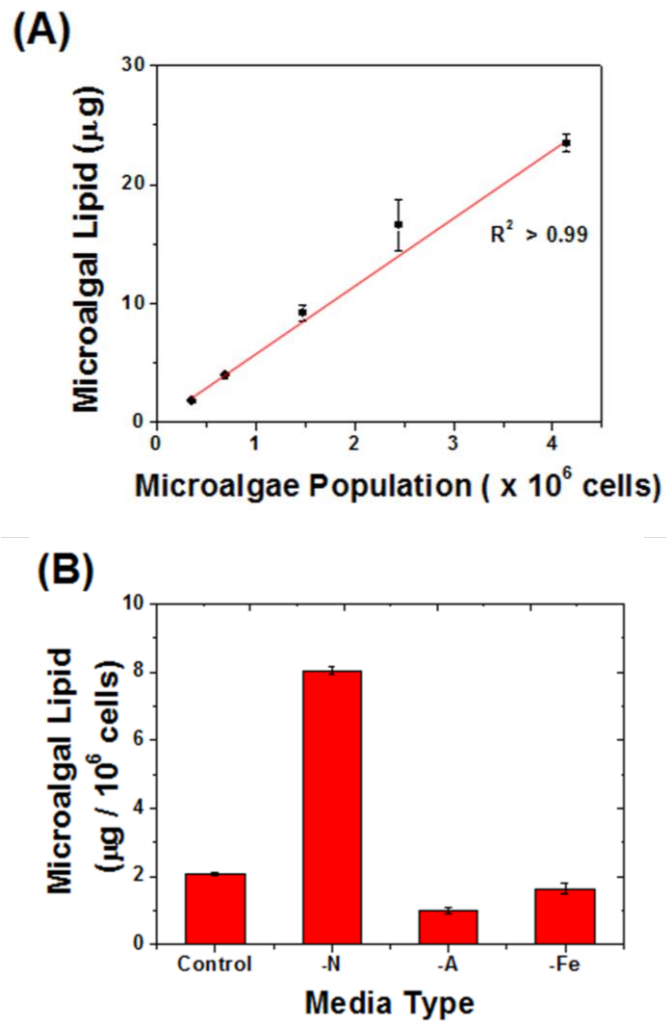


**Figure 2.9.** (A) Calibration curve between different microalgal (strain cc503) densities and microalgal lipid levels measured using the lab-on-a-disc. (B) Lipid accumulation in microalgae (strain cc503) cultured in different media. Control, complete medium; -N, nitrogen-deficient medium; -A, acetate-deficient medium; -Fe, iron-deficient medium.



As shown in **Figure 2.10A**, the quantity of microalgal lipid obtained by manual extraction was comparable to that automatically prepared using the lab-on-a-disc. Furthermore, the microalgal lipid quantified by the simple colorimetric detection method proposed was compared with the data measured by conventional GC-MS. As shown in **Figure 2.10B**, there is a highly linear correlation suggesting that the fully automated lab-on-a-disc using simple absorbance-based detection can provide microalgal lipid quantification that is as accurate as the conventional GC-MS methods, which require time-consuming and complex manual procedures. However, the relative error in the measured microalgal lipid amounts was high especially at low concentration of microalgae samples. This might be due to the handling errors in sample preparation steps and the contribution from other lipids in GC-MS detection.

### **Comparison of the microalgal lipid quantification by colorimetric detection and GC-MS**

Two microalgal lipid detection method; TG-based colorimetric detection and GC-MS, were compared in detail. As shown in **Figure 2.10**, two methods provide a good correlation. However, the relative error in the quantification is not small especially at low concentration of microalgae samples as shown in **Figure 2.11**. We believe this discrepancy stems from the differences in the detection mechanism and the level of complexity in the sample preparation steps. The TG-based absorbance detection method is only measuring TG without prior sample preparation step. Therefore, the error bar is much smaller than GC-MS but the total lipid amount might be smaller. The lipid amount measured by GC-MS contains not only TG but also other lipids. In the solvent extraction method using hexane and ethanol mixture, it is reported that more than 80 % of the lipid compositions in the extracted lipid is TG.<sup>116</sup> Even if TG might be the most dominant fraction, the small portion of other lipids may also affect the final results. Furthermore, we believe the complicated sample pretreatment steps from transesterification to FAMES purification in GC-MS detection cause handling errors and therefore affect the relatively large error bars in our GC-MS experiments.

### **Lipid quantification of the cc503 microalgae strain**

A microalgae strain (cc503, wall-less) was cultured under nutrient deficiencies: nitrogen-deficient medium (-N), acetate-deficient medium (-A), iron-deficient medium (-Fe), or control medium, as shown in **Figure 2.9**.

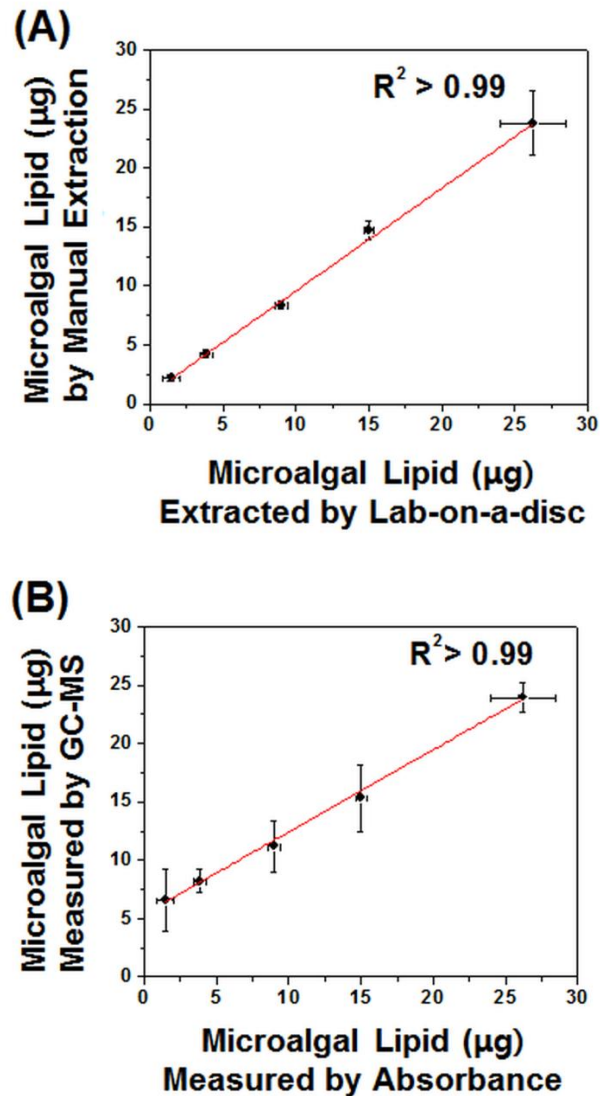


**Figure 2.10.** Correlation curves (A) to compare the microalgal lipid (strain cc125) extracted by lab-on-a-disc and by a manual process, and (B) to demonstrate the correlation of the microalgal lipid amounts measured by colorimetric assay and by gas chromatography - mass spectrometer (GC-MS) analysis. Each point derives from three repeated experiments ( $n = 3$ ).

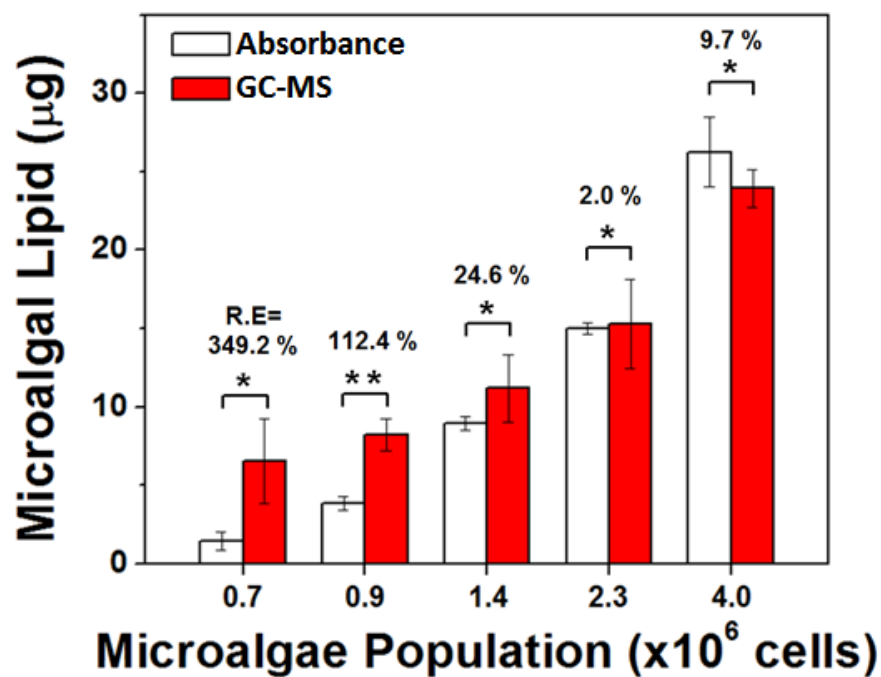


**Figure 2.11.** Comparison of the microalgal lipid amount measured by absorbance detection and GC-MS (microalgae strain: cc125). Data represent mean  $\pm$  standard deviation of three independent experiments. R.E represents relative errors between two methods. \* $P > 0.05$  and \*\* $P < 0.05$ .

### 2.4.3 Conclusions

We demonstrated a novel n-hexane-compatible lab-on-a-disc for rapid on-site monitoring of microalgal lipid contents by a serial process from cell sampling through colorimetric lipid detection. Through the miniaturization, integration, and automation of microalgal lipid quantification steps on a small disc, microalgal lipid contents were successfully determined using a small volume of sample ( $\leq 500 \mu\text{L}$ ) within a short span of time ( $\leq 13 \text{ min}$ ). We anticipate that this point-of-care test system, as with similar previously reported portable instruments,<sup>96</sup> will make an immense contribution to the commercial production of microalgal-based biofuels by providing rapid, cost-effective, user-friendly on-site quantification of microalgal lipids. Furthermore, to the best of our knowledge, this work is the first of its kind to extend the use of centrifugal microfluidic technology to energy and biomedical applications.

## CHAPTER 3. Lab-on-a-disc for simultaneous determination of total phenolic content and antioxidant activity of beverage samples

### 3.1 Introduction

#### 3.1.1 Total phenolic content and antioxidant activity

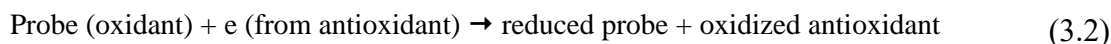
Phenolic compound (polyphenols) are composed of a chemically heterogeneous group, containing a phenol group (a functional hydroxyl group in an aromatic ring) in its basic structure.<sup>125, 126</sup> These compounds generally are categorized as phenolic acids and analogs, flavonoids, tannins, stilbenes, curcuminoids, coumarins, lignans, quinones, and others based on the number of phenolic rings and of the structural elements that link these rings. Phenolic compounds are also widespread constituents of medical plants, fruits, vegetables, and beverages (e.g. fruit juice, tea, beer, and wine).<sup>127</sup> There has been promoted in the potential health benefits of dietary phenolic compounds as antioxidant and may protect from oxidative stress and some diseases because of their possible beneficial effects on human health.<sup>94</sup> The determination of phenolic compound in food and beverages have been commonly reported in term of “total phenolic content”. The Folin-Ciocalteu (FC) method based on electron transfer reaction between FC reagent and containing of phenolic compounds, it was widely used as a conventional method for determination of the sum of phenolic compounds in various products.<sup>125</sup> The gallic acid was employed as the standard solution for FC assay. The FC reagent consists of phosphotungstic and phosphomolybdic acids, the reagent was a strong oxidant.<sup>61</sup> The FC reagent oxidizes one or two electrons from phenolic compounds antioxidants to form some blue compounds such as  $(\text{PMo}_0\text{W}_{11}\text{O}_{40})^{4-}$ .<sup>128</sup> FC reagent react with phenolic compounds under alkaline conditions. Under this condition, phenolic compounds can dissociate phenolic proton, lead to phenolate anion which is capable of reducing the FC reagent. It can be expressed by<sup>128</sup>



The reduction of FC reagent leads to formation of the blue species that is conveniently detectable using a spectrophotometer.

Antioxidants activity (AA) of phenolic compounds was an important parameter in food science, nutritional and medical studies.<sup>129</sup> The antioxidant activity was defined as potential compounds that can delay, inhibit, or prevent oxidation reaction of oxidizable materials by scavenging or neutralizing free radicals and reactive oxygen species (ROS).<sup>61</sup> The antioxidant activity is related to the presence of antioxidant compounds for protection harmful oxidation in biological system. There are several

methods for the measurement of antioxidant activity including 2,2-diphenyl-1-picrylhydrazyl radical (DPPH radical) assay, trolox equivalent antioxidant capacity (TEAC) assay, and ferric reducing antioxidant power (FRAP) assay.<sup>130</sup> These methods were based on reaction between two components in a reaction mixture; antioxidants (phenolic compounds) and oxidant (probe), according to electron transfer reaction as follows:<sup>130</sup>



The probe itself is an oxidant (or free radical) that can receive an electron from the antioxidant, resulting color changes of the probe. The level of color change is proportion to the antioxidant activity. The color change stop when the reaction is reached the end point.<sup>130</sup> This reaction can be measured by spectrophotometer detection. Trolox solution was used as a common standard for the calibration curve of the method.<sup>131</sup> The antioxidant activity determination is recommended to evaluate from two methods as minimum, therefore normally combined more than one method to measure antioxidant activity in order to give comprehensive information on the total antioxidant activity of food and beverages.<sup>129, 132</sup> There are many publications determined the content of phenolic compounds by FC method and its antioxidant activity by DPPH, TEAC and FRAP methods. The excellent linear correlation between phenolic compounds concentration and antioxidant activity of phenolic compounds often found. Therefore both total phenolic content and antioxidant activity evaluation have become a routine assay in study phenolic antioxidants.<sup>133</sup>

### **3.1.2 Importance of total phenolic content analysis and antioxidant activity evaluation in beverage samples**

Food analysis is an emerging area which requires advanced science and technology to meet the increasing demand in modern society for food safety and health. As people pay more attention in the quality of life and health issues, there is a recent trend to link food and health issues together. Therefore, food and beverage companies started to use ingredients known to improve human health such as phenolic compounds. The amount of these kinds of health-aid additives become one of a decisive factor in food and beverage consumption.<sup>134</sup> The presence of natural antioxidants in food and beverages, such as total phenolic compound and its antioxidant activity has attracted considerable interests because of its potential function for health-aid and therapeutic effects. They are known to play important roles against harmful oxygen radicals or highly reactive oxygen species (ROS) by scavenging or neutralizing free radicals.<sup>61</sup> ROS is known to be closely associated with accelerated aging and diseases such as arteriosclerosis or cancer.<sup>62</sup> Recently, food and beverage companies are promoting the presence of

antioxidants in their products for the potential health benefits in the diet. Therefore, quantification methods for total phenolic content and antioxidant activity in the food and beverages have gained much attention in order to measure the phenolic compounds and thereby to guarantee the quality of the products.

### 3.2 Available methods for total phenolic content and antioxidant activity

Analytical methods for determination of total phenolic content and antioxidant evaluation in different types of sample with analysis time required are shown in **Table 3.1**. Conventionally, total phenolic content and antioxidant activity detection were conducted using chromatographic methods; (GC)<sup>135</sup> and high performance liquid chromatography (HPLC)<sup>136</sup> or using colorimetric methods. Both GC and HPLC analyses are powerful for separating and identifying the total phenolic content components in the complex sample but both required complicated sample preparation, long analysis time and expensive operating machine. Therefore, both GC and HPLC methods are not practical for routine analysis in point of care test settings.

The traditional colorimetric method is frequently used for determination of total phenolic content and antioxidant activity because of its easier availability in many laboratories. A Folin-Ciocalteu (FC) method is commonly used for determination of the total phenolic content in plant extracts and beverages.<sup>128</sup> The most common methods widely used for evaluation of antioxidant activity in food products and dietary supplements are based on radical scavenging, such as 2,2-diphenyl-1-picrylhydrazyl radical (DPPH),<sup>61</sup> trolox equivalent antioxidant capacity (TEAC)<sup>137</sup> assay, and ferric reducing antioxidant power (FRAP) assay.<sup>138</sup> These colorimetric methods are simpler than conventional GC or HPLC analysis but it also requires

**Table 3.1.** Analytical methods for determination of total phenolic content and antioxidant evaluation in different types of sample with analysis time required.

Method	Sample	Analysis time
<b><i>Total phenolic content</i></b>		
GC-MS <sup>135</sup>	Moringa peregrine (plant)	70 min
HPLC-UV <sup>136</sup>	Grape juice	60 min
Spectrophotometer <sup>139</sup> (based on FC reaction)	Commercial beverage	90 min
Flow injection analysis <sup>63</sup> (based on FC reaction)	Food product	5 min
Sequential injection analysis <sup>64</sup> (based on FC reaction)	Wine	5 min
Lab-on-a-chip <sup>3</sup> (based on acidic potassium permanganate chemiluminescence)	Honey	10 min
<b><i>Antioxidant activity</i></b>		
Spectrophotometer <sup>61</sup> (based on DPPH reaction)	Food	30 min
Spectrophotometer <sup>138</sup> (based on FRAP reaction)	Teas	30 min
Spectrophotometer <sup>140</sup> (based on TEAC reaction)	Vegetable juices	30 min
SIA <sup>141</sup> (based on ABTS reaction)	Ginger beverages	1.5 min
Lab-on-a-chip <sup>6</sup> (based on DPPH reaction)	Nutrients	10 min



time consuming steps and labor-intensive manual handling. Additionally, recent studies claimed that it is necessary to combine more than one method to measure antioxidant activity in beverage samples since the antioxidant activity of food and beverage samples are determined by a mixture of different antioxidants with different mechanisms of actions. Therefore, the automation and integration of more than one detection methods are required to avoid many labor-intensive manual handling and long reaction time.

To automate method base on colorimetric reaction, flow injection analysis (FIA)<sup>63</sup> and sequential injection analysis (SIA)<sup>64</sup> have been developed for determination of total phenolic content of wine and beer samples. These methods have novelty in reducing the time, labor and handling errors from manual experiment. However, it required complicated pumping and tubing in FIA, and it required large sample and reagent volume in SIA. Also, both methods did not measure both total phenolic content and antioxidant activity.

Recently, lab-on-a-chip system has been employed for a simple one-step reaction and detection of total phenolic content and antioxidant activity in microfluidic channels. It has been developed for determination of total phenolic content in honey<sup>3</sup> and a lab-on-a-chip device has also been developed a two-compartment microfluidic device that minimizes the dynamic of liver metabolism and the subsequent antioxidant activity of food components by Jungwoo Lee and coworkers.<sup>6</sup> They used 2,2-diphenyl-1-picrylhydrazyl radical (DPPH) method for antioxidant activity detection. Both lab-on-a-chip based total phenolic content and antioxidant activity detection have novelty in automating the complicated steps and reducing the sample and reagent volume. However, this technique requires external syringe pumps and external interconnects to induce fluid movement. In addition, both studies cannot detect total phenolic content and antioxidant activity simultaneously, and also in Lee's work, they only used DPPH method for antioxidant activity detection.

Centrifugal microfluidic system called lab-on-a-disc has garnered much attention as analytical device for automating and integrating complicated assay in variety field such as clinical,<sup>86</sup> environmental,<sup>5</sup> chemical engineering<sup>14</sup> and food application.<sup>2</sup> In lab-on-a-disc system, a simple motor is used to rotate the microfluidic disc device and then, centrifugal force is the driving force for fluidic or particles transported through microchannels. By controlling fluid direction using valves, all process from sample metering to detection could be integrated and automatically conducted on a rotating disc device.<sup>106, 142, 143</sup> As taking advantages describe above, lab-on-a-disc can be an ideal solution to overcome the limitation of previous total phenolic content and antioxidant activity detection such as huge consumption of reagents, requiring complex pumping, expensive cost, long analysis time and labor intensive manual handling, and minimal amount of instrument.

In this work, we present a new fully integrated lab-on-a-disc system for simultaneous determination of total phenolic content and antioxidant activity detection from different beverage samples (teas, fruit juices, beer and wines). Lab-on-disc platform was designed and developed the all-in-one device for three different colorimetric detections including FC, DPPH and FRAP methods. The optimization of sample and reagent volume consumption, mixing time of three colorimetric reaction (FC, DPPH and FRAP) and sample dilution ratio for the integration on a disc were investigated. The full automation of all steps such as sample filtering, metering, mixing, reaction and final colorimetric detection was demonstrated. The lab-on-a-disc method was validated with the conventional method for total phenolic content and antioxidant activity analysis in different beverage samples.

### 3.3 Simultaneous determination of total phenolic contents and antioxidant activity of beverage sample using lab-on-a-disc

#### 3.3.1 Experimental details

##### Chemical and reagents

Gallic acid monohydrate (purity  $\geq 98.0\%$ , ACS reagent), trolox (6-hydroxy-2,5,7,8-tetramethylchromane-2-carboxylic acid, iron (II) sulfate heptahydrate, ACS reagent, (purity  $\geq 99.0\%$ ), 2.0 N Folin-Ciocalteu reagent (FC reagent), 2,2-diphenyl-1-picrylhydrazyl radical (DPPH $\bullet$   $\approx 90.0\%$ ), 2,2'-azinobis(3-ethylbenzothiazolin-6-sulfonate) diammonium salts (ABTS  $\approx 98.0\%$ ), 2,4,6-tris(2-pyridyl)-s-triazine (TPTZ, puriss, purity  $\geq 99.0\%$ ), potassium persulfate (purity  $\geq 99.0\%$ ), sodium acetate anhydrous (purity  $\geq 99.0\%$ ) and iron (III) chloride hexahydrate puriss. p.a., ACS reagent, crystallized, 98.0–102% (RT) and hydrogen peroxide (H<sub>2</sub>O<sub>2</sub>) were purchased from Sigma-Aldrich (St. Louis, MO, USA). Methanol and ethanol of gradient grade were obtained from Mallinckrodt (Dublin 15, Ireland).

##### Preparation of standard solution

The gallic acid standard stock solution (5000  $\mu\text{g mL}^{-1}$ ) was prepared in methanol before diluting to concentrations of 20, 100, 400, 500 and 1000  $\mu\text{g mL}^{-1}$ , respectively. The trolox stock solution (5.0 mM) was also dissolved in methanol before diluting to concentrations of 0.25, 0.50, 1.0, 1.5 and 2.0 mM, respectively. The Fe (II) stock solution was prepared in deionized water before diluting to concentrations of 0.1, 0.2, 0.5, 0.8, 1.0, 2.0, 5.0, 8.0 and 10.0 mM, respectively.

### Sample preparation

Beverage samples (green tea, black tea, orange juice, grape juice, apple juice, red wine, white wine, and beer) were purchased from a local market in Ulsan city (South Korea). Green tea and black tea, the samples were prepared by pouring 200 mL of deionized water at 100 °C in to a beaker with tea bag (about 1.5 g of leaves) and by brewing for 5 min. For fruit juice, the samples were centrifuged at 3000 rpm for 10 min. For alcoholic samples were accurately weighed into 30 g portions. The alcoholic samples were degassed for 10 min. All of samples were diluted with methanol for FC and DPPH methods and diluted with deionized water for FRAP method before analysis.

### Disc design and fabrication

A disc device was designed and fabricated by Mr. Yubin Kim in Prof. Y.K. Cho's laboratory at Ulsan National Institute of Science and Technology (UNIST) in South Korea. A disc contains five identical units for total phenolic content and antioxidant activity detection, each starting from a 20  $\mu$ L minimum beverage sample. Each unit consists of chambers for sample loading, metering, waste storing, diluting and interference eliminating, reagent storing and optical detection (**Figure 3.1B**).

For disc fabrication, our disc is made by assembling four layers of polycarbonate (PC). A detail layout of the disc fabrication is shown in **Figure 3.2**. The top layer (1 mm thick) has a sample flow channel, inlets, and vent holes. The middle polycarbonate (PC) film (0.125 mm thick) contains a carbon pattern for valving purposes. Detail valving protocol is explained previously.<sup>14</sup> Briefly, upon laser irradiation, the carbon dot areas are burned and punctured, allowing liquid to pass through the channel. The middle layer (5 mm thick) contains chambers for storing samples and reagents. All the chambers, inlets, vent holes and channels were cut into the PC plate using a computer numerical control (CNC) milling machine (3D Modeling Machine; M&I CNC Lab, Korea). Finally, 1 mm the bottom layer was assembled to the middle layer to provide an optically clear surface for precise colorimetric detection. The optical path length was 5.125 mm, which equal to the thickness of the middle layer and the PC film. (**Figure 3.2**) In this disc fabrication, all layers were assembled using the thermal fusion assembly technique. There was no leakage even when the discs were rotated at spin speeds as high as 6,000 rpm. Laser-irradiated carbon dot valves were adopted because the previously used ferrowax valves are not solvent-tolerant. Carbon dots were patterned on the surface of the 0.125 mm PC film using a laser printer (DocuCentre-IV C2263, Fuji Xerox Co. Ltd., Japan) and were irradiated using a BS808T2000C-MOUNT laser diode (Best-Sources Industry (HK) Co. Ltd., China).

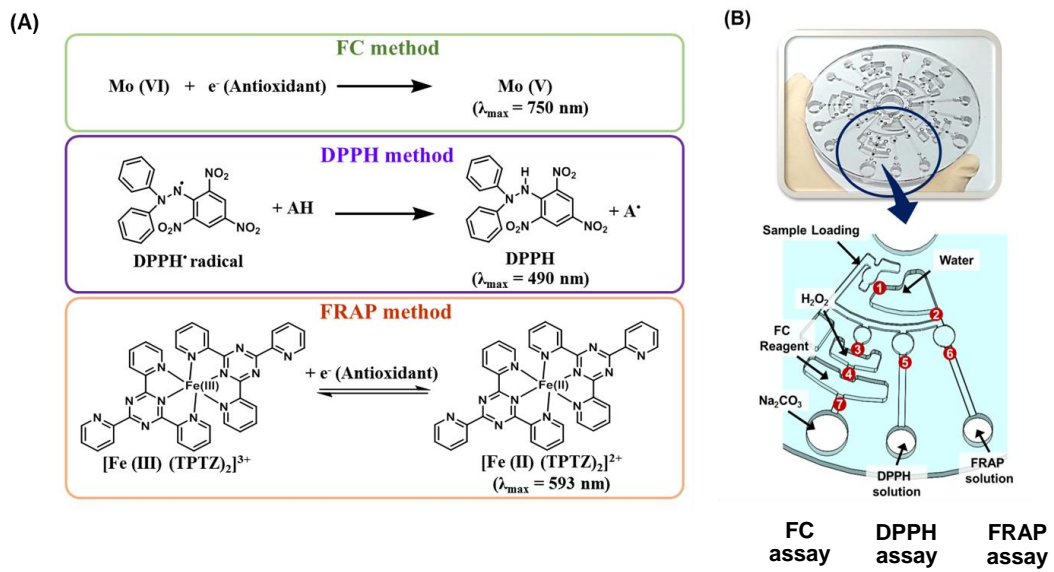


**Figure 3.1.** (A) Colorimetric reactions of FC, DPPH and FRAP methods and (B) overview of disc design.

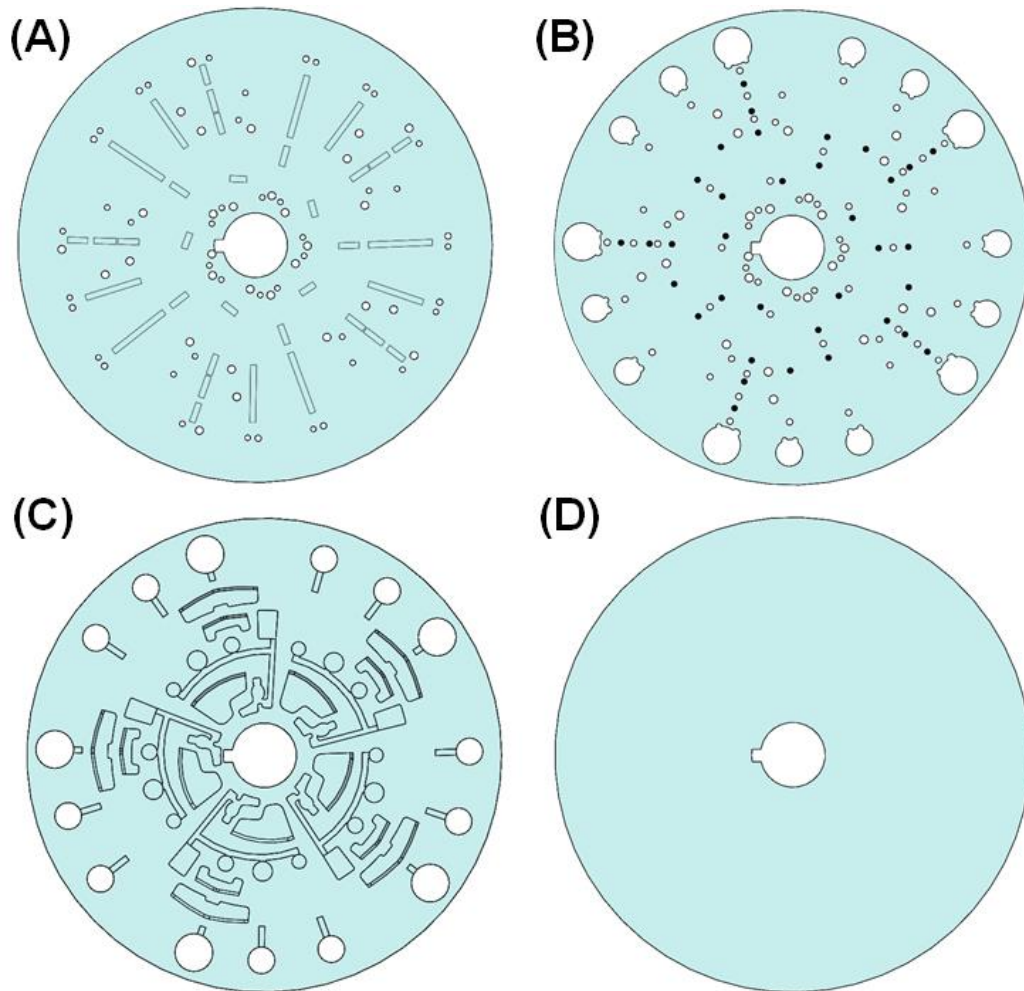


**Figure 3.2.** The lab-on-a-disc is composed of 4 layers of polycarbonate (PC). (A) Top layer containing sample inlet holes, vent holes, and flow channels. (B) Polycarbonate (PC) film (0.125 mm thick) containing carbon dot patterns, inlets, vent hole, and open holes for optical detection. (C) Middle layer disc (5 mm thick) containing sample and reagent chambers. (D) Bottom layer (1 mm thick). The diameter of the disc is 120 mm.

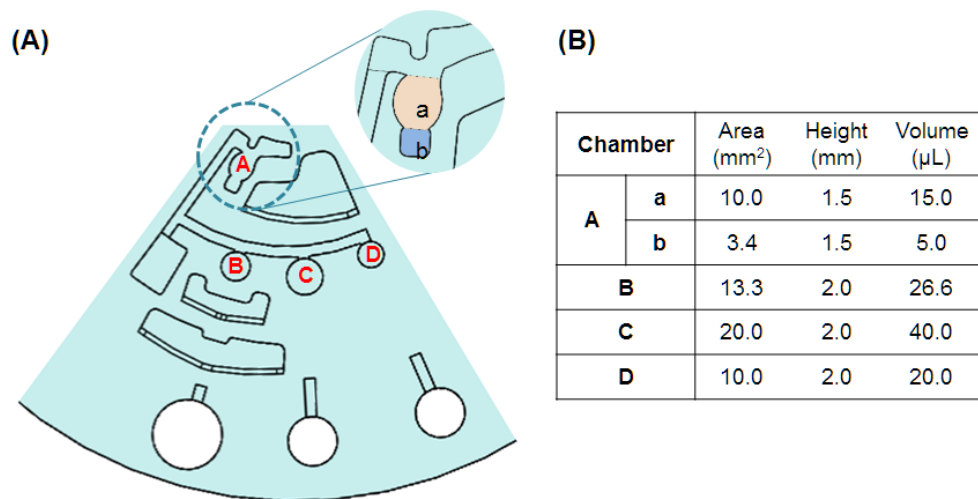


**Figure 3.3.** The disc layout with detailed information about the chamber design. (A) the design of the microfluidic layout, and (B) the volume of metering chambers.

### **Disc operation procedure: Integrated FC, DPPH and FRAP assays**

The experimental set-up is shown in **Figure 3.4**. The lab-on-a-disc device was mounted on a programmable spinning motor. The laser-irradiated carbon dot valves could selectively melt and opened by a laser diode (Best-Sources Industry (HK) Co. Ltd., China). Colorimetric detection of target analytes was conducted using an optical fiber-coupled spectrometer (MAYA2000 Pro, Ocean Optics, FL, USA).

The detailed procedure of the disc operation is summarized in **Table 3.2**. This method was developed and conducted by Mr. Yubin Kim. First, 20  $\mu\text{L}$  of the beverage sample was measured, the excess beverage sample was discarded, and the colloidal particles in beverage sample were precipitated. The supernatant (15  $\mu\text{L}$ ) of beverage was then transferred to the dilution chamber containing 135  $\mu\text{L}$  of deionized water. For dilution and mixing, disc was rotated at  $\pm 3000$  rpm for 20 sec. The diluted beverage samples were transferred to metering chamber for FC, DPPH and FRAP reaction respectively. For FC reaction, the metered (27  $\mu\text{L}$ ) sample was mixed with 13  $\mu\text{L}$  of  $\text{H}_2\text{O}_2$  solution and then 240  $\mu\text{L}$  of 0.2 N FC reagent. Then, FC reagent treated solution was transferred to next FC reaction chamber containing of 160  $\mu\text{L}$  of  $\text{Na}_2\text{CO}_3$  solution. Simultaneously other metered samples; 40  $\mu\text{L}$  and 20  $\mu\text{L}$  for DPPH and FRAP, respectively, were transferred to reaction chamber; containing DPPH solution (160  $\mu\text{L}$ ) and FRAP solution (180  $\mu\text{L}$ ), respectively. After transferring, the disc was rotated at  $\pm 3000$  rpm for 5 min for mixing. After mixing, supernatant of final solution of FC reaction was transferred to detection chamber. Finally, the absorbance results of each reaction were measured using a fiber-coupled spectrometer.

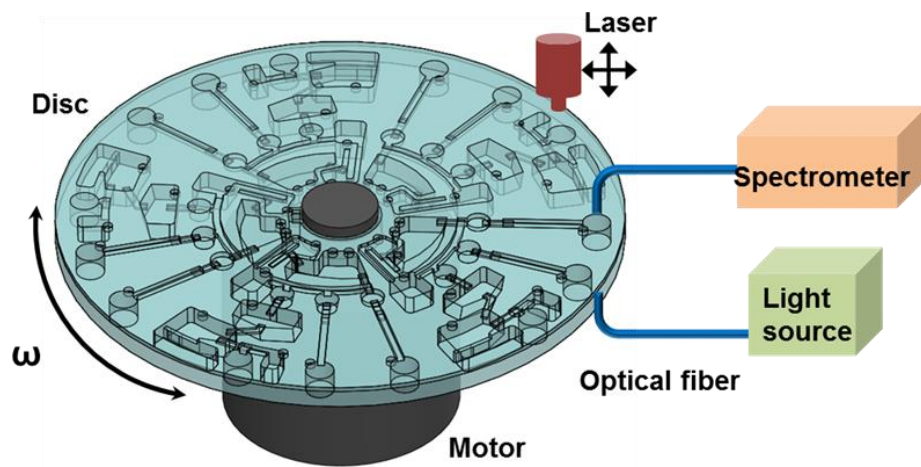


**Figure 3.4.** Experimental design for the simultaneous determination of total phenolic content and antioxidant activity using three colorimetric reactions on lab-on-a-disc device. The motor for rotating the disc, the laser to irradiate the carbon dot, the portable spectrometer, the optical fiber, and the light sources are integrated into our experimental set-up.



**Table 3.2.** Spin program used for total phenolic content and antioxidant activity detection in our lab-on-a-disc.

Step	Spin speed (rpm)	Time <sup>a</sup>	Operation
1	3000	1 min	The beverage sample is metered and particles in beverage form a sediment in bottom of chamber.
2	3000	5 sec	Valve #1 is opened to transfer the metered beverage sample to dilution chamber.
3	±3000 <sup>b</sup>	20 sec	The disc is shaken for mixing the beverage sample with water dilution.
4	3000	5 sec	Valve #2 is opened to transfer the sample to metering chambers for FC, DPPH and FRAP reaction.
5	3000	5 sec	Valve #3 is opened to transfer the metered sample to H <sub>2</sub> O <sub>2</sub> containing chamber to remove the ascorbic acid interference.
6	3000	5 sec	Valve #4 is opened to transfer the H <sub>2</sub> O <sub>2</sub> treated sample to 1 <sup>st</sup> FC reaction chamber.
7	3000	20 sec	Valve #5, #6 and #7 are opened to transfer the FC reagent treated solution to 2 <sup>nd</sup> FC reagent chamber, to transfer the metered samples to DPPH and FRAP reaction chamber respectively.
8	±3000 <sup>b</sup>	5 min	The disc is shaken for mixing the FC reagent treated solution with Na <sub>2</sub> CO <sub>3</sub> , metered samples with DPPH and FRAP respectively.
<b>Total Time</b>		<b>7 min</b>	

<sup>a</sup> Time includes the acceleration time to reach the target speed (0.2 sec), deceleration time to stop the rotation (0.2 sec), and the time for laser actuation to open the carbon dot valve (1 sec).

<sup>b</sup> ± 3,000 rpm: rotation at 3,000 rpm clockwise and counterclockwise.

### Method for determination of total phenolic content

Total phenolic content in beverage samples were determined by using the Folin-Ciocalteu (FC) colorimetric method described by Kim *et al.*<sup>139</sup> with some modification. In manual experiments, 500  $\mu\text{L}$  of the diluted sample or standard solution of gallic acid was mixed with 2.5 mL of 0.2 N Folin-Ciocalteu (FC) reagent and 2 mL of 20% sodium carbonate ( $\text{Na}_2\text{CO}_3$ ). After 90 min, the absorbance was measured at 750 nm using a microplate reader (Infinite M200, TECAN, South Korea). The results were expressed in gallic acid equivalent using a gallic acid standard curve ( $0\text{--}500 \mu\text{g mL}^{-1}$ ). The chemical reactions for determination of total phenolic content are described as follow: polyphenol in beverage samples reacted with FC reagent under basic condition (20% sodium carbonate). Dissociation of a phenolic proton leads to a phenolate anion which a capable of reducing FC reagent. The phenolate is reduced the yellow of Folin-Ciocalteu reagent active changing it into a blue color (**Figure 3.1B**).

### Method for determination of antioxidant activity based on 2,2-diphenyl-1-picrylhydrazyl radical (DPPH) assay

The DPPH radical scavenging activity was determined by using the method of Kim *et al.*<sup>139</sup> with some modifications. Briefly, 200  $\mu\text{L}$  of sample and standard solution (Trolox) was mixed with 800  $\mu\text{L}$  of 0.6 mM DPPH solution (yielding an absorbance of  $1.0 \pm 0.2$  at 490 nm). The mixture was allowed to react for 10 min at room temperature in the dark. The absorbance was then analyzed at 490 nm using a microplate reader. The results were calculated using the following formula:

$$\text{DPPH radical scavenging activity (\%)} = (A_{\text{control}} - A_{\text{std/sample}}) \times 100. \quad (3.3)$$

The chemical reactions for determination of antioxidant activity are described as follow:  $\text{DPPH}^\bullet$  free radical reacted with antioxidant (standard solution or samples). Antioxidant can donate a hydrogen atom to  $\text{DPPH}^\bullet$  and thus decrease the concentration of the stable free radical ( $\text{DPPH}^\bullet$ ), causing in the color change from violet to pale yellow (**Figure 3.1B**).

### Method for determination of antioxidant activity based on ferric reducing antioxidant power (FRAP) assay

The reducing antioxidant power was determined by using a ferric reducing ability of plasma (FRAP) assay described by Stratil *et al.*<sup>62</sup> with some modification. Briefly, the FRAP reagent contained 2.5 mL of 10.0 mM TPTZ solution in 40.0 mM HCl plus 2.5 mL of 20.0 mM  $\text{FeCl}_3$  and 25 mL of 300.0 mM acetate buffer, pH 3.60, was freshly prepared. An aliquot of 50  $\mu\text{L}$  of the standard solution or samples and 50  $\mu\text{L}$  of deionized water were added to 900 mL of FRAP reagent and incubated in a water bath at

37 °C for 30 min. After this time, the absorbance was measured at 593 nm using a microplate reader. The calibration curve was constructed using ferrous sulfate (0–7.5 mM) and the reducing power was expressed as Fe (II) equivalent concentration. The chemical reactions for determination of antioxidant activity are described as follow: the reduction of the ferric-tripyridyltriazine (Fe (III)-TPTZ) complex to the ferrous form (Fe (II)-TPTZ) in the presence of antioxidants. This reduction indicates the increasing of blue color from ferric form (Fe III) to ferrous form (Fe II) (**Figure 3.1B**).

### 3.3.2 Results and discussion

#### Investigation of reduced volume consumption (sample and reagent) for disc experiment

The volume of sample and reagent consumption of FC, DPPH and FRAP methods were investigated prior to the development of lab-on-a-disc system. The consumption of sample and reagent volumes for determination of total phenolic content (FC method) and antioxidant activity (DPPH and FRAP methods) were studied using the spectrophotometric method (manual method). **Table 3.3** presents the comparison of sample volume and reagent volume consumption between original scale and reduced scale of sample and reagent consumption for lab-on-a-disc device. The conventional methods to measure TPC and AA requires large volume of reagent of 4500  $\mu\text{L}$ , 800  $\mu\text{L}$ , and 900  $\mu\text{L}$  to manually perform each experiment of FC, DPPH, and FRAP methods, respectively (see **Table 3.3**). In order to prepare the fully integrated lab-on-a-disc for simultaneous tests of three methods, the reduced volume of reagent was investigated at 360  $\mu\text{L}$ , 160  $\mu\text{L}$ , and 180  $\mu\text{L}$  for FC, DPPH, and FRAP methods, respectively. The reagent volume was reduced to obtain comparable sensitivity and dynamic range when compared to batch methods with utilizing of at least 200  $\mu\text{L}$  for final volume of detection chamber. **Figure 3.5** shows well-agreement in correlation between sensitivity obtained from original volume consumed and after reduced volume for each method. The correlation curves confirm that the reduced sample and reagent volume consumption of FC, DPPH and FRAP methods (disc scale) are valid, when comparing with the original scale with the correlation coefficient 0.994, 0.992 and 0.999 for FC, DPPH and FRAP methods, respectively (**Figure 3.5A, B and C**).

**Table 3.3.** Applied condition in manual procedure for FC, DPPH and FRAP methods (original volume from batch method and reduced volume for disc method) and mixing time.

Colorimetric method	Reagent volume ( $\mu\text{L}$ )		Sample volume ( $\mu\text{L}$ )		Mixing time (min)	
	Original	Reduced	Original	Reduced	Manual	Disc
FC	4500	360	500	40	90	5
DPPH	800	160	200	40	10	5
FRAP	900	180	100	20	30	5

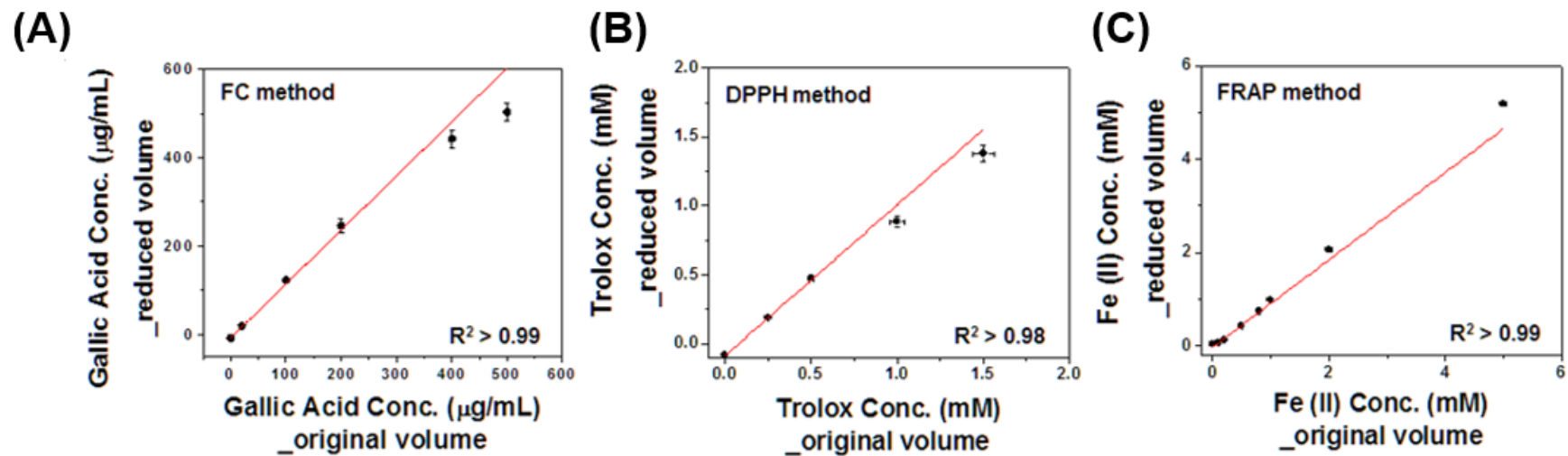


**Figure 3.5.** Investigations of reduced volume of reagent by manual method. Correlation curves to compare the results conducted by using original volume of reagent and reduced volume of reagent for (A) FC (B) DPPH and (C) FRAP reactions, respectively.

### Optimal mixing time of reaction for the integration on a disc

The reaction time for FC, DPPH and FRAP method was optimized for the rapid and simultaneous tests of three independent assays. The investigation of reaction time for FC, DPPH and FRAP methods were carried out in rotating disc (**Figure 3.6**). According to the reaction time of FC, DPPH and FRAP reactions in manual method were established at 90, 10 and 30 min, respectively. In FC method, the first reaction of mixing the diluted sample with FC reagent is rapid but the second reaction of mixing with  $\text{Na}_2\text{CO}_3$  solution requires long reaction time of 90 min. Thus, we optimized the second reaction of FC method. The mixing time of FC reaction in a disc system was studied in the range of 0–90 min as shown in **Figure 3.6A**. There was no significant decrease in the detection signal at higher than 5 min. Therefore, the minimum reaction time for first and second reactions of FC method on a disc was obtained as 5 min which was as a suitable condition for total phenolic content analysis.

For DPPH reaction, the mixing time was investigated in the range of 0–10 min in a disc system as shown in **Figure 3.6B**. The detection signal was not significantly reduced if the mixing time is longer than 2.5 min. In FRAP reaction, **Figure 3.6C** illustrates the mixing time of FRAP reaction study in a disc system (0–30 min). We observed that the absorbance of the reduced Fe (II)-TPTZ complex was stable after 2.5 min mixing time. Thus, we suspected that minimum reaction time for DPPH and FRAP reaction was obtained as 2.5 min. However, for simultaneous test of FC, DPPH and FRAP methods on a disc, the reaction time was fixed as 5 min for 2<sup>nd</sup> FC, DPPH and FRAP method. Thus, the total reaction time was 5 min for simultaneous reaction of FC, DPPH and FRAP method. These results show that our lab-on-a-disc reduced the reaction time by 18 times for FC, by 2 times for DPPH and by 6 times for FRAP method (see **Table 3.3**). Since the disc is designed to accomplish the three-independent analysis, the minimum reaction time was determined to be 5 min in order to guarantee to obtain the signal of detection in the same levels as given from condition of original mixing time.

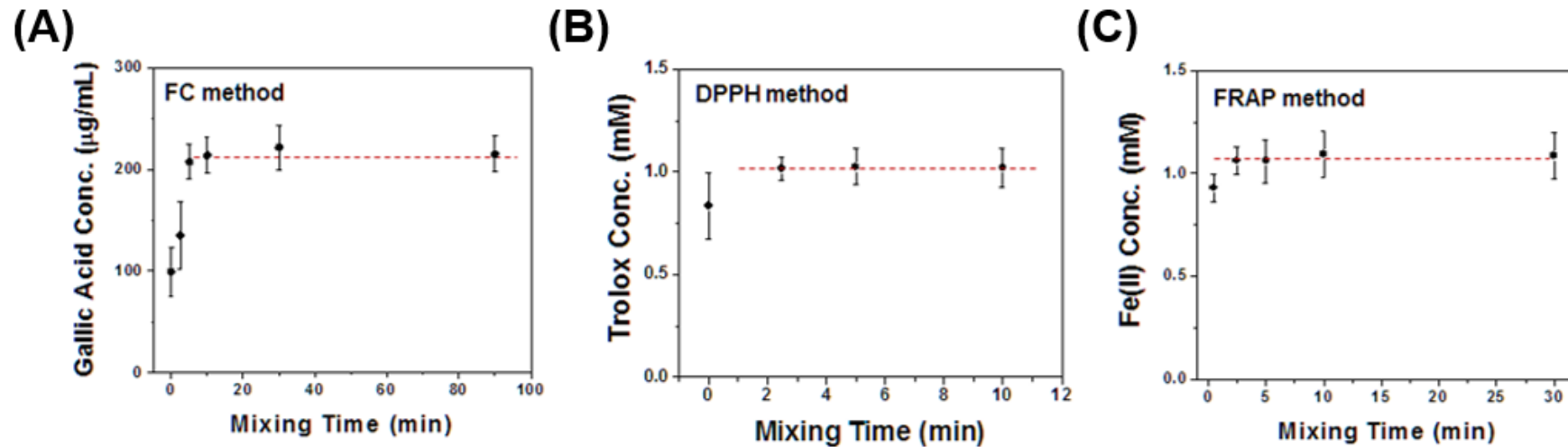


**Figure 3.6.** The investigation of reduced mixing time of (A) FC, (B) DPPH and (C) FRAP methods on a disc. Mixing condition on a disc was  $\pm 3,000$  rpm clockwise and counterclockwise with acceleration time to reach the target speed (0.2 sec) and deceleration time to stop the rotation (0.2 sec). The volume of reagents was reduced to from the 200  $\mu\text{L}$  of final detection volume for each method. Note that the mixing time of first reaction of FC method was fixed to 40 sec.

### **Beverage sample dilution ratio for the integration on a disc**

For lab-on-a-disc system, the beverage samples required the sample dilution step with deionized water before analysis. Therefore, eight beverages samples dilution ratio for determination of total phenolic content (FC method) and antioxidant activity (DPPH and FRAP methods) were studied using the spectrophotometric method (manual method) before integrated to lab-on-a-disc system. The dilution ratio of beverage samples were studied in the range of 1x, 3x, 9x and 27x (sample: deionized water), respectively. The results show that every beverage samples show high linear correlation with correlation coefficients ( $r^2$ ) > 0.997 (data no shown) when the dilution ratio was less than 9x for FC, DPPH and FRAP methods. Thus, the dilution ratio (9x) was chosen for suitable of beverage samples dilution.

### **Disc operation: CCD image visualization for method performance testing**

Schematic illustrations of sequential steps for detecting FC, DPPH and FRAP methods are shown in **Figure 3.7**, with corresponding captured images from a movie recorded using a charge-coupled device (CCD) camera. First, real beverage sample (in this image, grape juice was used) and reagents were loaded into the lab-on-a-disc (**Figure 3.7A**) and 15  $\mu$ L of beverage sample was metered (**Figure 3.7B**). Subsequently, colloidal particles in beverage sample was subjected to sedimentation by spinning 3000 rpm for 1 min, and the supernatant beverage sample was transferred to dilution chamber (**Figure 3.7C**). The diluted sample was transferred to metering chambers for FC, DPPH and FRAP methods (**Figure 3.7D**). For FC method, one of metered diluted sample was treated by  $H_2O_2$  which has been popularly used to remove the interference effect of ascorbic acid. (**Figure 3.7E**) Then, 1<sup>st</sup> FC reaction was conducted from the  $H_2O_2$  treated diluted sample (**Figure 3.7E**). After 1<sup>st</sup> FC reaction, other reactions including 2<sup>nd</sup> FC, DPPH and FRAP reaction were conducted simultaneously (**Figure 3.7F**). In 2<sup>nd</sup> FC reaction, the color of solution changed to blue and white particles were precipitated.

In DPPH reaction, the dark-violet color of DPPH solution was changed to yellowish-violet color, and in FRAP reaction, the yellow color of FRAP solution was change to navy color (**Figure 3.7F & 3.7G**). As spinning disc, precipitated white particles were subject to sedimentation and the supernatant blue color solution was used for colorimetric detection of total phenolic compound. After finishing the mixing step, the absorbance of all resulting solutions including FC, DPPH and FRAP reactions was measured (**Figure 3.7H**).



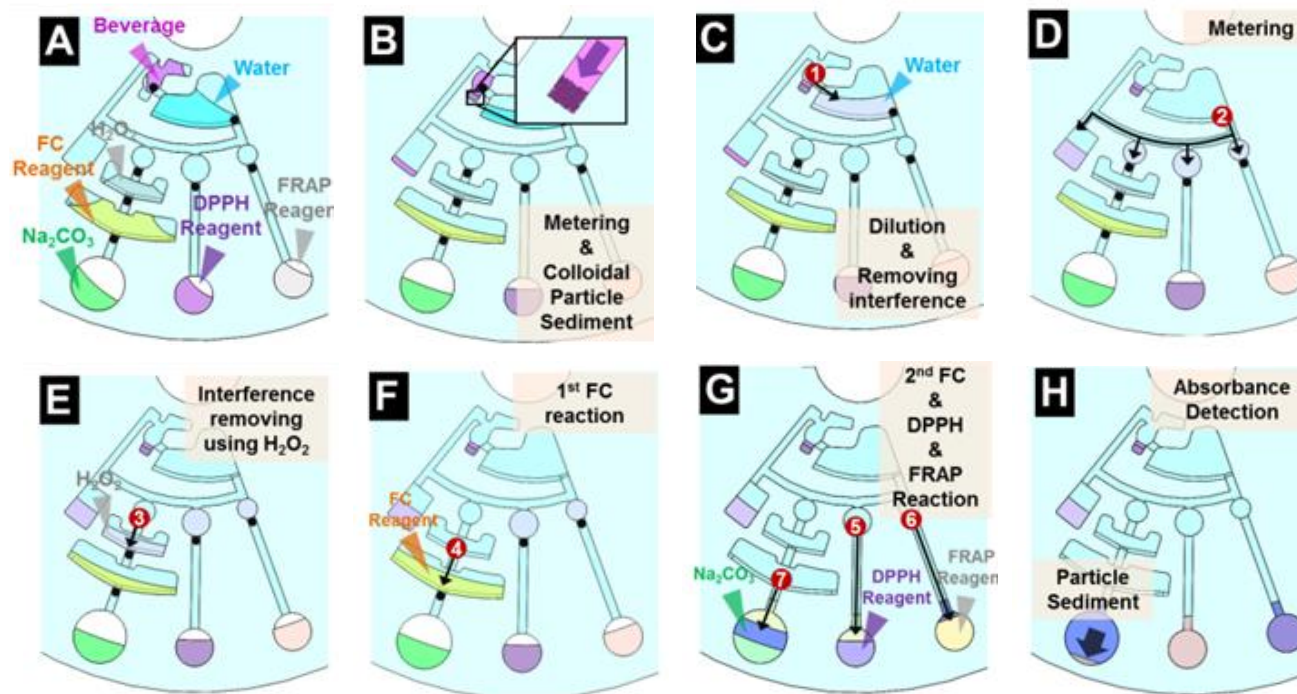


**Figure 3.7.** Illustration of the processes used to total phenolic content and antioxidant activity detection on a disc. (A) Beverage sample was loaded onto the disc, the excess sample was transferred to the metering chamber, and 15  $\mu\text{L}$  of beverage sample was metered. (B) After spinning at 3,000 rpm to sediment the colloidal particle, (C) valve #1 was opened to transfer the supernatant into dilution chamber and the disc was shaken for mixing. Then, (D) valve #2 was opened to transfer the diluted beverage sample to metering chamber for each reaction. Subsequently, (E) valve #3 was opened to transfer the diluted beverage sample to  $\text{H}_2\text{O}_2$  containing chamber to remove the interference in FC method. (F) Valve #4 was opened to transfer  $\text{H}_2\text{O}_2$  treated diluted beverage sample to 1<sup>st</sup> FC reaction chamber. Then, (G) valve #5 was opened to transfer the 1<sup>st</sup> FC reacted solution to 2<sup>nd</sup> FC reaction chamber. Simultaneously, valve #6 and #7 were opened to transfer metered beverage sample to DPPH reaction chamber and FRAP reaction chamber respectively. Then, (H) disc was shaken for mixing and precipitated white particles in 2<sup>nd</sup> FC reaction chamber were sediment. Finally, the absorbance was measured using an optical fiber-coupled spectrometer (QE65000, Ocean Optics, FL, USA) to detect the total phenolic content and antioxidant activity (750 nm for FC method, 490 nm for DPPH method and 593 nm for FRAP method).

### Analytical characteristic of lab-on-a-disc system

The analytical characteristic of lab-on-a-disc method for determination of total phenolic content (FC method) and antioxidant activity (DPPH and FRAP) are shown in **Table 3.4**. In total phenolic content analysis (FC method), calibration curve was linear over the concentration range of 0–500  $\mu\text{g mL}^{-1}$ , with  $r^2 > 0.998$  for gallic acid. In antioxidant activity detection (DPPH and FRAP methods), calibration curves were linear over the concentration range of 0–1.5 mM for trolox and 0–5.0 for Fe (II), with  $r^2 > 0.990$  for both trolox and Fe (II). The limit of quantification (LOQ) of FC method was 48  $\mu\text{g mL}^{-1}$  and for DPPH and FRAP were 0.3 mM and 0.2 mM, respectively.

### Application of lab-on-disc for analysis of total phenolic content and antioxidant activity in three types of drinks (tea, juice and alcoholic)

The total phenolic content and antioxidant activity of eight different kinds of beverage samples were evaluated in our lab-on-a-disc platform as shown in **Figure 3.8**. Among three types of juice sample; apple juice shows the highest total phenolic content and antioxidant activity. For tea samples, black tea shows higher total phenolic content and antioxidant activity compared to green tea. For alcoholic samples, red wine shows 3–4 times higher total phenolic content and ~3–5 times higher antioxidant activity compared to beer or white wine samples. The results of total phenolic content amount in red wine, beer and white wine is similar with reported result.<sup>144</sup> In detail, this results correspond with the fact that grape skin has majority of phenolic compounds including tannins, quercetin and kaempferol glucosides and glucuronides, gallic acid and its glucosides, caftaric and coumaric acid.<sup>145</sup> Also, the total phenolic content and antioxidant activity of red wine are much higher than that of beer, which is also corresponding to the literature. It is known that dietary intake of polyphenols is on the order of 200 mg/day. From our results, around 89 ml of red wine, 149 ml of apple juice and 167 ml of black tea per day are enough to fulfill the dietary intake of polyphenol respectively.<sup>63, 146</sup> The real sample determinations by lab-on-a-disc methods were insignificant different with the results analyzed by conventional batch method based on paired t-test (at 95% confidence level;  $P > 0.05$ ) (**Figure 3.8**).

Since the antioxidant activity of food and beverage samples are determined by a mixture of different antioxidants with different mechanisms of actions, it is highly recommended to use multiple methods to test total phenolic content and antioxidant activity. Here, FC, DPPH, and FRAP methods were simultaneously conducted with eight different beverage samples using our lab-on-a-disc platform. Samples throughput (25 samples per hour) for analysis of all three methods (FC, DPPH and FRAP) was achieved.

**Table 3.4.** Analytical characteristic of lab-on-a-disc method for determination of total phenolic content (FC method) and antioxidant activity (DPPH and FRAP).

Parameter	FC	DPPH	FRAP
Analysis time	7 min	7 min	7 min
Regression equation	$y = 0.004x + 0.332$	$y = 73.997x + 1.647$	$y = 0.718x + 0.038$
Coefficient of determination ( $r^2$ )	0.998	0.990	0.990
LOQ	$48 \mu\text{g mL}^{-1}$	0.3 mM	0.2 mM
Sample throughput	25 samples per hour		

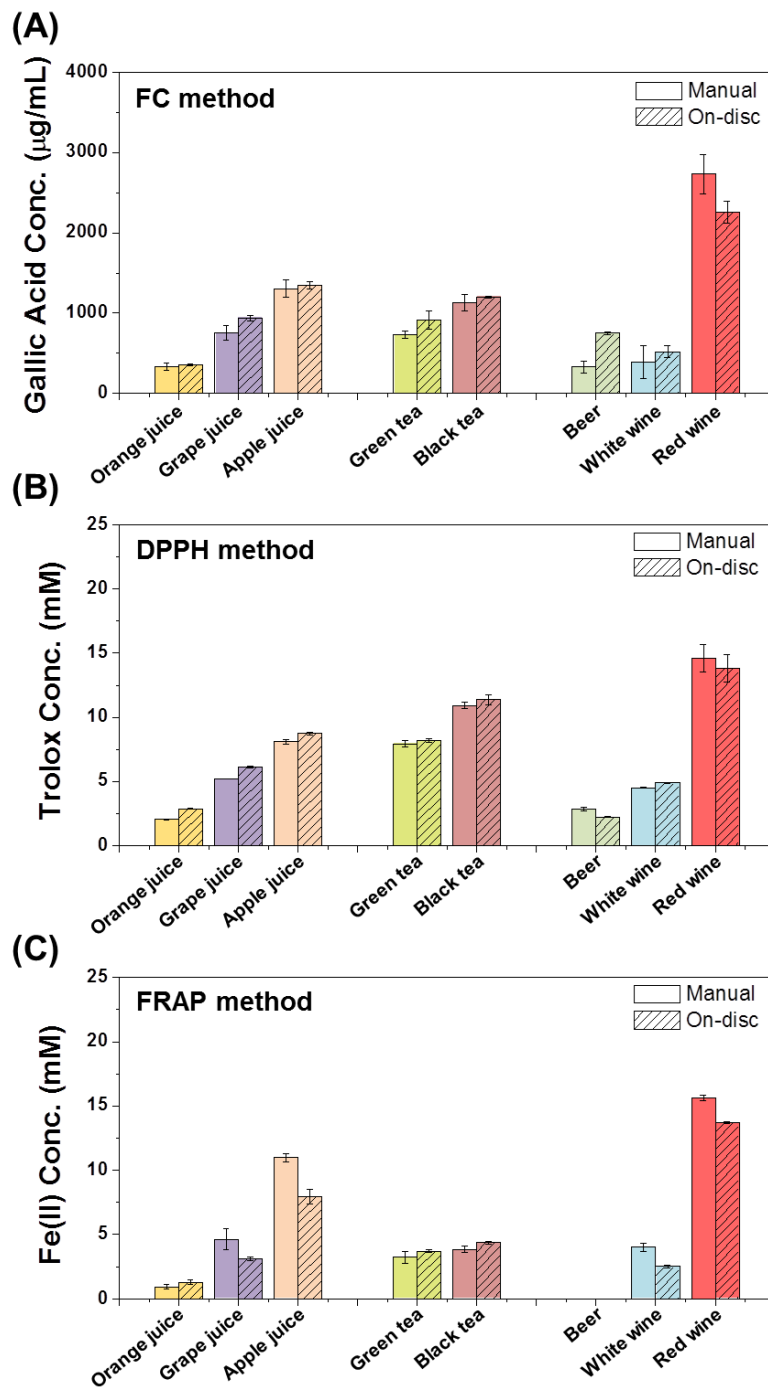


**Figure 3.8.** Total phenolic content and antioxidant analysis results by using manual (conventional) assay and on-disc assay from 8 different beverage samples. (A) FC method, (B) DPPH method and (C) FRAP method.

### **Evaluation of correlation between total phenolic content and antioxidant activity of sample**

As shown in **Figure 3.9**, a regression analysis was performed using Pearson's correlation coefficient ( $r$ ) to correlate the on-disc total phenolic content and antioxidant activity results by various methods (FC, DPPH and FRAP). The results from eight different beverage sample shows good correlation; FC vs DPPH shows  $r > 0.9224$ , FC vs FRAP shows  $r > 0.7935$ , DPPH vs FRAP shows  $r > 0.8703$ . Because of the same basic principles of the applied methods for the determination of total phenolic content and the antioxidant activity (redox properties), one can expect a high correlation of determined values among all methods.<sup>62</sup> There was strong correlation between DPPH value and total phenolic content (FC), FRAP value and total phenolic content (FC) of the beverage samples tested, indicating the number of phenolic hydroxyl groups is a major determinant of antioxidant power of beverage samples which the phenolic compounds may be contributed significantly to the antioxidant activity of the investigated beverage samples. These results was supported by pervious literature who reported such good correlation between total phenolic content and antioxidant activity.<sup>147-149</sup>

### **3.3.3 Conclusions**

A lab-on-a-disc method was successfully developed for integrated and automated analysis of total phenolic content and antioxidant activity from beverage samples. The full automation of all steps such as sample filtering, metering, mixing, reaction and final colorimetric detection for determination of total phenolic content and antioxidant activity were demonstrated within 7 min. The all-in-one device for three different colorimetric detections including FC method for total phenolic content, and DPPH and FRAP methods for antioxidant activity was applied for the diverse beverage samples including tea, juice and alcoholic drink. The lab-on-a-disc method was successfully validated with the conventional method for total phenolic content and antioxidant activity analysis in different beverage samples. The total phenolic content and antioxidant activity values obtained from our lab-on-a-disc method showed relatively good correlation. We expect that our device presented here to prove practical utility by providing a fast, simple and cost-effective method for the analysis of total phenolic content and antioxidant activity from beverage samples.

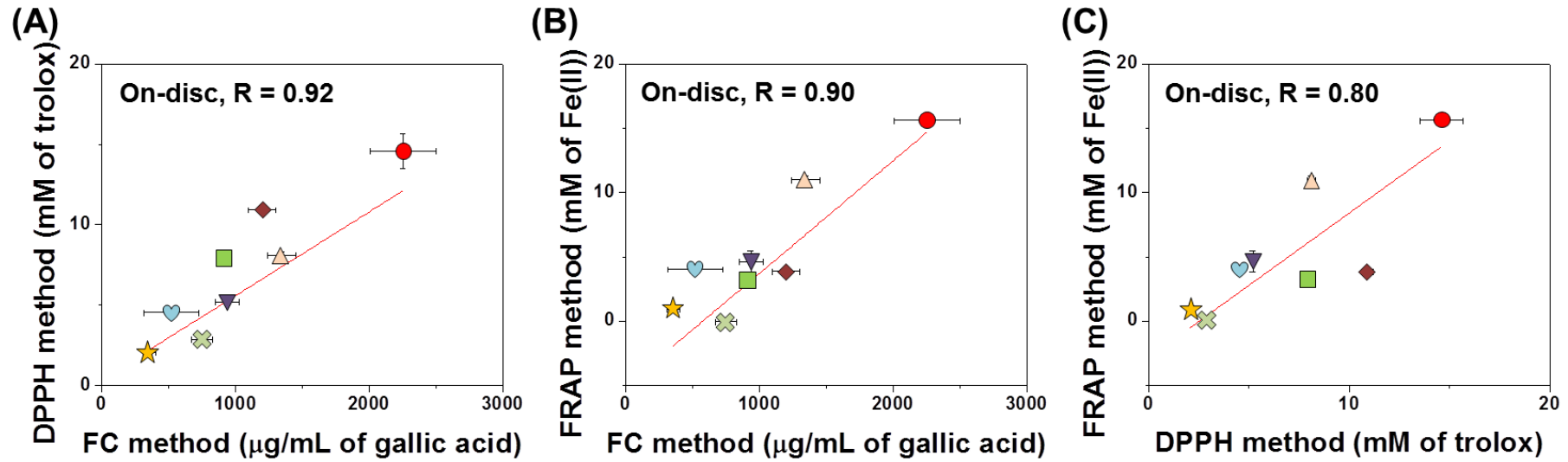


**Figure 3.9.** Correlation curves of on-disc real sample evaluation results between (A) FC and DPPH method, (B) FC and DPPH method, and (C) DPPH and FRAP method.

## CHAPTER 4. Absorbance and luminescence detection on a disc

Among the various detection techniques in lab-on-a-disc, optical detection is very common for several reasons. First, in usual, optical detectors are integrated into the operating devices, which makes it possible to keep the disposable cartridges cheap. In second, a multitude of detection locations on a spinning disc can be analyzed sequentially by spinning, which only needs a single detector. Third, the spinning rotors can precisely position readout cavities relative to the detector position, which enables the alignment of the optical detection system without additional cost. In this chapter we will review existing detection systems that for lab-on-a-disc allow for the visual detection of the assay result, followed by methods for absorbance- and chemiluminescence-based detection. And also, we will introduce our bench top disc analyzer for on-disc absorbance and chemiluminescence detection

### 4.1 History of on-disc absorbance and luminescence detection

#### On-disc absorbance detection

The basic principle of absorbance detection is followed by beer's law. The absorbance of solution will depend directly on the concentration of the absorbing molecules and the pathlength traveled by light through the solution. Schematic illustration of absorbance detection and equation is shown in **Figure 4.1**

Kong *et al*, developed absorbance detection set-up for lab-on-a-disc. All spectral measurements were made using an absorbance instrumental configuration with components.<sup>20</sup> A full schematic of the absorbance instrumental configuration is shown in **Figure 4.2**. Measurements were made directly through chambers on the disk (absorbance path length of 1.4 mm). The absorbing wavelength range used for the calculations was 745.04–745.95 nm, while the non-absorbing wavelength range used was 475.03–475.84 nm.

Grumann *et al*, introduced the total internal reflection for absorbance measurements.<sup>21</sup> A light beam directed onto the disc plane was deflected by a disc-integrated V-groove and passed through a microfluidic chamber in the azimuthal direction. A following V-groove deflected the light beam out of the disc plane to the optical detector. Therefore, the overall path length for the absorption measurement (and the sensitivity) was increased from 1 mm to 10 mm.

Czugala *et al*, showed a paired emitter detector diode (PEDD) device for absorbance detection.<sup>22</sup> In the PEDD setup, two LED were used. One LED served as the light source and it was placed above the disc, while the other LED, operated in the reverse bias mode, served as the light detector for the

transmission light. An improved sensitivity and signal-to-noise ratio as taking advantages of a low cost, small size, and low power consumption, were reported and it compared with the standard setup using an LED and a photodiode.

Ding *et al.*, showed an in-line, miniature, low-cost and portable spectrophotometric detection system can be used for rapid protein determination and calibration in lab-on-a-disc platform.<sup>85</sup> Their portable detection analyzer is configured with paired emitter and detector diodes, which is the light beam between both paired LEDs is collimated having enhanced system tolerance. They claim that their approach could be widely used methods for high throughput assays required a large number of parallel reactions, such as protein drug screening and drug solubility measurement, density calibration in drug discovery and development



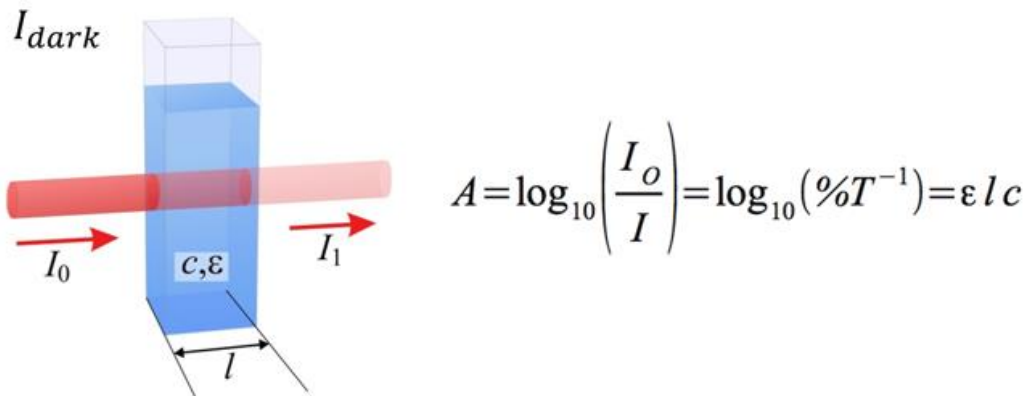


**Figure 4.1.** Schematic illustration of absorbance detection where  $I_0$  = Initial light intensity,  $I$  = light intensity after transmitting target solution,  $T$  = Transmittance,  $\epsilon$  = the molar attenuation coefficient of that material,  $l$  = optical pathlength.

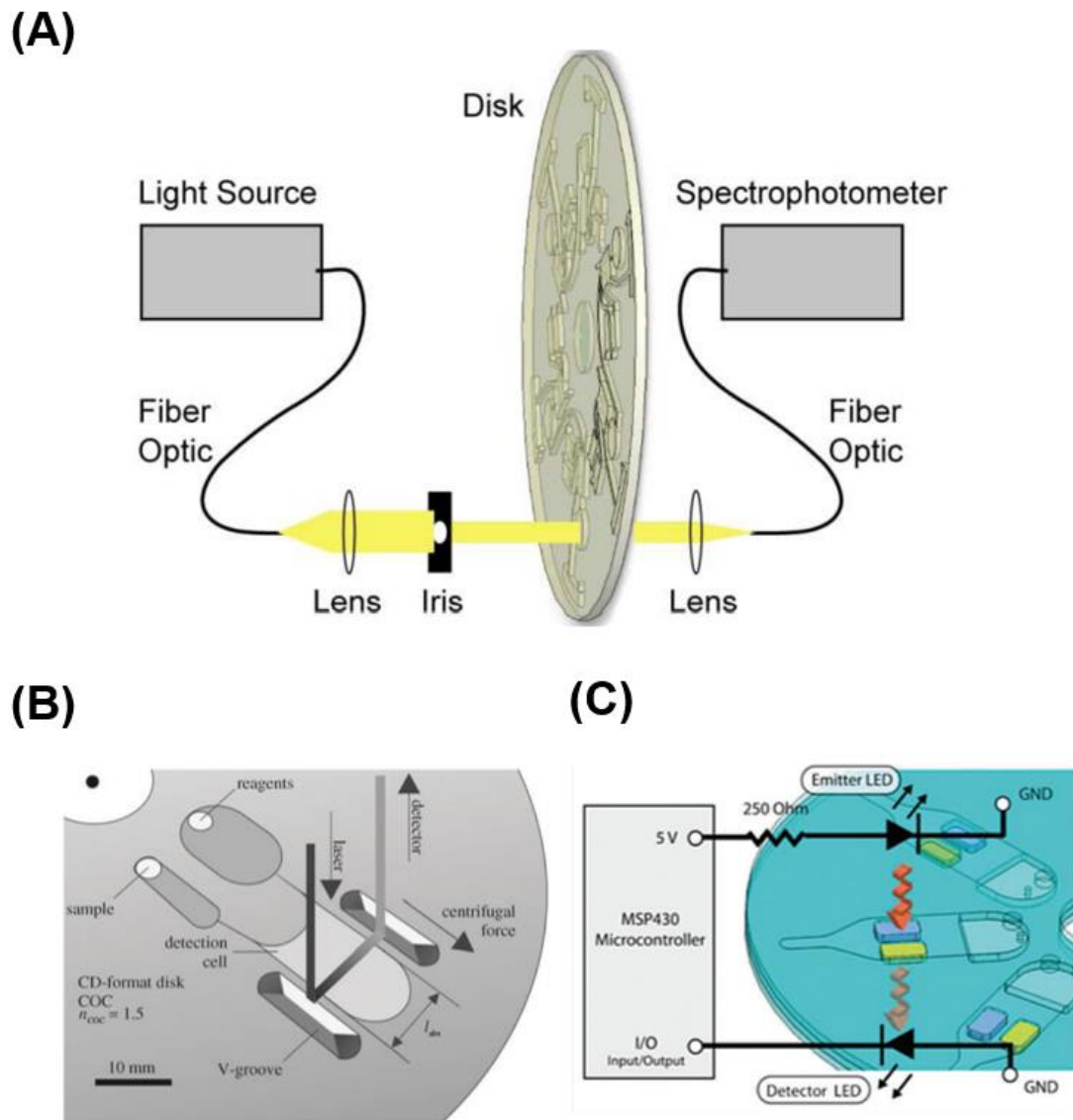


**Figure 4.2.** Schematic illustration of (A) absorbance detection set-up for lab-on-a-disc,<sup>20</sup> (B) the total internal reflection for absorbance measurements in lab-on-a-disc,<sup>21</sup> (C) paired emitter detector diode (PEDD) device for absorbance detection in lab-on-a-disc.<sup>22</sup>

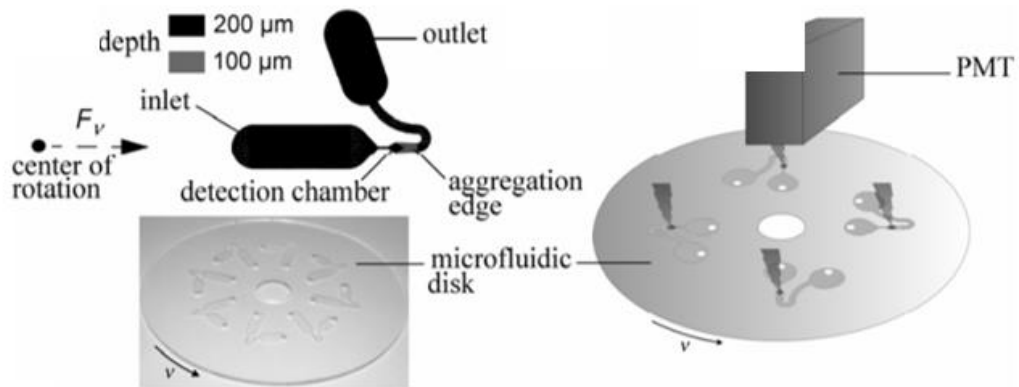
### **On-disc chemiluminescence detection**

Chemiluminescence is the emission of light as a result of a chemical reaction. Certain compounds achieve excited energy states in specific chemical reactions and emit light following a transition to ground state. The wavelength of the light emitted by a molecule in chemiluminescence is the same as in its fluorescence, the energy levels of the molecules being the same. The difference comes from a different excitation process. If the energy of the chemical reaction is lower than required for attaining the excited state, the chemiluminescence does not occur. Also, the deactivation of the excited molecule by nonradiative processes such as collisions with other molecules takes place for chemiluminescence similarly to fluorescence.

In 2006, Riegger *et al*, developed a versatile concept for the automated protocols and high-speed (< 1s) read of parallel chemiluminescent ELISAs. It is suited for the early diagnosis of acute myocardial infarction where three distinct cardiac markers, e.g. Myoglobin, Troponin-I, and CK-MB, have to be detected simultaneously. The simple concept is implemented in a modular setup comprising a PMT, a centrifuge, and an disposable disc with passive fluidic structures which can thus readily be made by standard polymer micromachining.<sup>23</sup>

Czilwik *et al*, developed a LabDisk player which integrate detector to measure chemiluminescent signal by immunoassay for human C-reactive protein. The device can operate programmed spinning protocols and is integrated with integrated chemiluminescence detection unit (Fluo Sens. QIAGEN Lake Constance, Stockach, Germany).<sup>24</sup>

(A)



(B)

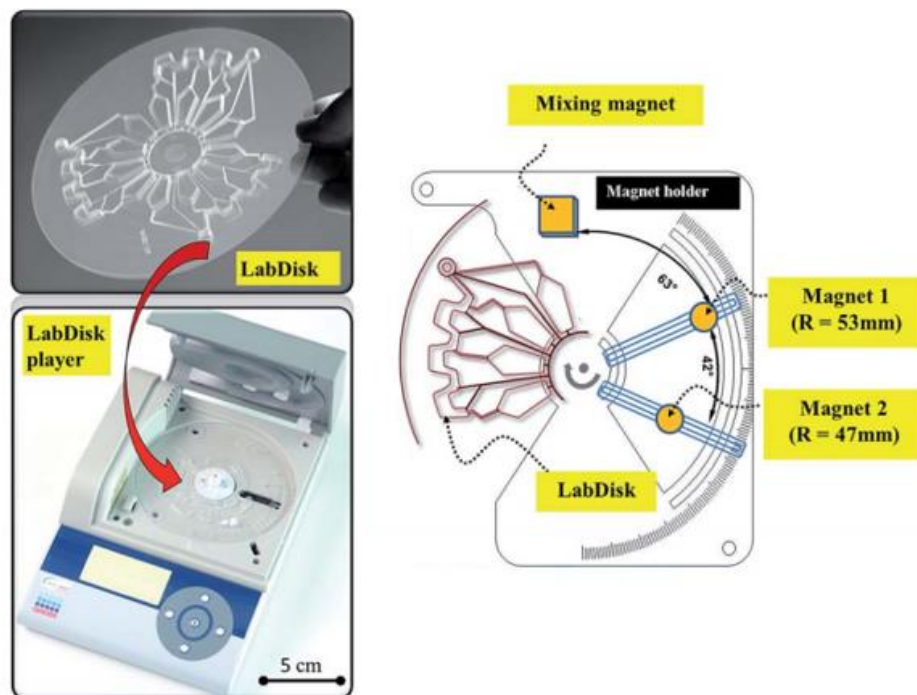


**Figure 4.3.** (A) Schematic image of versatile concept for the automated protocols and high-speed ( $< 1$  s) read of parallel chemiluminescent ELISAs,<sup>23</sup> (B) illustration of LabDisk player which integrate detector to measure chemiluminescent signal by immunoassay for human C-reactive protein.<sup>24</sup>

## 4.2 On-disc absorbance detection

### Experimental set-up

In this section, we introduced the disc analyzer for on-disc absorbance detection. This analyzer provides wide range of absorbance signal which is from 300 nm to 1000 nm wavelength. Working principle of our disc analyzer is very simple. We simply adapted previous absorbance scanning set-up from other group (**Figure 4.2A**).<sup>20</sup> But we made our own software using LabVIEW to control the absorbance scanning and data processing to increase the accuracy of absorbance.

As shown in **Figure 4.4**, schematic image of optical analyzer for absorbance detector and optical elements used for building up. There are 5 main optical components including optical fiber (60  $\mu$ m optical diameter), collimating lens, iris, portable spectrometer coupled with optical fiber and light source coupled with optical fibers.

Operation protocol is very simple. Using customized software in **Figure 4.4C**, all operation including motor control, zero-position, absorbance detection can be controlled. In brief, after loading the disc on disc analyzer, user just type the location of chamber to analyze and target wavelength. Then, absorbance of each chambers is measured and stored as excel file.

For disc, optical pathlength was 5.14 mm (5mm thickness of disc main body + 2 \* 0.07 mm of double adhesive tapes). This optical pathlength can be reduced or increased by choosing different thickness of disc body.

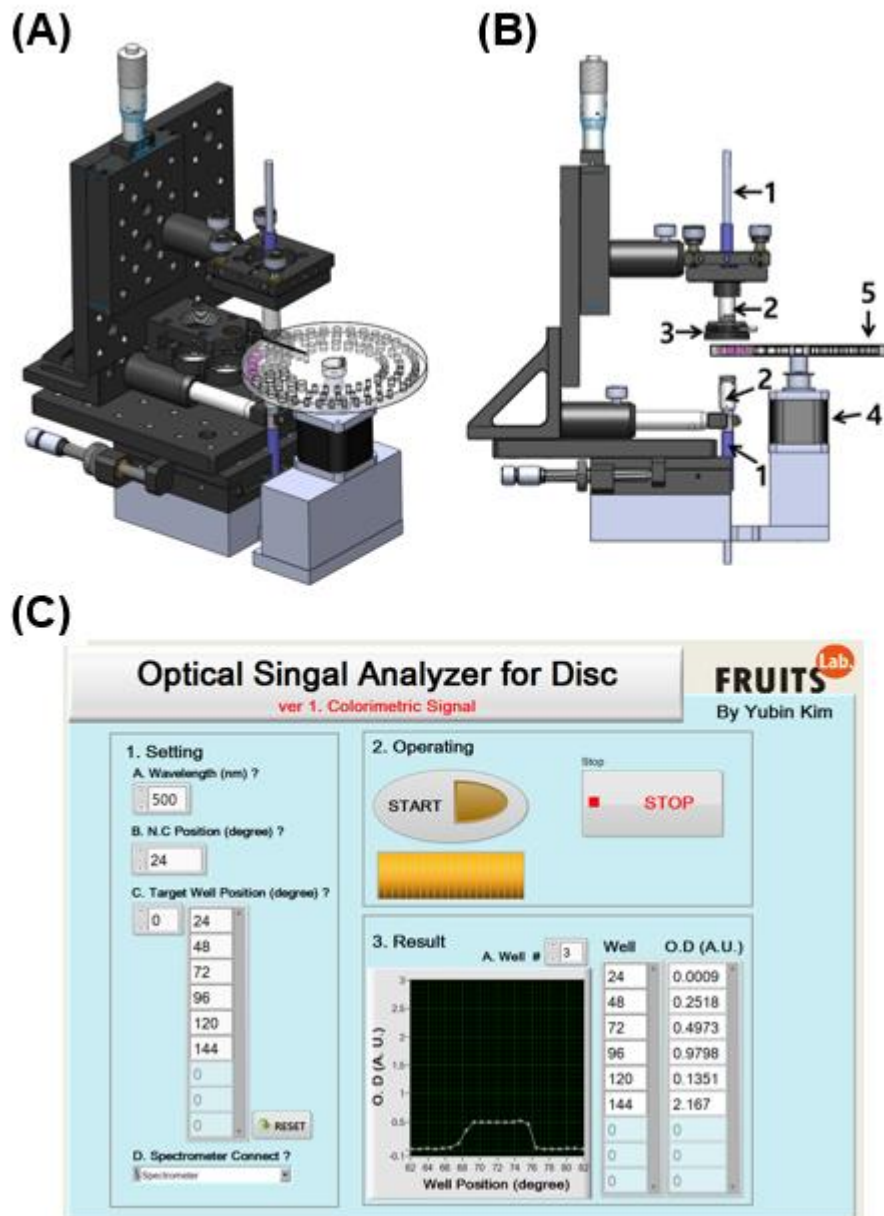


**Figure 4.4.** (A) Schematic image of optical analyzer for absorbance detection (B) Side view and optical elements; 1. Optical fiber (60 um optical diameter), 2. collimating lens, 3. iris, 4. motor, 5. lab-on-a-disc. (C) Image of customized software to operate the optical analyzer for absorbance.

### **Absorbance error caused by scratched surface**

One of main absorbance error was diffraction of light from scratched surface. As shown in **Figure 4.3**, compared to clear surface chamber, scratched surface chamber shows instable absorbance results. The absorbance error is below 0.1 optical density (OD, same with absorbance) which will be very critical in low OD detection. To avoid this, disc surface should be handled carefully during disc fabrication. If scratch occurred on the surface, solvent surface treatment can be used to clear the surface.

### **On-disc absorbance data using disc analyzer**

To investigate the absorbance measurement specs of our disc analyzer we loaded the dye solution (absorbance wavelength at 500 nm) with dilution on a disc and measure the absorbance using disc analyzer. As shown in Figure 4.6A, absorbance from whole concentration (log scale) range of dye solution was measured. OD value shows saturation around 2.0 and below  $1/2^5$  to 0 concentration range, OD shows high linearity ( $R^2 > 0.99$ , **Figure 4.6B**). As shown in **Figure 4.6C**, measured OD value of our disc analyzer was compared with that of conventional spectrometer (Tecan, Infinite® 200 PRO). High linear correlation between OD value from disc analyzer and OD value from conventional spectrometer was obtained ( $R^2 > 0.99$ ). For conventional spectrometer, 96 well plated was used.

For low OD detection (under 0.1 OD), we tested our disc analyzer with low concentration of dye solution. As shown in **Figure 4.7**, measured low OD value of our disc analyzer was compared with that of commercial spectrometer (Tecan, Infinite® 200 PRO). High linear correlation between low OD value from disc analyzer and low OD value from commercial spectrometer was obtained ( $R^2 > 0.99$ ). For commercial spectrometer, 10 mm pathlength cuvette was used. The limit of detection (LOD) of our disc analyzer is 0.01 OD.

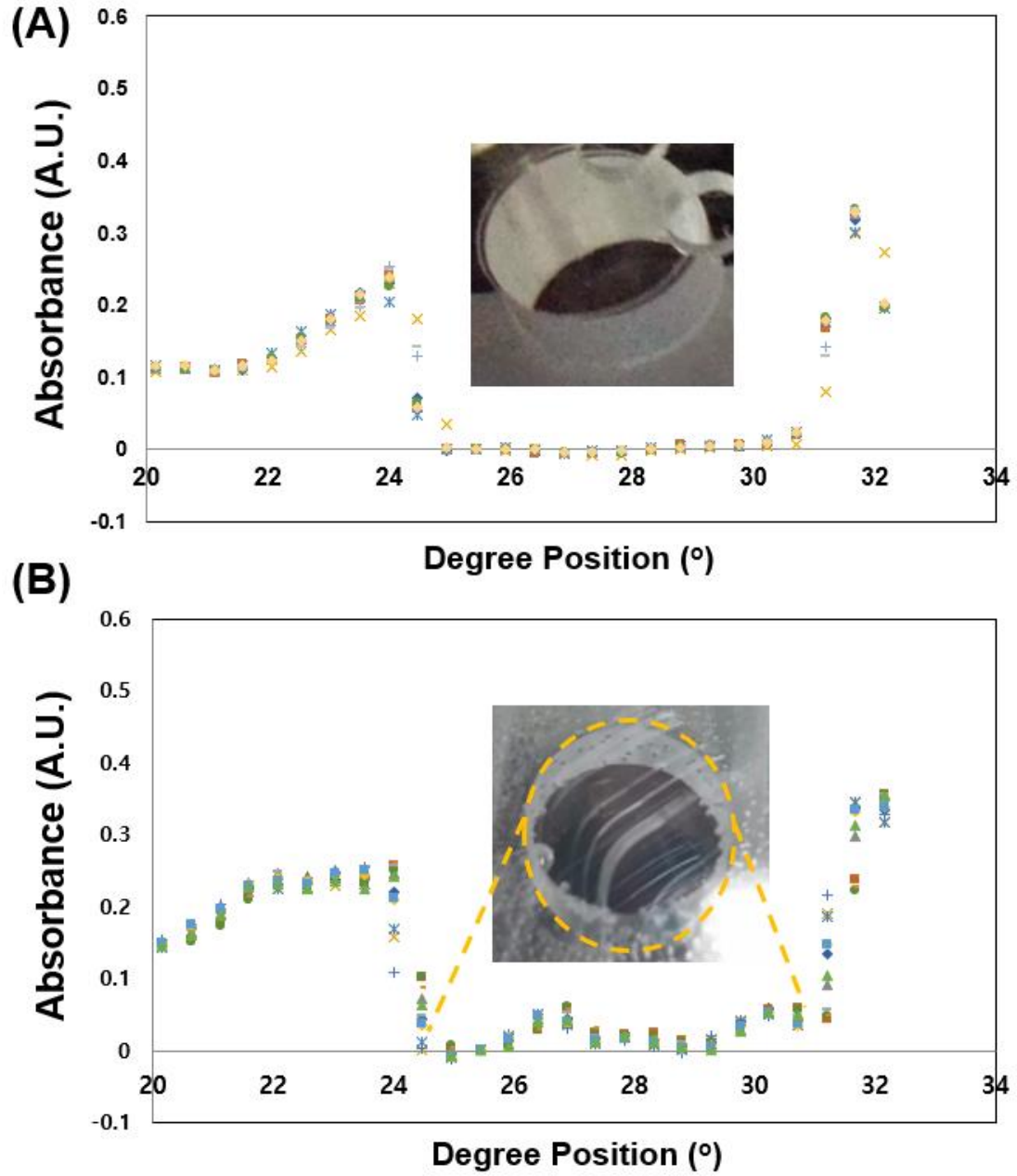


**Figure 4.5.** Absorbance data by radial position of chamber (A) chamber with clear surface (B) chamber with scratched surface.



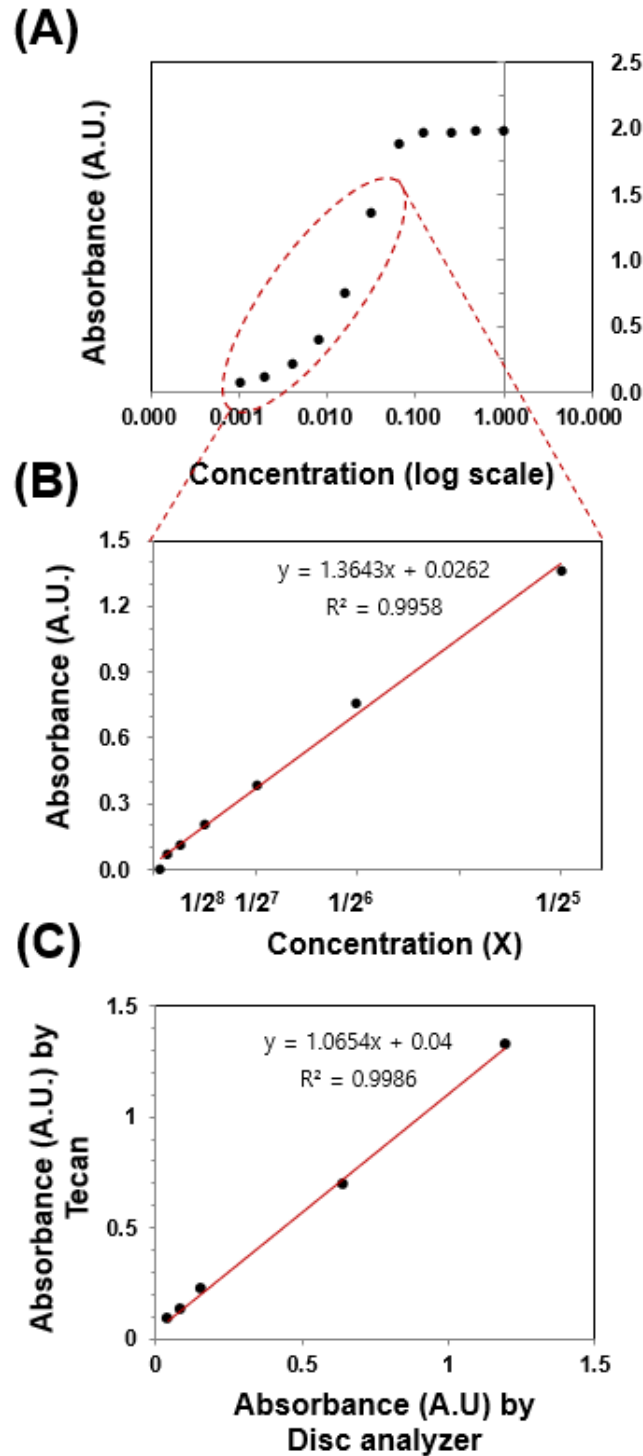


**Figure 4.6.** Absorbance data of our disc analyzer. Absorbance from (A) whole concentration (log scale) (B)  $1/2^5$  to 0 concentration (C) comparison with conventional spectrometer (Tecan, Infinite® 200 PRO). For conventional spectrometer, 96 well plated was used.

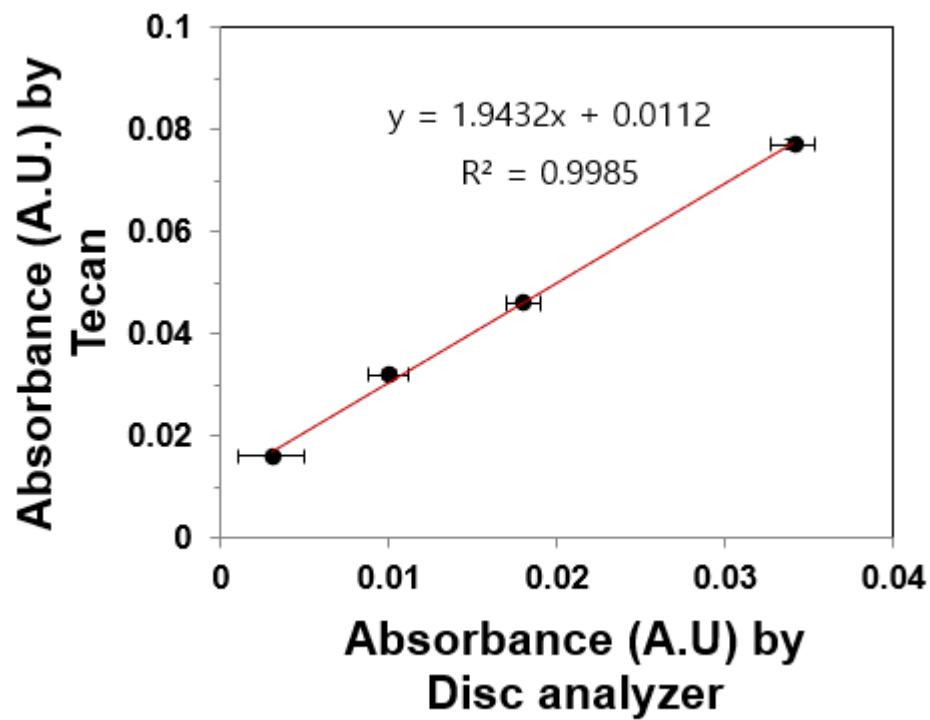


**Figure 4.7.** Comparison with commercial spectrometer (Tecan, Infinite® 200 PRO) in small absorbance range (under 0.1 OD). For conventional spectrometer, 10 mm pathlength cuvette was used.

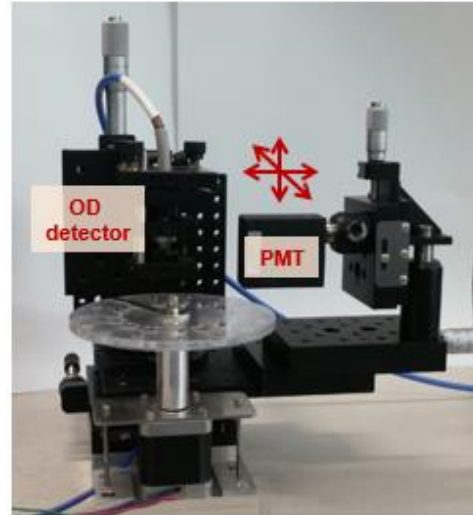
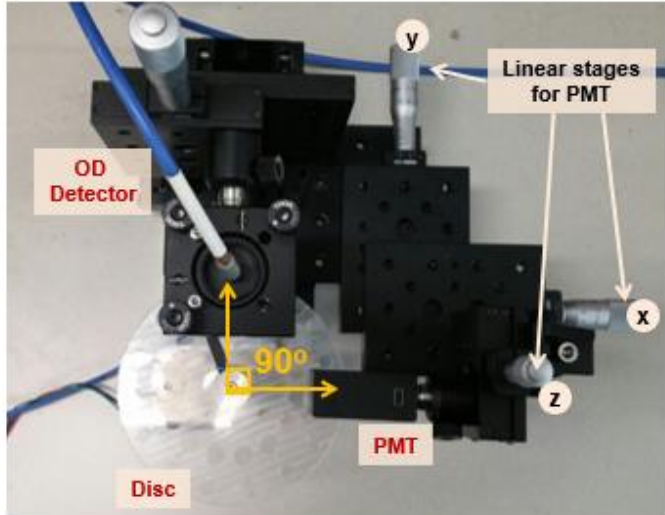
### 4.3 On-disc luminescence detection set-up

#### Experimental set-up

In this section, we introduced the disc analyzer for chemiluminescence detection. This analyzer provides the chemiluminescence signal on a disc. Working principle of our disc analyzer for chemiluminescence is very simple. We simply adapted previous chemiluminescence detection set up from other group (**Figure 4.3A**).<sup>23</sup> But we made our own software using LabVIEW to control the chemiluminescence scanning and we investigated the ferrofluid barrier to block the signal from other sample chamber. (**Figure 4.9** and **4.10**)

As shown in **Figure 4.8A**, real image of disc analyzer for chemiluminescence is introduced. From the device set up of disc analyzer for absorbance detection we added PMT detector and linear stages for on-disc chemiluminescence detection. OD detecting optical fiber and PMT shows 90<sup>0</sup> degree. In real operation of chemiluminescence detection, all set-up was installed in light blocking black box. To block the all light from outside we used double door and black silicon which absorb the light. Because PMT was very sensitive to light (~ few photons can be detected), special care was needed.

(A)



(B)

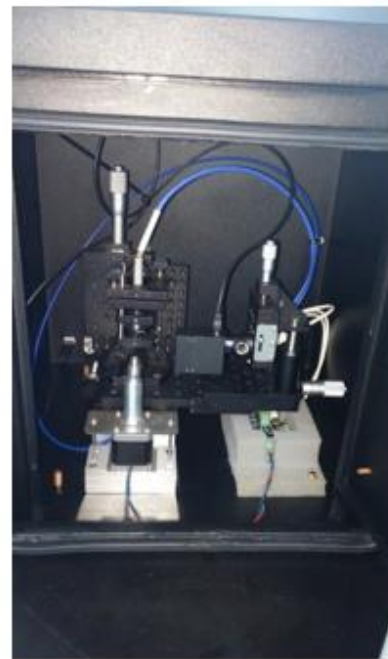


**Figure 4.8.** (A) Image of disc analyzer for absorbance and chemiluminescence detection. (B) Light blocking black box for containing disc analyzer.

### Effect of ferrofluid chemiluminescence barrier

In this section, we investigated the ferrofluid barrier to block the signal from other sample chamber (**Figure 4.9** and **4.10**). Chemiluminescence can transmit chamber to chamber in disc which is composed of polycarbonate. We measured how much chemiluminescence are transmitted when chamber to chamber angle is 24°. CRP solution was used as chemiluminescence sample of center chamber.

As shown in **Figure 4.9**, 2.9 % of chemiluminescence signal in center chamber affected to next detection chamber without ferrofluid barrier (left bar graph). 2.9 % of chemiluminescence signal will be very critical when next detection chamber shows low chemiluminescence signal whereas center chamber shows high chemiluminescence signal. Then, we tested in same condition except adding ferrofluid barrier. As shown in **Figure 4.9**, 0.6 % of chemiluminescence signal was transfer to next detection chamber with ferrofluid barrier (right bar graph). Around 2.3% of chemiluminescence signal in center chamber was blocked by ferrofluid barrier. 80% of chemiluminescence transmittance was blocked.

Finally, as shown in **Figure 4.10**, we tested the effect of ferrofluid chemiluminescence barrier in a whole disc which has 24° chamber to chamber angle difference. We put CRP solution as chemiluminescence sample in center chamber (C1). The nearest chamber C2 and C15 chamber shows 0.12% chemiluminescent affection from C1 chamber. From C3 to C14, very small chemiluminescence signal (< 0.04%) was obtained. Chemiluminescent affection was obtained by using below equation.

$$\frac{\textit{Photon signal from C\#} - \textit{Blank singal}}{\textit{Photon signal from C1} - \textit{Blank signal}} \times 100$$

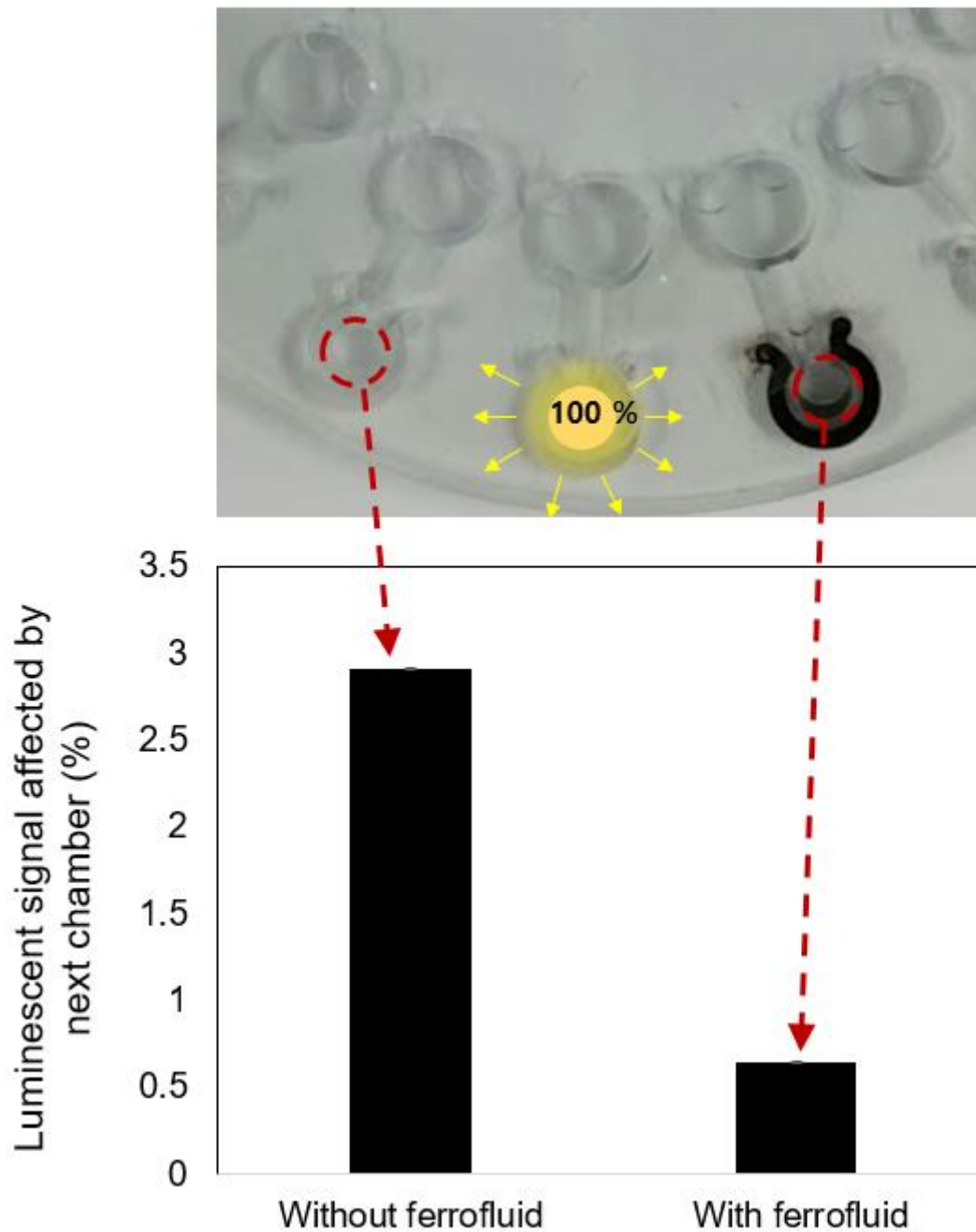


**Figure 4.9.** Effect of ferrofluid chemiluminescence barrier. CRP solution was used as chemiluminescence sample of center chamber. 2.9 % of chemiluminescence signal in center chamber affected to next detection chamber without ferrofluid barrier (left bar graph) and 0.63 % of chemiluminescence signal was transfer to next detection chamber with ferrofluid barrier (right bar graph).

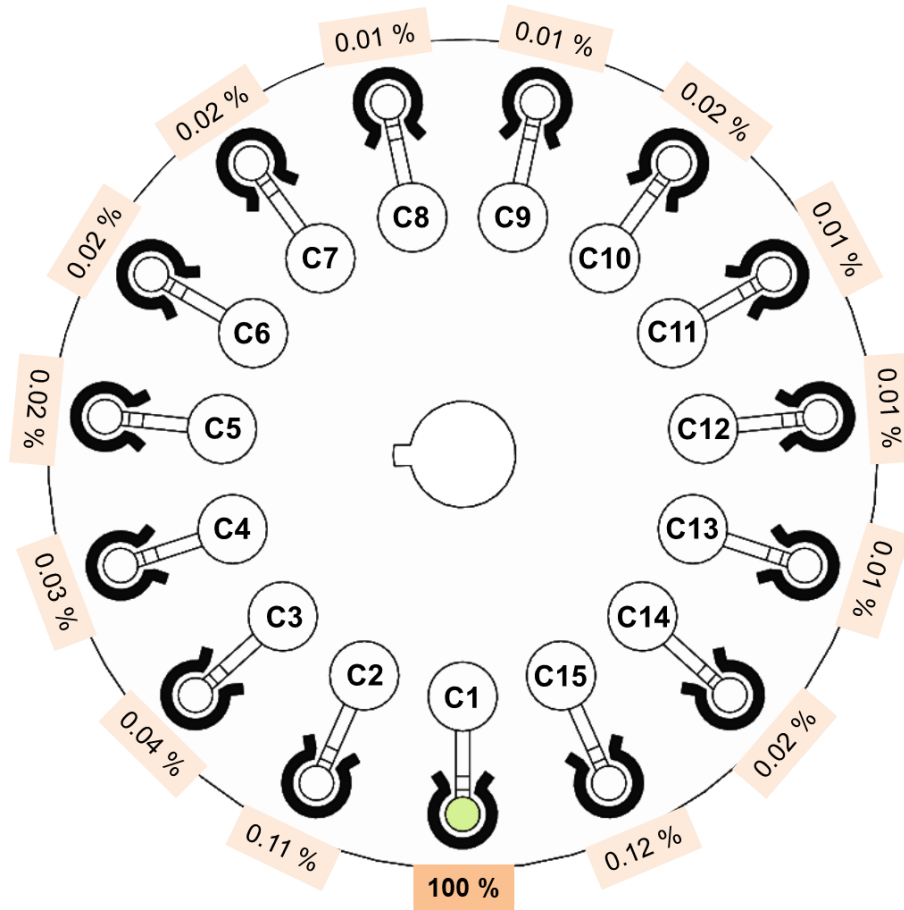


**Figure 4.10.** Effect of ferrofluid chemiluminescence barrier in whole disc. CRP solution was used as chemiluminescence sample of center chamber (C1).

### **On-disc chemiluminescence signal using disc analyzer**

To investigate the chemiluminescence signal measurement specs of our disc analyzer, we loaded the CRP solution with dilution on a disc and measure the chemiluminescence using disc analyzer. As shown in **Figure 4.11A**, chemiluminescence from whole concentration range of CRP solution was measured. From 0.01 to 0 concentration range of CRP solution, standard calibration curve shows high linearity ( $R^2 > 0.99$ ). In low concentration range of CRP solution (0.0001 to 0), standard calibration curve shows relatively low linearity ( $R^2 > 0.92$ ).

Chemiluminescence signal comparison results between commercial spectrometer (PerkinElmer, EnVision 2105 Multimode Plate Reader) and disc analyzer was given in **Figure 4.12**. Chemiluminescence comparison of whole CRP concentration range are shown in **Figure 4.12A**. It shows high linear correlations between commercial spectrometer and our disc analyzer. In relatively low CRP concentration range, both commercial spectrometer and disc analyzer shows high linear correlation ( $R^2 > 0.99$ ). For commercial spectrometer, white 96 well plated was used.



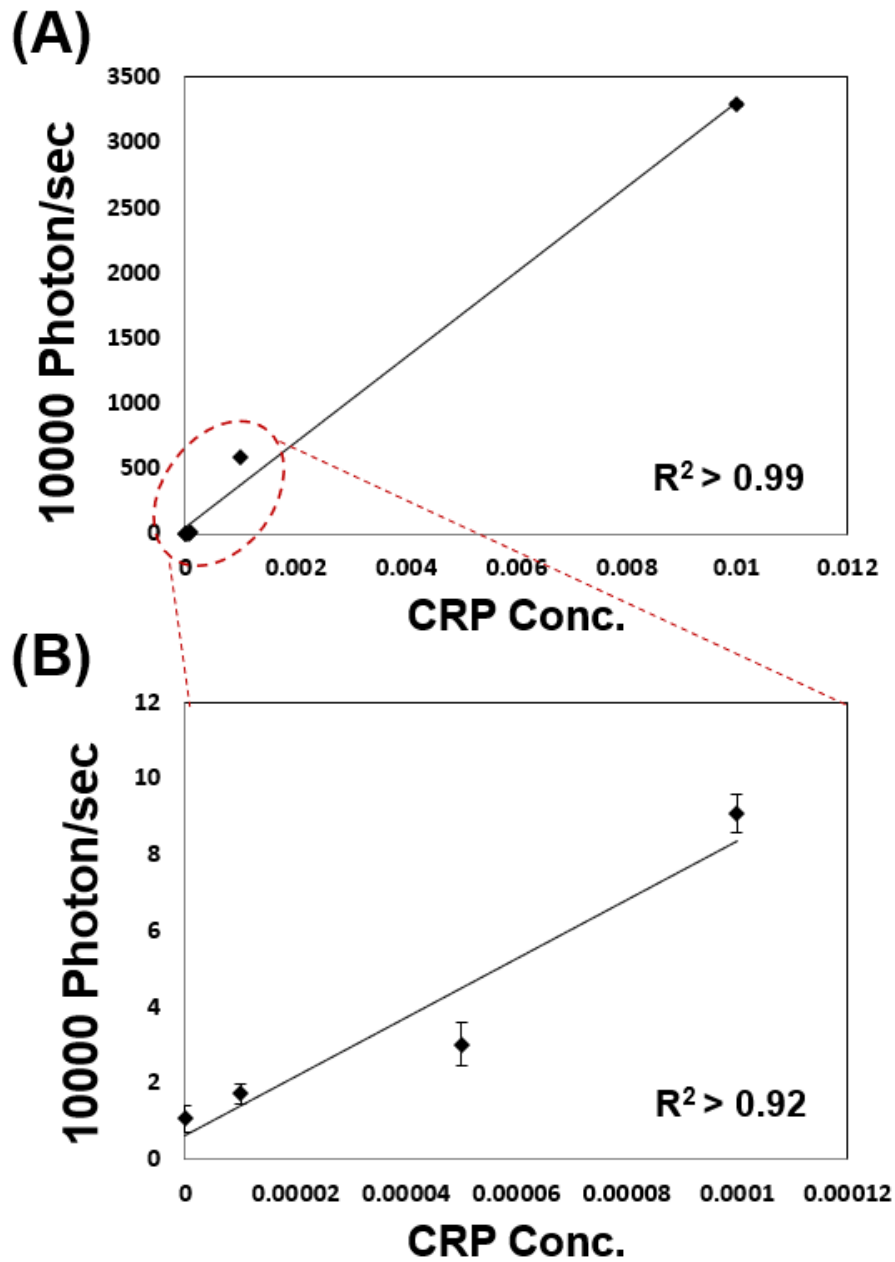


**Figure 4.11.** Chemiluminescence data using our disc analyzer. Chemiluminescence from (A) whole concentration range (B) 0.0001 to 0 concentration. C-Reactive protein (CRP) was used as chemiluminescence sample solution.

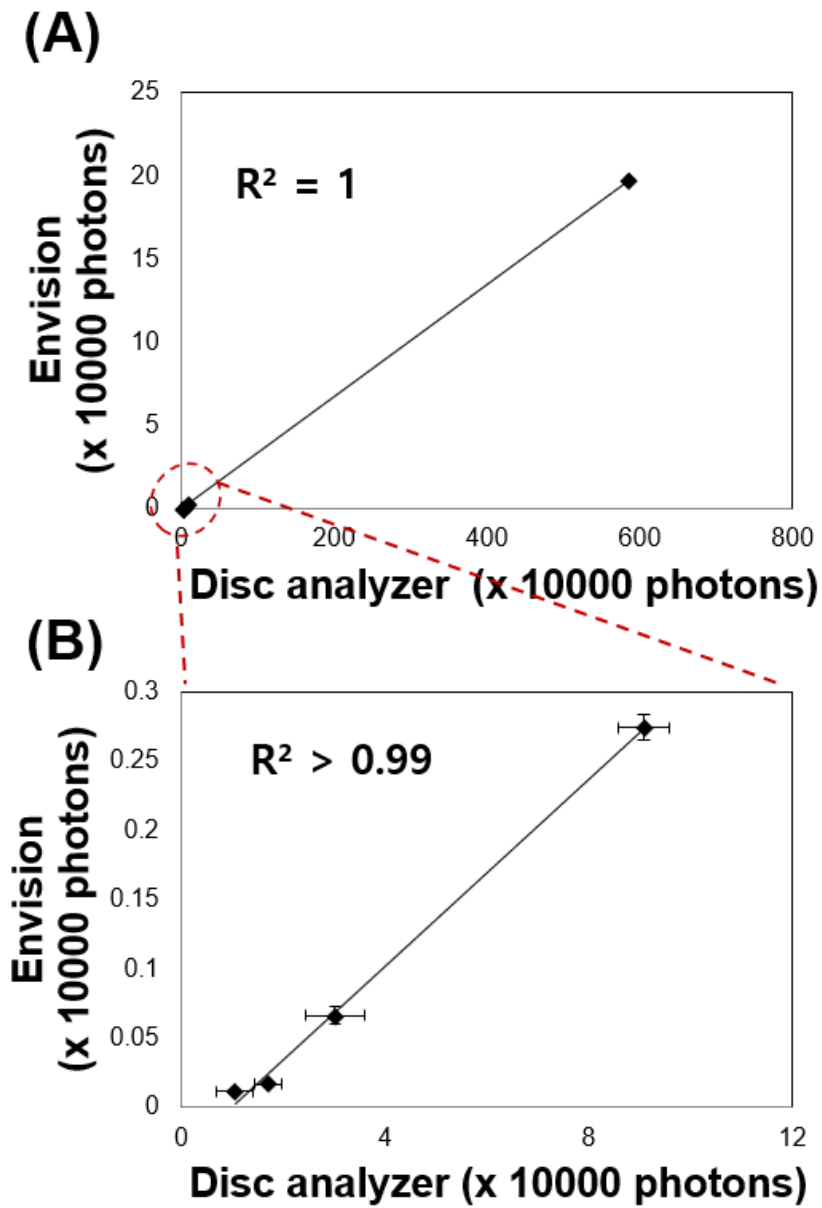


**Figure 4.12.** Chemiluminescence comparison data between conventional spectrometer (PerkinElmer, EnVision 2105 Multimode Plate Reader) (A) whole CRP concentration range and (B) in low concentration range.

#### 4.4 Conclusions

Our bench top disc analyzer for optical signal detection from lab-on-a-disc is introduced. The detection system is a custom-built machine using the following parts: step motor, optomechanical components, translation stages, light source, optical density detector, and commercially available PMT. The optomechanical parts and step motor are assembled to hold the device, and the motor can rotate the disc. The detection is performed by both optical density detector and PMT fixed on the optomechanical parts, and it is located above the detection chambers of the device. For optical density detection (colorimetric absorbance detection), OD detector coupled optical fiber and light source coupled optical fiber are aligned, and disc detection chamber are aligned between optical fiber. For chemiluminescence detection, as manipulating the step motor, the detection chambers are aligned right below the detection zone of PMT. By using LabVIEW software, we made customized software for colorimetric absorbance detection and chemiluminescence detection. Using this, certain position of disc chamber can be chosen and the signal from it can be detection. We agree that this is not the first development of disc analyzer for optical signal detection. But we hope our trials and error to build up this customizing bench top disc analyzer can help to following research who want to apply lab-on-a-disc for various applications.

All the on-disc optical detection results in chapter 2 and 3 are obtained by using our disc analyzer.

#### 4.4.1 On-going portable disc analyzer

For on-site use of lab-on-a-disc, portable lab-on-a-disc analyzer is necessary. We are developing a portable lab-on-a-disc spinning device. Schematic illustration of portable lab-on-a-disc analyzer is shown **Figure 4.13A, B, C, and D**. In this device, five wavelength LED & Photodiode for absorbance detection, BLDC motor with encode driver for motion control, rechargeable battery pack for portability, laser actuation for valving and camera module for disc imaging will be integrated. All part module will be controlled by raspberry-pi board.

As a preliminary sensing test, we detected the 540 nm wavelength absorbance with lab-on-a-disc having 5.14 mm pathlength. The result shows that dynamic range is 0 – 2 OD which is proper for general absorbance detection, and limit of detection was 0.03 OD with very low CV % (0.67).

As the future works, we will test other functional parts including 4 more LED and photodiode pair, motor spinning rpm and torque with integrating lab-on-a-disc, laser module for valving and camera module for imaging the disc. We believe our new portable lab-on-a-disc analyzer can be used for on-site detection of various application such as microalgal lipid quantification, and total phenolic and antioxidant compound detection from beverage sample.

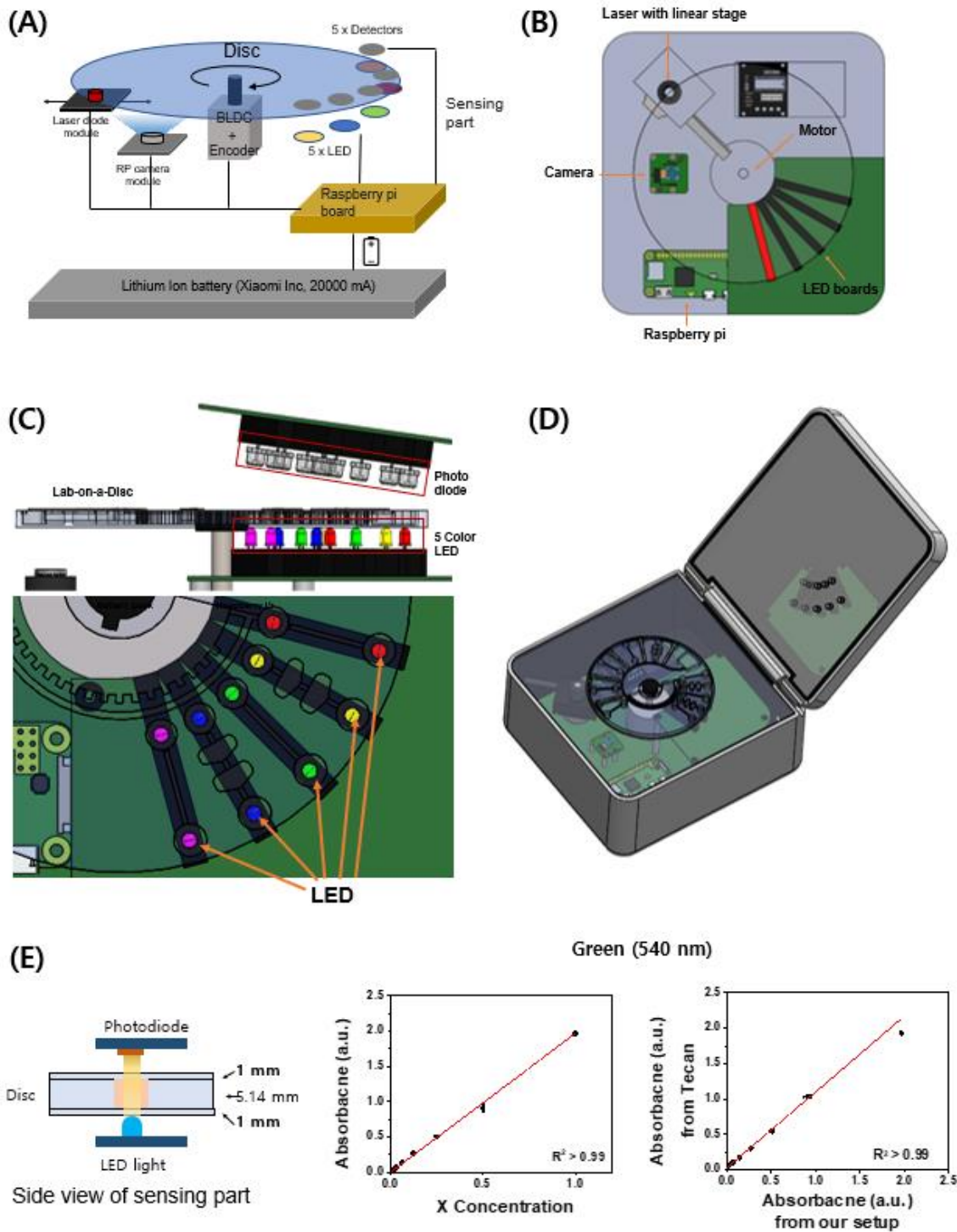


**Figure 4.13.** Schematic illustration presenting (A) functional module (B) top-view of board (C) detection module (D) expected image of device. (E) Scheme of side view of sensing part, overall pathlength for absorbance detection is 5.14 mm. Dynamic range is 0 – 2 OD, and limit of detection is 0.03 OD with 0.67 % CV.

## CHAPTER 5. General conclusions and future perspectives

### 5.1 General conclusions

In conclusion, we demonstrated two major applications to expand the use of lab-on-a-disc toward microalgal lipid quantification and natural antioxidants determination in beverage sample. Advance on lab-on-a-disc fabrication & valving technique allow us to use the organic solvent such as ethanol and hexane which can't be used in existing lab-on-a-disc platform because of incompatibility.

For biofuel applications, we have developed a fully integrated centrifugal microfluidic device for rapid on-site quantification of lipids from microalgal samples. The fully automated serial process involving cell sedimentation and lysis, liquid-liquid extraction, and colorimetric detection of lipid contents was accomplished within 13 min using a lab-on-a-disc. The presented organic solvent-tolerable (for n-hexane, ethanol) microfluidic disc was newly fabricated by combining thermal fusion bonding and carbon dot based valving techniques. A hexane compatible lab-on-a-disc composed of solvent resistive bonding and valving technique to expand the application of lab-on-a-disc to organic solvent based chemical engineering problems such as microalgal lipid extraction. For solvent resistive bonding, adhesive-free thermal fusion assembling (TFA) was used for assembling the disc components. TFA is a process which fuses more than one material via hot embossing. For solvent resistive valving technique, a thin thermoplastic film with laser printed carbon dots were inserted and bonded between top and bottom discs. The carbon dots absorb the laser energy and melt the underline thermoplastic film substrate, thereby open the fluidic passage. The similar valving technique was previously demonstrated but it was not compatible with organic solvents because it used the solvent incompatible adhesives to assemble the microfluidic device. It is expected that this novel platform will possibly contribute towards sustainable biofuel applications by providing a practical solution for on-site monitoring of lipid accumulation in microalgal samples, thus providing imperative contribution towards energy and environmental purposes of centrifugal microfluidic technology. Furthermore, to the best of our knowledge, this work is the first of its kind to extend the use of centrifugal microfluidic technology to energy and biomedical applications.

In addition, we developed a fully integrated and automated lab-on-a-disc for the rapid determination of the total phenolic content (TPC) and antioxidant activity (AA) of beverage samples. The simultaneous measurements of TPC and AA on a spinning disc was achieved by integrating three independent analytical techniques: TPC measured using the Folin–Ciocalteu method, AA measured using the 2,2-diphenyl-1-picrylhydrazyl radical (DPPH) and the ferric reducing antioxidant power methods. The TPC and AA of 8 different beverage samples, including various fruit juices, tea, wine and beer, were analyzed. Unlike conventional labor-intensive processes for measuring TPC and AA, our

fully automated platform offers one-step operation and rapid analysis. We expect our device to see wide application due to its ability to provide fast, simple, and cost-effective analyses of TPC and AA of beverage samples.

For disc analyzer, we developed the on-disc optical detection set-up. Disc analyzer system is a custom-built machine using the following parts: step motor, optomechanical components, translation stages, light source, optical density detector, and commercially available PMT. The optomechanical parts and step motor are assembled to hold the device, and the motor can rotate the disc. The detection is performed by both optical density detector and PMT fixed on the optomechanical parts, and it is located above the detection chambers of the device. For optical density detection (colorimetric absorbance detection), OD detector coupled optical fiber and light source coupled optical fiber are aligned, and disc detection chamber are aligned between optical fiber. For chemiluminescence detection, as manipulating the step motor, the detection chambers are aligned right below the detection zone of PMT. By using LabVIEW software, we made customized software for colorimetric absorbance detection and chemiluminescence detection. Using this, certain position of disc chamber can be chosen and the signal from it can be detection.

## 5.2 Future perspective

### 5.2.1 Microfluidic in biofuel production

In this section, we will give our expectation of future role of microfluidics to help the biofuel production.

In 21 centuries, there have been many developments in biofuels technologies. One of main problems of biofuel industry was to find the proper microalgae strain with optical culture conditions for microalgae to accumulate more lipid. Microfluidic technology shows important roles in high-throughput screening of strain selection and culture conditions to find the optimal microalgal fuel production conditions (**Chapter 1.1.1**).

Even if there have been huge developments in biofuel industry, industrial production of microalgal lipid still have some problems. One of main problems is industrial microalgae culture system is not simple and not equal to culture conditions in laboratory which are totally regulated for experiments.

#### **Ecosystems in microalgae – other organisms**

In huge microalgae farm, complicated ecosystem (e.g. microalgae with predators and symbiosis of microalgae-bacteria) is existed and it is different with laboratory experiment. It is difficult to maintain selected species with high productivity contents. Also, overbreeding of microalgae may cause bloom which may disrupt the ecological balance, so it is very important to control their growth.

#### **Negative case**

In negative cases, microalgae can be attacked by many predators. Microalgae are prone to attack by fungi, rotifers, viruses or other predators. Consequently, microalgal pond collapse is a critical issue that companies must solve to produce microalgal biofuels cost-effectively. In plant growing industry, microbial infections are a common feature. Thus, there have been many developments of antibiotics and other strategies to combat them. However, in microalgal biofuel industry, this microalgae-predator relationship is not fully understood. Thus, the first step for microalgal biofuel industry will be figure out all the competitors which reducing the microalgal biofuel production as attacking or competing with microalgae and affect to lipid accumulation.

#### **Positive case**

However, there also some positive case of microalgae – other microorganisms. Recent studies showed that some microalgae-bacteria relationship (symbiosis) increase the microalgal growth and biofuel production. As shown in Figure 5.1A, microalgae and symbiotic bacteria exchanged the



nutrients which are deficient to each other but essential for the growth. Microalgae gives dissolved organic matter to symbiotic bacteria and after symbiotic bacteria using it, then symbiotic bacteria give inorganic nutrients which containing sulfur, nitrogen, phosphate which are essential for microalgae growing. This virtuous circle will be benefit for both microalgae and bacteria. Thus, it is nowadays realized that microalgae–bacteria consortia may be utilized to improve algal biomass production and to enrich the biomass with valuable chemical and energy compounds.

For both negative (predator) and positive (symbiotic bacteria) case in microalgae biofuel industry, however, still there are many unknown problems and not enough studies carry out because this is early stage and there are so many combinations to be tested. We should test the all possible combinations of various microalgae strains, various symbiotic bacteria and diverse culture conditions.

### **Potential approach mimic microalgae-other organisms using microfluidics**

We believed that microfluidic research can help to solve this and contribute to understanding of microalgae – other organism (predators and symbiotic bacteria) as providing high-throughput co-culture and screening (analysis) set-up. As shown in Figure 5.1B, one of possible applications will be the droplet encapsulation-based co-culture and high-throughput analysis.

In our humble opinions, next generation microfluidic microalgae biofuel research trends will be focused on studying microalgae-other organisms communications to understand their eco-system.

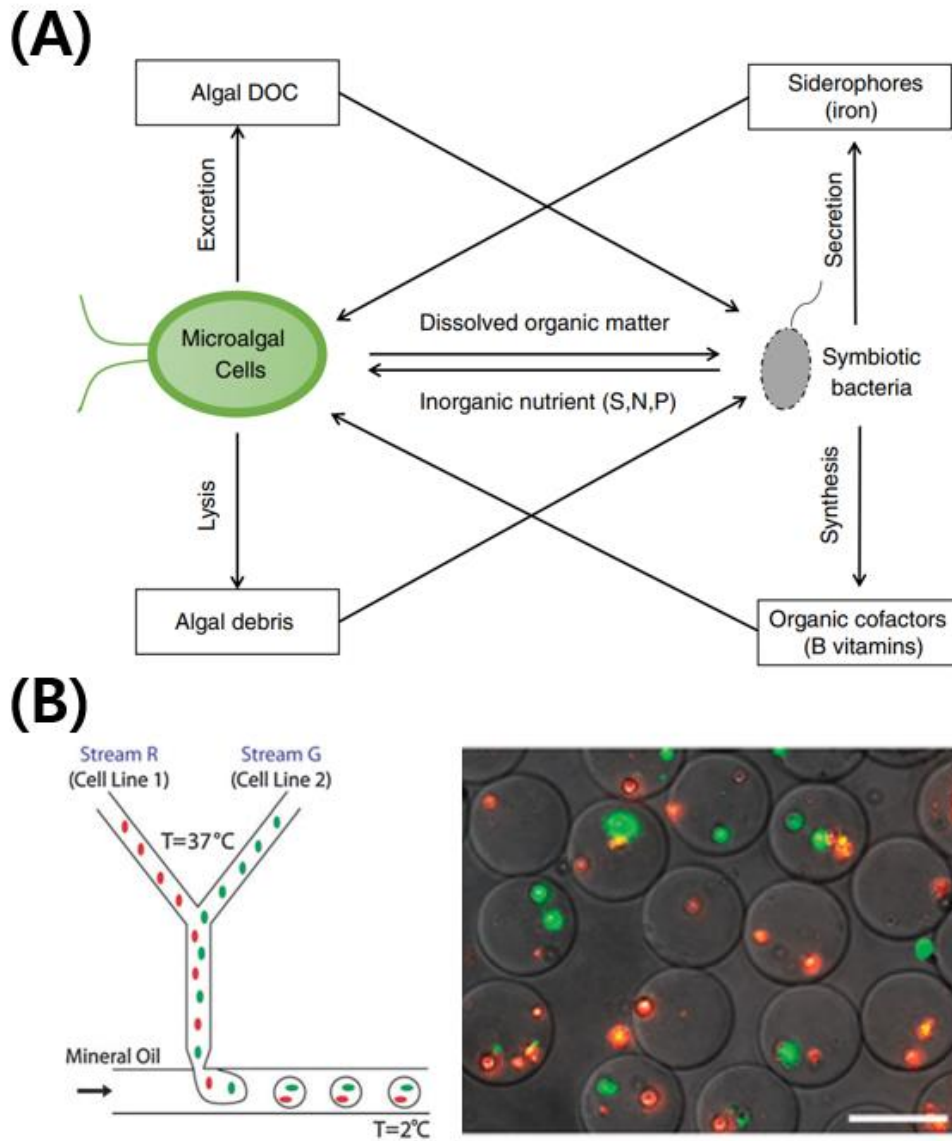


**Figure 5.1.** Schematic illustration presenting (A) symbiotic metabolic pathway between microalgae cell and symbiotic bacteria.<sup>25</sup> (B) possible application to study the symbiosis of microalgae and bacteria; high-throughput combinatorial cell co-culture using microfluidics.<sup>26</sup>

## 5.2.2 Microfluidics in food nutrient determination

In this section, we will give our expectation of future role of microfluidics to help the quantify the food nutrients using microfluidics. In chapter 1, we just review the microfluidic device for antioxidant detection. Here, we will give little big scope of microfluidic use for food nutrient detection including antioxidants, amino acid, etc. Then, we will give our future perspective of microfluidic roles for food nutrient detection.

As shown in **Table 5.1**, 15 microfluidic (microchip) researches are summarized with various categories (nutrient species, sample type, microfluidic device type, sample preparation method, detection method). Various nutrients such as biogenic amines, antioxidants, vanillin, total isoflavones, amino acids from alcoholic beverage (wine, sakes and beers), tea, milk and fruits have been analyzed by microfluidic device including capillary electrophoresis (CE) and micro structured imprinted plastic chip. For detection, fluorescence detection and electrochemical detection was used, and most of CE detection was conducted by electrochemical detection. For sample preparation, all microfluidic device needs additional off-chip sample preparation such as off-chip dilution, fluorescence dye labelling, filtration and extraction (solid-liquid).

From the summary of existing food nutrients detection approaches, we found that all microfluidic approaches need sample preparation steps additionally and it takes additional labor force, materials and instruments. Thus, as far as we know, except our approach (**chapter 3**), there is no sample-to-answer microfluidic device in food nutrients detection.

As we showed and discussed in chapter 1, 2 and 3, one of major advantages of lab-on-a-disc is full integration and automation of all required processes (sample to answer manner). Especially in sample preparation, lab-on-a-disc shows special advantages such as serial dilution<sup>150</sup>, extraction of target sample (solid-liquid, liquid-liquid extraction).<sup>14, 105</sup> and filtration<sup>8</sup> as using centrifugal force and simple valving for flow control. And also, lab-on-a-disc platform has been developed in detection parts such as electrochemical<sup>107</sup> and optical detection (chapter 4).

Recently one good example for lab-on-a-disc for food detection has been published. Loo *et al*, showed fast sample-to-answer analysis of genetically modified (GM) papaya using lab-on-a-disc for field use.<sup>151</sup> It proved that lab-on-a-disc platform can be used even in genetic detection of food. Thus, in our humble opinion, we expected that there are many potential applications in food nutrient detection area as using lab-on-a-disc for sample to answer manner which is simple and user-friendly.

**Table 5.1.** Research lists of food nutrient analysis using microfluidics.

	<b>Nutrients</b>	<b>Sample</b>	<b>Microchip</b>	<b>Sample preparation</b>	<b>Device for detection</b>
1 <sup>152</sup>	Biogenic amines (tyramine, histamine)	Wines, sakes, beers	Separation in MCE	Off-chip dilution and labelling with fluorescamine	Separation in MCE followed by fluorescence detection
2 <sup>67</sup>	Antioxidants (rutin, etc.), vitamins (ascorbic acid, etc.)	Apples and natural vanilla beans	Glass CE microchip	Off-chip extraction, pulverization, macerated, dilution and filtration	Glass CE microchip using CNTs as electrode
3 <sup>68</sup>	Antioxidants (catechin, rutin, etc.)	Apples, pears, wines, green tea	CE microchip	Off-chip extraction, dilution, and filtration	Adaption of traditional analytical methods on MCE with electrochemical detection
4 <sup>153</sup>	Vanillin, ethyl vanillin	Vanillin beans, tea	Glass CE chip	Off-chip extraction, dilution, and filtration	Glass CE chip, electrochemical detection
5 <sup>154</sup>	Proteins ( $\beta$ -conglycinin, glycinin)	Soybeans flour	SDS CE, Agilent 2100 bioanalyzer	Off-chip protein denaturation and filtration	Agilent 2100 bioanalyzer with epifluorescent detection
6 <sup>155</sup>	Amino acids (Arg, Gln, etc.)	Sports beverage, jelly-form beverage, tablet-form	CE microchip	Off-chip extraction and filtration	Detection with less than 10 min of total analysis time
7 <sup>69</sup>	Total isoflavones, antioxidant (arbutin, rutin, etc.)	Apples, pears	Glass CE microchip	Off-chip extraction and filtration	Glass CE microchip with MWCNTs based electrode as a flow injection system for analysis of total isoflavones and as a separation system for antioxidants detection
8 <sup>156</sup>	Folic acid	Infant formula powder	Microchannel microchip	Powder dissolved in water filtered and diluted	ELISA assay on surface of microchannel

**Table 5.1.** Research lists of food nutrient analysis using microfluidics. (*continued*)

	<b>Nutrients</b>	<b>Sample</b>	<b>Microchip</b>	<b>Sample preparation</b>	<b>Device for detection</b>
9 <sup>157</sup>	Biogenic amines (tryptamine, tyramine), amino acid (tryptophan)	Rice wine, beer	CZE microchip	Off-chip dilution	Electrochemical detection
10 <sup>158</sup>	Vanillin, ethyl vanillin	Vanilla pod, Vanilla sugar	CZE microchip	Off-chip extraction and dilution	Electrochemical detection (end channel)
11 <sup>159</sup>	Total isoflavones	Soy milk	Glass CE microchip	Off-chip extraction and dilution	Electrochemical detection (end channel)
12 <sup>70</sup>	Antioxidant (chlorogenic)	Red wine	Glass CE microchip	Dilution and filtration, off-chip	Electrochemical detection (SPE electrode)
13 <sup>71</sup>	Antioxidants (catechins)	Green tea extract (nutraceutical)	PDMS CE, microchip	Solid-liquid extraction and filtration, off-chip	Electrochemical detection
14 <sup>72</sup>	Antioxidant (arbutin, ascorbic acid)	Pear pulps and commercial juices	Glass CE microchip	Juice filtration or solid-liquid extraction and filtration, off-chip	Electrochemical detection
15 <sup>160</sup>	Amino acids (theanine, Arg, Gln)	Green tea	PMMA microchip	Extraction and filtration and derivatization of amino acids, off-chip	LIF detection

\*CNTs : carbon nanotubes, CE: capillary electrophoresis, MWCNTs : Multi-walled carbon nanotubes, ELISA : enzyme-linked immunosorbent assay, CZE : capillary zone electrophoresis, SPE : screen printed electrode, Arg : arginine, Gln : glutamine, LIF : laser-induced fluorescence

## References

1. Burtis, C. A.; Anderson, N. G.; Mailen, J. C.; Scott, C. D.; Tiffany, T. O.; Johnson, W. F., Development of a Miniature Fast Analyzer. *Clinical Chemistry* **1972**, *18* (8), 753-+.
2. Kim, T.-H.; Park, J.; Kim, C.-J.; Cho, Y.-K., Fully Integrated Lab-on-a-Disc for Nucleic Acid Analysis of Food-Borne Pathogens. *Analytical Chemistry* **2014**, *86* (8), 3841-3848.
3. Al Lawati, H. A. J.; Al Haddabi, B.; Suliman, F. O., A novel microfluidic device for estimating the total phenolic/antioxidant level in honey samples using a formaldehyde/potassium permanganate chemiluminescence system. *Analytical Methods* **2014**, *6* (18), 7243-7249.
4. M. Madou; Kellogg, G., The LabCD: A centrifuge-based microfluidic platform for diagnostics. *Proc. SPIE Systems and Technologies for Clinical Diagnostics and Drug Discovery* **1998**, 80.
5. Hwang, H.; Kim, Y.; Cho, J.; Lee, J.-y.; Choi, M.-S.; Cho, Y.-K., Lab-on-a-Disc for Simultaneous Determination of Nutrients in Water. *Analytical Chemistry* **2013**, *85* (5), 2954-2960.
6. Lee, J.; Choi, J.-r.; Ha, S. K.; Choi, I.; Lee, S. H.; Kim, D.; Choi, N.; Sung, J. H., A microfluidic device for evaluating the dynamics of the metabolism-dependent antioxidant activity of nutrients. *Lab on a Chip* **2014**, *14* (16), 2948-2957.
7. Xu, W.; Kim, T.-H.; Zhai, D.; Er, J. C.; Zhang, L.; Kale, A. A.; Agrawalla, B. K.; Cho, Y.-K.; Chang, Y.-T., Make caffeine visible: a fluorescent caffeine “Traffic Light” detector. *Scientific reports* **2013**, *3*.
8. Woo, H.-K.; Sunkara, V.; Park, J.; Kim, T.-H.; Han, J.-R.; Kim, C.-J.; Choi, H.-I.; Kim, Y.-K.; Cho, Y.-K., Exodisc for Rapid, Size-Selective, and Efficient Isolation and Analysis of Nanoscale Extracellular Vesicles from Biological Samples. *ACS Nano* **2017**, *11* (2), 1360-1370.
9. Lee, S. K.; Yi, G. R.; Yang, S. M., High-speed fabrication of patterned colloidal photonic structures in centrifugal microfluidic chips. *Lab on a Chip* **2006**, *6* (9), 1171-1177.
10. Bruchet, A.; Taniga, V.; Descroix, S.; Malaquin, L.; Goutelard, F.; Mariet, C., Centrifugal microfluidic platform for radiochemistry: Potentialities for the chemical analysis of nuclear spent fuels. *Talanta* **2013**, *116*, 488-494.
11. Strohmeier, O.; Keller, M.; Schwemmer, F.; Zehnle, S.; Mark, D.; von Stetten, F.;

Zengerle, R.; Paust, N., Centrifugal microfluidic platforms: advanced unit operations and applications. *Chemical Society Reviews* **2015**.

12. Madou, M.; Zoval, J.; Jia, G.; Kido, H.; Kim, J.; Kim, N., LAB ON A CD. *Annual Review of Biomedical Engineering* **2006**, *8* (1), 601-628.

13. Park, J.-M.; Cho, Y.-K.; Lee, B.-S.; Lee, J.-G.; Ko, C., Multifunctional microvalves control by optical illumination on nanoheaters and its application in centrifugal microfluidic devices. *Lab on a Chip* **2007**, *7* (5), 557-564.

14. Kim, Y.; Jeong, S.-N.; Kim, B.; Kim, D.-P.; Cho, Y.-K., Rapid and Automated Quantification of Microalgal Lipids on a Spinning Disc. *Analytical Chemistry* **2015**, *87* (15), 7865-7871.

15. Kim, T.-H.; Sunkara, V.; Park, J.; Kim, C.-J.; Woo, H.-K.; Cho, Y.-K., A lab-on-a-disc with reversible and thermally stable diaphragm valves. *Lab on a Chip* **2016**, *16* (19), 3741-3749.

16. Grumann, M.; Geipel, A.; Riegger, L.; Zengerle, R.; Ducrée, J., Batch-mode mixing on centrifugal microfluidic platforms. *Lab on a Chip* **2005**, *5* (5), 560-565.

17. Honda, N.; Lindberg, U.; Andersson, P.; Hoffmann, S.; Takei, H., Simultaneous multiple immunoassays in a compact disc-shaped microfluidic device based on centrifugal force. *Clinical chemistry* **2005**, *51* (10), 1955-1961.

18. Lee, B. S.; Lee, J.-N.; Park, J.-M.; Lee, J.-G.; Kim, S.; Cho, Y.-K.; Ko, C., A fully automated immunoassay from whole blood on a disc. *Lab on a Chip* **2009**, *9* (11), 1548-1555.

19. Focke, M.; Stumpf, F.; Roth, G.; Zengerle, R.; von Stetten, F., Centrifugal microfluidic system for primary amplification and secondary real-time PCR. *Lab on a Chip* **2010**, *10* (23), 3210-3212.

20. Kong, M. C. R.; Salin, E. D., Spectrophotometric Determination of Aqueous Sulfide on a Pneumatically Enhanced Centrifugal Microfluidic Platform. *Analytical Chemistry* **2012**, *84* (22), 10038-10043.

21. Grumann, M.; Steigert, J.; Riegger, L.; Moser, I.; Enderle, B.; Riebeseel, K.; Urban, G.; Zengerle, R.; Ducrée, J. J. B. M., Sensitivity enhancement for colorimetric glucose assays on whole blood by on-chip beam-guidance. **2006**, *8* (3), 209-214.

22. Czugala, M.; Gorkin Iii, R.; Phelan, T.; Gaughran, J.; Curto, V. F.; Ducrée, J.;

- Diamond, D.; Benito-Lopez, F., Optical sensing system based on wireless paired emitter detector diode device and ionogels for lab-on-a-disc water quality analysis. *Lab on a Chip* **2012**, *12* (23), 5069-5078.
23. L. Riegger, J. S., M. Grumann, S. Lutz, G. Olofsson, M. Khayyami, W. Bessler, K. Mittenbuehler, R. Zengerle and J. Ducreé, Disk-based parallel chemiluminescent detection of diagnostic markers for acute myocardial infarction. In *Miniaturized Systems for Chemistry and Life Sciences ( $\mu$ TAS 2006)* 2006; pp 819-821.
24. Czilwik, G.; Vashist, S. K.; Klein, V.; Buderer, A.; Roth, G.; von Stetten, F.; Zengerle, R.; Mark, D., Magnetic chemiluminescent immunoassay for human C-reactive protein on the centrifugal microfluidics platform. *RSC Advances* **2015**, *5* (76), 61906-61912.
25. Yao, S.; Lyu, S.; An, Y.; Lu, J.; Gjermansen, C.; Schramm, A., Microalgae-bacteria symbiosis in microalgal growth and biofuel production: a review. *J Appl Microbiol* **2019**, *126* (2), 359-368.
26. Tumarkin, E.; Tzadu, L.; Csaszar, E.; Seo, M.; Zhang, H.; Lee, A.; Peerani, R.; Purpura, K.; Zandstra, P. W.; Kumacheva, E., High-throughput combinatorial cell co-culture using microfluidics. *Integr Biol-Uk* **2011**, *3* (6), 653-662.
27. Reyes, D. R.; Iossifidis, D.; Auroux, P.-A.; Manz, A., Micro total analysis systems. 1. Introduction, theory, and technology. *Analytical Chemistry* **2002**, *74* (12), 2623-2636.
28. Auroux, P.-A.; Iossifidis, D.; Reyes, D. R.; Manz, A., Micro total analysis systems. 2. Analytical standard operations and applications. *Analytical Chemistry* **2002**, *74* (12), 2637-2652.
29. Vilknér, T.; Janásek, D.; Manz, A., Micro Total Analysis Systems. Recent Developments. *Analytical Chemistry* **2004**, *76* (12), 3373-3386.
30. Dittrich, P. S.; Tachikawa, K.; Manz, A., Micro total analysis systems. Latest advancements and trends. *Analytical Chemistry* **2006**, *78* (12), 3887-3908.
31. Mark, D.; Haerberle, S.; Roth, G.; von Stetten, F.; Zengerle, R., Microfluidic lab-on-a-chip platforms: requirements, characteristics and applications. *Chemical Society Reviews* **2010**, *39* (3), 1153-1182.
32. Le, H. P., Progress and trends in ink-jet printing technology. *Journal of Imaging Science and Technology* **1998**, *42* (1), 49-62.



33. Terry, S. C.; Jerman, J. H.; Angell, J. B., A gas chromatographic air analyzer fabricated on a silicon wafer. *Electron Devices, IEEE Transactions on* **1979**, *26* (12), 1880-1886.
34. Manz, A.; Miyahara, Y.; Miura, J.; Watanabe, Y.; Miyagi, H.; Sato, K., Design of an open-tubular column liquid chromatograph using silicon chip technology. *Sensors and Actuators B: Chemical* **1990**, *1* (1), 249-255.
35. Shoji, S.; Esashi, M.; Matsuo, T., Prototype miniature blood gas analyser fabricated on a silicon wafer. *Sensors and Actuators* **1988**, *14* (2), 101-107.
36. Van Lintel, H.; Van de Pol, F.; Bouwstra, S., A piezoelectric micropump based on micromachining of silicon. *Sensors and Actuators* **1988**, *15* (2), 153-167.
37. Verpoorte, E.; Manz, A.; Lüdi, H.; Bruno, A.; Maystre, F.; Krattiger, B.; Widmer, H.; Van der Schoot, B.; De Rooij, N., A silicon flow cell for optical detection in miniaturized total chemical analysis systems. *Sensors and Actuators B: Chemical* **1992**, *6* (1), 66-70.
38. Erickson, R. A.; Jimenez, R., Microfluidic cytometer for high-throughput measurement of photosynthetic characteristics and lipid accumulation in individual algal cells. *Lab on a Chip* **2013**, *13* (15), 2893-2901.
39. Bae, S.; Kim, C. W.; Choi, J. S.; Yang, J. W.; Seo, T. S., An integrated microfluidic device for the high-throughput screening of microalgal cell culture conditions that induce high growth rate and lipid content. *Analytical and bioanalytical chemistry* **2013**, *405* (29), 9365-74.
40. Lim, H. S.; Kim, J. Y. H.; Kwak, H. S.; Sim, S. J., Integrated Microfluidic Platform for Multiple Processes from Microalgal Culture to Lipid Extraction. *Analytical Chemistry* **2014**, *86* (17), 8585-8592.
41. Michalak, I.; Chojnacka, K., Algae as production systems of bioactive compounds. *Eng Life Sci* **2015**, *15*.
42. Markou, G.; Nerantzis, E., Microalgae for high-value compounds and biofuels production: a review with focus on cultivation under stress conditions. *Biotechnol Adv* **2013**, *31*.
43. Yang, Y.-T.; Wang, C., Review of microfluidic photobioreactor technology for metabolic engineering and synthetic biology of cyanobacteria and microalgae. *Micromachines*. **2016**, *7*.
44. Hattab, M. A.; Ghaly, A.; Hammouda, A., Microalgae harvesting methods for industrial

production of biodiesel: critical review and comparative analysis. *Journal of Fundamentals of Renewable Energy and Applications* **2015**, 5 (2), 1-26.

45. Khanra, S.; Mondal, M.; Halder, G.; Tiwari, O. N.; Gayen, K.; Bhowmick, T. K., Downstream processing of microalgae for pigments, protein and carbohydrate in industrial application: a review. *Food Bioprod Process* **2018**, 110.

46. Ranjith Kumar, R.; Hanumantha Rao, P.; Arumugam, M., Lipid extraction methods from microalgae: a comprehensive review. *Front Energy Res* **2015**, 2.

47. Huang, M.; Joensson, H. N.; Nielsen, J., High-throughput microfluidics for the screening of yeast libraries. *Methods Mol Biol* **2018**, 1671.

48. Chen, K. L.; Crane, M. M.; Kaeberlein, M., Microfluidic technologies for yeast replicative lifespan studies. *Mech Ageing Dev* **2017**, 161.

49. Foudeh, A. M.; Fatanat Didar, T.; Veres, T.; Tabrizian, M., Microfluidic designs and techniques using lab-on-a-chip devices for pathogen detection for point-of-care diagnostics. *Lab Chip* **2012**, 12.

50. Wang, H.-Y.; Bernarda, A.; Huang, C.-Y.; Lee, D.-J.; Chang, J.-S., Micro-sized microbial fuel cell: a mini-review. *Bioresour Technol* **2011**, 102.

51. Juang, Y.-J.; Chang, J.-S., Applications of microfluidics in microalgae biotechnology: a review. *Biotechnol J* **2016**, 11.

52. Kim, H. S.; Devarenne, T. P.; Han, A., Microfluidic systems for microalgal biotechnology: a review. *Algal Res* **2018**, 30.

53. Kim, H. S.; Weiss, T. L.; Thapa, H. R.; Devarenne, T. P.; Han, A., A microfluidic photobioreactor array demonstrating high-throughput screening for microalgal oil production. *Lab on a Chip* **2014**, 14 (8), 1415-1425.

54. Kaminski, T. S.; Garstecki, P., Controlled droplet microfluidic systems for multistep chemical and biological assays. *Chem Soc Rev* **2017**, 46.

55. Lee, D.-H.; Bae, C. Y.; Han, J.-I.; Park, J.-K., In Situ Analysis of Heterogeneity in the Lipid Content of Single Green Microalgae in Alginate Hydrogel Microcapsules. *Analytical Chemistry* **2013**.

56. Kwak, H. S.; Kim, J. Y. H.; Na, S. C.; Jeon, N. L.; Sim, S. J., Multiplex microfluidic

system integrating sequential operations of microalgal lipid production. *Analyst* **2016**, *141* (4), 1218-1225.

57. Kim, H. S.; Devarenne, T. P.; Han, A., A high-throughput microfluidic single-cell screening platform capable of selective cell extraction. *Lab on a Chip* **2015**, *15* (11), 2467-2475.

58. Pan, J.; Stephenson, A. L.; Kazamia, E.; Huck, W. T. S.; Dennis, J. S.; Smith, A. G.; Abell, C., Quantitative tracking of the growth of individual algal cells in microdroplet compartments. *Integr Biol-Uk* **2011**, *3* (10), 1043-1051.

59. Kim, H. S.; Guzman, A. R.; Thapa, H. R.; Devarenne, T. P.; Han, A., A Droplet Microfluidics Platform for Rapid Microalgal Growth and Oil Production Analysis. *Biotechnology and Bioengineering* **2016**, *113* (8), 1691-1701.

60. Holcomb, R.; Mason, L.; Reardon, K.; Crokek, D.; Henry, C., Culturing and investigation of stress-induced lipid accumulation in microalgae using a microfluidic device. *Analytical and bioanalytical chemistry* **2011**, *400* (1), 245-253.

61. Pyrzynska, K.; Pekal, A., Application of free radical diphenylpicrylhydrazyl (DPPH) to estimate the antioxidant capacity of food samples. *Analytical Methods* **2013**, *5* (17), 4288-4295.

62. Stratil, P.; Klejdus, B.; Kubáň, V., Determination of Total Content of Phenolic Compounds and Their Antioxidant Activity in Vegetables Evaluation of Spectrophotometric Methods. *J. Agric. Food Chem.* **2006**, *54* (3), 607-616.

63. Magalhães, L. M.; Segundo, M. A.; Reis, S.; Lima, J. L. F. C.; Rangel, A. O. S. S., Automatic Method for the Determination of Folin–Ciocalteu Reducing Capacity in Food Products. *J. Agric. Food Chem.* **2006**, *54* (15), 5241-5246.

64. Moreno, C. L.; Rudner, P. C.; García, J. M. C.; Pavón, J. M. C., Development of a Sequential Injection Analysis Device for the Determination of Total Polyphenol Index in Wine. *Microchim. Acta* **2004**, *148* (1-2), 93-98.

65. Novo, P.; Moulas, G.; França Prazeres, D. M.; Chu, V.; Conde, J. P., Detection of ochratoxin A in wine and beer by chemiluminescence-based ELISA in microfluidics with integrated photodiodes. *Sensors and Actuators B: Chemical* **2013**, *176*, 232-240.

66. Escarpa, A., Lights and shadows on Food Microfluidics. *Lab on a Chip* **2014**, *14* (17), 3213-3224.

67. Crevillén, A. G.; Ávila, M.; Pumera, M.; González, M. C.; Escarpa, A., Food Analysis on Microfluidic Devices Using Ultrasensitive Carbon Nanotubes Detectors. *Analytical Chemistry* **2007**, *79* (19), 7408-7415.
68. Kovachev, N.; Canals, A.; Escarpa, A., Fast and Selective Microfluidic Chips for Electrochemical Antioxidant Sensing in Complex Samples. *Analytical Chemistry* **2010**, *82* (7), 2925-2931.
69. Crevillén, A. G.; Pumera, M.; González, M. C.; Escarpa, A., Towards lab-on-a-chip approaches in real analytical domains based on microfluidic chips/electrochemical multi-walled carbon nanotube platforms. *Lab on a Chip* **2009**, *9* (2), 346-353.
70. Scampicchio, M.; Wang, J.; Mannino, S.; Chatrathi, M. P., Microchip capillary electrophoresis with amperometric detection for rapid separation and detection of phenolic acids. *Journal of Chromatography A* **2004**, *1049* (1), 189-194.
71. Hompesch, R. W.; García, C. D.; Weiss, D. J.; Vivanco, J. M.; Henry, C. S., Analysis of natural flavonoids by microchip-micellar electrokinetic chromatography with pulsed amperometric detection. *Analyst* **2005**, *130* (5), 694-700.
72. Blasco, A. J.; Barrigas, I.; González, M. C.; Escarpa, A., Fast and simultaneous detection of prominent natural antioxidants using analytical microsystems for capillary electrophoresis with a glassy carbon electrode: A new gateway to food environments. *ELECTROPHORESIS* **2005**, *26* (24), 4664-4673.
73. Pires, N. M. M.; Dong, T.; Hanke, U.; Hoivik, N., Recent Developments in Optical Detection Technologies in Lab-on-a-Chip Devices for Biosensing Applications. *Sensors* **2014**, *14* (8), 15458-15479.
74. Collins, G. E.; Lu, Q.; Pereira, N.; Wu, P., Long pathlength, three-dimensional absorbance microchip. *Talanta* **2007**, *72* (1), 301-304.
75. Salimi-Moosavi, H.; Jiang, Y.; Lester, L.; McKinnon, G.; Harrison, D. J., A multireflection cell for enhanced absorbance detection in microchip-based capillary electrophoresis devices. **2000**, *21* (7), 1291-1299.
76. Billot, L.; Plecis, A.; Chen, Y., Multi-reflection based on chip label free molecules detection. *Microelectronic Engineering* **2008**, *85* (5), 1269-1271.

77. Noda, T.; Takao, H.; Yoshioka, K.; Oku, N.; Ashiki, M.; Sawada, K.; Matsumoto, K.; Ishida, M., Performance of absorption photometry microchip for blood hemoglobin measurement integrated with processing circuits and Si(110) 45° mirrors. *Sensors and Actuators B: Chemical* **2006**, *119* (1), 245-250.
78. Ma, B.; Zhou, X.; Wang, G.; Dai, Z.; Qin, J.; Lin, B., A hybrid microdevice with a thin PDMS membrane on the detection window for UV absorbance detection. **2007**, *28* (14), 2474-2477.
79. Ou, J.; Glawdel, T.; Ren, C. L.; Pawliszyn, J., Fabrication of a hybrid PDMS/SU-8/quartz microfluidic chip for enhancing UV absorption whole-channel imaging detection sensitivity and application for isoelectric focusing of proteins. *Lab on a Chip* **2009**, *9* (13), 1926-1932.
80. Snakenborg, D.; Mogensen, K. B.; Kutter, J. P., Optimization of Signal-to-Noise Ratio in Absorbance Detection by Integration of Microoptical Components. 2003; pp 841-844.
81. Mogensen, K. B.; Kutter, J. P., Optical detection in microfluidic systems. **2009**, *30* (S1), S92-S100.
82. Llobera, A.; Demming, S.; Wilke, R.; Büttgenbach, S., Multiple internal reflection poly(dimethylsiloxane) systems for optical sensing. *Lab on a Chip* **2007**, *7* (11), 1560-1566.
83. Ro, K. W.; Lim, K.; Shim, B. C.; Hahn, J. H., Integrated Light Collimating System for Extended Optical-Path-Length Absorbance Detection in Microchip-Based Capillary Electrophoresis. *Analytical Chemistry* **2005**, *77* (16), 5160-5166.
84. Pan, J.-Z.; Yao, B.; Fang, Q., Hand-held Photometer Based on Liquid-Core Waveguide Absorption Detection for Nanoliter-scale Samples. *Analytical Chemistry* **2010**, *82* (8), 3394-3398.
85. Ding, Z.; Zhang, D.; Wang, G.; Tang, M.; Dong, Y.; Zhang, Y.; Ho, H.-p.; Zhang, X., An in-line spectrophotometer on a centrifugal microfluidic platform for real-time protein determination and calibration. *Lab on a Chip* **2016**, *16* (18), 3604-3614.
86. Gorkin, R.; Park, J.; Siegrist, J.; Amasia, M.; Lee, B. S.; Park, J.-M.; Kim, J.; Kim, H.; Madou, M.; Cho, Y.-K., Centrifugal microfluidics for biomedical applications. *Lab on a Chip* **2010**, *10* (14), 1758-1773.
87. Park, J.; Sunkara, V.; Kim, T.-H.; Hwang, H.; Cho, Y.-K., Lab-on-a-Disc for Fully Integrated Multiplex Immunoassays. *Analytical Chemistry* **2012**, *84* (5), 2133-2140.

88. Burger, R.; Kirby, D.; Glynn, M.; Nwankire, C.; O'Sullivan, M.; Siegrist, J.; Kinahan, D.; Aguirre, G.; Kijanka, G.; Gorkin, R. A.; Ducrée, J., Centrifugal microfluidics for cell analysis. *Current Opinion in Chemical Biology* **2012**, *16* (3), 409-414.
89. Madou, M.; Zoval, J.; Jia, G.; Kido, H.; Kim, J.; Kim, N., Lab on a CD. *Annu. Rev. Biomed. Eng.* **2006**, *8*, 601-628.
90. Rocco, R. M., *Landmark papers in clinical chemistry*. Elsevier: 2005.
91. Kido, H.; Maquieira, A.; Hammock, B. D., Disc-based immunoassay microarrays. *Analytica chimica acta* **2000**, *411* (1), 1-11.
92. Lai, S.; Wang, S.; Luo, J.; Lee, L. J.; Yang, S.-T.; Madou, M. J., Design of a Compact Disk-like Microfluidic Platform for Enzyme-Linked Immunosorbent Assay. *Analytical Chemistry* **2004**, *76* (7), 1832-1837.
93. Zourob, M.; Elwary, S.; Turner, A. P., *Principles of Bacterial Detection: Biosensors, Recognition Receptors and Microsystems: Biosensors, Recognition Receptors, and Microsystems*. Springer: 2008.
94. Scalbert, A.; Manach, C.; Morand, C.; Remesy, C.; Jimenez, L., Dietary polyphenols and the prevention of diseases. *Crit. Rev. Food Sci. Nutr.* **2005**, *45* (4), 287-306.
95. Haerberle, S.; Brenner, T.; Zengerle, R.; Ducrée, J., Centrifugal extraction of plasma from whole blood on a rotating disk. *Lab on a Chip* **2006**, *6* (6), 776-781.
96. Lee, B. S.; Lee, Y. U.; Kim, H.-S.; Kim, T.-H.; Park, J.; Lee, J.-G.; Kim, J.; Kim, H.; Lee, W. G.; Cho, Y.-K., Fully integrated lab-on-a-disc for simultaneous analysis of biochemistry and immunoassay from whole blood. *Lab on a Chip* **2011**, *11* (1), 70-78.
97. Cho, Y.-K.; Lee, J.-G.; Park, J.-M.; Lee, B.-S.; Lee, Y.; Ko, C., One-step pathogen specific DNA extraction from whole blood on a centrifugal microfluidic device. *Lab on a Chip* **2007**, *7* (5), 565-573.
98. Park, J.-M.; Cho, Y.-K.; Lee, B.-S.; Lee, J.-G.; Ko, C., Multifunctional microvalves control by optical illumination on nanoheaters and its application in centrifugal microfluidic devices. *Lab Chip* **2007**, *7* (5), 557-564.
99. Ducrée, J.; Haerberle, S.; Lutz, S.; Pausch, S.; Stetten, F. v.; Zengerle, R., The

centrifugal microfluidic Bio-Disk platform. *Journal of Micromechanics and Microengineering* **2007**, *17* (7), S103-S115.

100. Badr, I. H.; Johnson, R. D.; Madou, M. J.; Bachas, L. G., Fluorescent ion-selective optode membranes incorporated onto a centrifugal microfluidics platform. *Analytical Chemistry* **2002**, *74* (21), 5569-5575.

101. Garcia-Cordero, J. L.; Kurzbuch, D.; Benito-Lopez, F.; Diamond, D.; Lee, L. P.; Ricco, A. J., Optically addressable single-use microfluidic valves by laser printer lithography. *Lab on a Chip* **2010**, *10* (20), 2680-2687.

102. Garcia-Cordero, J., *Development of Innovative Microfluidic Polymeric Technologies for Point-of-care & Integrated Diagnostics Devices*. 2019.

103. Thompson, B. L.; Ouyang, Y. W.; Duarte, G. R. M.; Carrilho, E.; Krauss, S. T.; Landers, J. P., Inexpensive, rapid prototyping of microfluidic devices using overhead transparencies and a laser print, cut and laminate fabrication method. *Nat Protoc* **2015**, *10* (6), 875-886.

104. Tang, M.; Wang, G.; Kong, S.-K.; Ho, H.-P., A Review of Biomedical Centrifugal Microfluidic Platforms. *Micromachines* **2016**, *7* (2), 26.

105. Duford, D. A.; Xi, Y.; Salin, E. D., Enzyme Inhibition-Based Determination of Pesticide Residues in Vegetable and Soil in Centrifugal Microfluidic Devices. *Analytical Chemistry* **2013**, *85* (16), 7834-7841.

106. Jung, J. H.; Park, B. H.; Oh, S. J.; Choi, G.; Seo, T. S., Integration of reverse transcriptase loop-mediated isothermal amplification with an immunochromatographic strip on a centrifugal microdevice for influenza A virus identification. *Lab on a Chip* **2015**, *15* (3), 718-725.

107. Kim, T.-H.; Abi-Samra, K.; Sunkara, V.; Park, D.-K.; Amasia, M.; Kim, N.; Kim, J.; Kim, H.; Madou, M.; Cho, Y.-K., Flow-enhanced electrochemical immunosensors on centrifugal microfluidic platforms. *Lab on a Chip* **2013**, *13* (18), 3747-3754.

108. Focke, M.; Stumpf, F.; Faltin, B.; Reith, P.; Bamarni, D.; Wadle, S.; Müller, C.; Reinecke, H.; Schrenzel, J.; Francois, P., Microstructuring of polymer films for sensitive genotyping by real-time PCR on a centrifugal microfluidic platform. *Lab on a Chip* **2010**, *10* (19), 2519-2526.

109. Lutz, S.; Weber, P.; Focke, M.; Faltin, B.; Hoffmann, J.; Müller, C.; Mark, D.; Roth, G.; Munday, P.; Armes, N., Microfluidic lab-on-a-foil for nucleic acid analysis based on

isothermal recombinase polymerase amplification (RPA). *Lab on a Chip* **2010**, *10* (7), 887-893.

110. Stumpf, F.; Schwemmer, F.; Hutzenlaub, T.; Baumann, D.; Strohmeier, O.; Dingemanns, G.; Simons, G.; Sager, C.; Plobner, L.; von Stetten, F.; Zengerle, R.; Mark, D., LabDisk with complete reagent prestorage for sample-to-answer nucleic acid based detection of respiratory pathogens verified with influenza A H3N2 virus. *Lab Chip* **2016**, *16* (1), 199-207.

111. Chisti, Y., Biodiesel from microalgae. *Biotechnology Advances* **2007**, *25* (3), 294-306.

112. Sharma, K. K.; Schuhmann, H.; Schenk, P. M., High Lipid Induction in Microalgae for Biodiesel Production. *Energies* **2012**, *5* (5), 1532-1553.

113. Li, Y.; Ghasemi Naghdi, F.; Garg, S.; Adarme-Vega, T.; Thurecht, K.; Ghafor, W.; Tannock, S.; Schenk, P., A comparative study: the impact of different lipid extraction methods on current microalgal lipid research. *Microbial Cell Factories* **2014**, *13* (1), 14.

114. Madou, M. J.; Kellogg, G. J., LabCD: a centrifuge-based microfluidic platform for diagnostics. *Proc. SPIE* **1998**, *3259*, 80-93.

115. Jung, J. H.; Park, B. H.; Choi, Y. K.; Seo, T. S., A microbead-incorporated centrifugal sample pretreatment microdevice. *Lab on a Chip* **2013**, *13* (17), 3383-3388.

116. Chen, M.; Liu, T.; Chen, X.; Chen, L.; Zhang, W.; Wang, J.; Gao, L.; Chen, Y.; Peng, X., Subcritical co-solvents extraction of lipid from wet microalgae pastes of *Nannochloropsis* sp. *European Journal of Lipid Science and Technology* **2012**, *114* (2), 205-212.

117. Larkum, A. W. D.; Ross, I. L.; Kruse, O.; Hankamer, B., Selection, breeding and engineering of microalgae for bioenergy and biofuel production. *Trends in Biotechnology* **2012**, *30* (4), 198-205.

118. Hooper, J. K., *The Chlamydomonas Sourcebook. A Comprehensive Guide to Biology and Laboratory Use.* Elizabeth H. Harris. Academic Press, San Diego, CA, 1989. xiv, 780 pp., illus. \$145. *Science* **1989**, *246* (4936), 1503-1504.

119. Cakmak, T.; Angun, P.; Demiray, Y. E.; Ozkan, A. D.; Elibol, Z.; Tekinay, T., Differential effects of nitrogen and sulfur deprivation on growth and biodiesel feedstock production of *Chlamydomonas reinhardtii*. *Biotechnology and Bioengineering* **2012**, *109* (8), 1947-1957.

120. Johnson, X.; Alric, J., Interaction between Starch Breakdown, Acetate Assimilation, and



Photosynthetic Cyclic Electron Flow in *Chlamydomonas reinhardtii*. *Journal of Biological Chemistry* **2012**, 287 (31), 26445-26452.

121. Liu, Z.-Y.; Wang, G.-C.; Zhou, B.-C., Effect of iron on growth and lipid accumulation in *Chlorella vulgaris*. *Bioresource Technology* **2008**, 99 (11), 4717-4722.

122. Fajardo, A. R.; Cerdán, L. E.; Medina, A. R.; Fernández, F. G. A.; Moreno, P. A. G.; Grima, E. M., Lipid extraction from the microalga *Phaeodactylum tricornutum*. *European Journal of Lipid Science and Technology* **2007**, 109 (2), 120-126.

123. Miller, R.; Wu, G.; Deshpande, R. R.; Vieler, A.; Gärtner, K.; Li, X.; Moellering, E. R.; Zäuner, S.; Cornish, A. J.; Liu, B.; Bullard, B.; Sears, B. B.; Kuo, M.-H.; Hegg, E. L.; Shachar-Hill, Y.; Shiu, S.-H.; Benning, C., Changes in Transcript Abundance in *Chlamydomonas reinhardtii* following Nitrogen Deprivation Predict Diversion of Metabolism. *Plant Physiology* **2010**, 154 (4), 1737-1752.

124. Khotimchenko, S. V.; Yakovleva, I. M., Lipid composition of the red alga *Tichocarpus crinitus* exposed to different levels of photon irradiance. *Phytochemistry* **2005**, 66 (1), 73-79.

125. Dai, J.; Mumper, R. J., Plant Phenolics: Extraction, Analysis and Their Antioxidant and Anticancer Properties. *Molecules* **2010**, 15 (10), 7313-7352.

126. Crozier, A.; Jaganath, I. B.; Clifford, M. N., Dietary phenolics: chemistry, bioavailability and effects on health. *Nat. Prod. Rep.* **2009**, 26 (8), 1001-1043.

127. Tsao, R., Chemistry and Biochemistry of Dietary Polyphenols. *Nutrients* **2010**, 2 (12), 1231-1246.

128. Sanchez-Rangel, J. C.; Benavides, J.; Heredia, J. B.; Cisneros-Zevallos, L.; Jacobo-Velazquez, D. A., The Folin-Ciocalteu assay revisited: improvement of its specificity for total phenolic content determination. *Analytical Methods* **2013**, 5 (21), 5990-5999.

129. Perez-Jimenez, J.; Arranz, S.; Taberner, M.; Diaz-Rubio, M. E.; Serrano, J.; Goni, I.; Saura-Calixto, F., Updated methodology to determine antioxidant capacity in plant foods, oils and beverages: Extraction, measurement and expression of. *Food Res. Int.* **2008**, 41 (3), 274-285.

130. Huang, D. J.; Ou, B. X.; Prior, R. L., The chemistry behind antioxidant capacity assays. *J. Agric. Food Chem.* **2005**, 53 (6), 1841-1856.

131. Stratil, P.; Kuban, V.; Fojtova, J., Comparison of the phenolic content and total antioxidant activity in wines as determined by spectrophotometric methods. *Czech Journal of Food Sciences* **2008**, *26* (4), 242-253.
132. Frankel, E. N.; Meyer, A. S., The problems of using one-dimensional methods to evaluate multifunctional food and biological antioxidants. *J. Sci. Food Agric.* **2000**, *80* (13), 1925-1941.
133. Stratil, P.; Klejdus, B.; Kubáň, V., Determination of phenolic compounds and their antioxidant activity in fruits and cereals. *Talanta* **2007**, *71* (4), 1741-1751.
134. García-Cañas, V.; Simó, C.; Herrero, M.; Ibáñez, E.; Cifuentes, A., Present and Future Challenges in Food Analysis: Foodomics. *Analytical Chemistry* **2012**, *84* (23), 10150-10159.
135. Al-Owaisi, M.; Al-Hadiwi, N.; Khan, S. A., GC-MS analysis, determination of total phenolics, flavonoid content and free radical scavenging activities of various crude extracts of *Moringa peregrina* (Forssk.) Fiori leaves. *Asian Pacific Journal of Tropical Biomedicine* **2014**, *4* (12), 964-970.
136. Spanos, G. A.; Wrolstad, R. E., Influence of processing and storage on the phenolic composition of Thompson Seedless grape juice. *J. Agric. Food Chem.* **1990**, *38* (7), 1565-1571.
137. Leccese, A.; Bartolini, S.; Viti, R., Total Antioxidant Capacity and Phenolics Content in Apricot Fruits. *International Journal of Fruit Science* **2007**, *7* (2), 3-16.
138. Benzie, I. F. F.; Szeto, Y. T., Total Antioxidant Capacity of Teas by the Ferric Reducing/Antioxidant Power Assay. *J. Agric. Food Chem.* **1999**, *47* (2), 633-636.
139. Kim, D.-B.; Shin, G.-H.; Lee, Y.-J.; Lee, J. S.; Cho, J.-H.; Baik, S.-O.; Lee, O.-H., Assessment and comparison of the antioxidant activities and nitrite scavenging activity of commonly consumed beverages in Korea. *Food Chemistry* **2014**, *151*, 58-64.
140. Wootton-Beard, P. C.; Moran, A.; Ryan, L., Stability of the total antioxidant capacity and total polyphenol content of 23 commercially available vegetable juices before and after in vitro digestion measured by FRAP, DPPH, ABTS and Folin-Ciocalteu methods. *Food Res. Int.* **2011**, *44* (1), 217-224.
141. Chan-Eam, S.; Teerasong, S.; Damwan, K.; Nacapricha, D.; Chaisuksant, R., Sequential injection analysis with electrochemical detection as a tool for economic and rapid evaluation of total antioxidant capacity. *Talanta* **2011**, *84* (5), 1350-1354.

142. Burger, R.; Kurzbuch, D.; Gorkin, R.; Kijanka, G.; Glynn, M.; McDonagh, C.; Ducree, J., An integrated centrifugo-opto-microfluidic platform for arraying, analysis, identification and manipulation of individual cells. *Lab on a Chip* **2015**, *15* (2), 378-381.
143. Strohmeier, O.; Keil, S.; Kanat, B.; Patel, P.; Niedrig, M.; Weidmann, M.; Hufert, F.; Drexler, J.; Zengerle, R.; von Stetten, F., Automated nucleic acid extraction from whole blood, *B. subtilis*, *E. coli*, and Rift Valley fever virus on a centrifugal microfluidic LabDisk. *RSC Advances* **2015**, *5* (41), 32144-32150.
144. Lugasi, A.; Hóvári, J., Antioxidant properties of commercial alcoholic and nonalcoholic beverages. *Food / Nahrung* **2003**, *47* (2), 79-86.
145. Felice, F.; Zambito, Y.; Di Colo, G.; D'Onofrio, C.; Fausto, C.; Balbarini, A.; Di Stefano, R., Red grape skin and seeds polyphenols: Evidence of their protective effects on endothelial progenitor cells and improvement of their intestinal absorption. *European Journal of Pharmaceutics and Biopharmaceutics* **2012**, *80* (1), 176-184.
146. Pellegrini, N.; Serafini, M.; Colombi, B.; Del Rio, D.; Salvatore, S.; Bianchi, M.; Brighenti, F., Total Antioxidant Capacity of Plant Foods, Beverages and Oils Consumed in Italy Assessed by Three Different In Vitro Assays. *The Journal of Nutrition* **2003**, *133* (9), 2812-2819.
147. Katalinic, V.; Milos, M.; Kulisic, T.; Jukic, M., Screening of 70 medicinal plant extracts for antioxidant capacity and total phenols. *Food Chemistry* **2006**, *94* (4), 550-557.
148. Rapisarda, P.; Tomaino, A.; Lo Cascio, R.; Bonina, F.; De Pasquale, A.; Saija, A., Antioxidant Effectiveness As Influenced by Phenolic Content of Fresh Orange Juices. *J. Agric. Food Chem.* **1999**, *47* (11), 4718-4723.
149. Tawaha, K.; Alali, F. Q.; Gharaibeh, M.; Mohammad, M.; El-Elimat, T., Antioxidant activity and total phenolic content of selected Jordanian plant species. *Food Chemistry* **2007**, *104* (4), 1372-1378.
150. Kim, T.-H.; Kim, C.-J.; Kim, Y.; Cho, Y.-K., Centrifugal microfluidic system for a fully automated N-fold serial dilution. *Sensors and Actuators B: Chemical* **2018**, *256*, 310-317.
151. Loo, J. F.-C.; But, G. W.-C.; Kwok, H.-C.; Lau, P.-M.; Kong, S.-K.; Ho, H.-P.; Shaw, P.-C., A rapid sample-to-answer analytical detection of genetically modified papaya using loop-mediated isothermal amplification assay on lab-on-a-disc for field use. *Food Chemistry* **2019**, *274*, 822-830.

152. Jayarajah, C. N.; Skelley, A. M.; Fortner, A. D.; Mathies, R. A., Analysis of Neuroactive Amines in Fermented Beverages Using a Portable Microchip Capillary Electrophoresis System. *Analytical Chemistry* **2007**, *79* (21), 8162-8169.
153. Ávila, M.; Zougagh, M.; Escarpa, A.; Ríos, Á., Fast single run of vanilla fingerprint markers on microfluidic-electrochemistry chip for confirmation of common frauds. *ELECTROPHORESIS* **2009**, *30* (19), 3413-3418.
154. Blazek, V.; Caldwell, R. A., Comparison of SDS gel capillary electrophoresis with microfluidic lab-on-a-chip technology to quantify relative amounts of 7S and 11S proteins from 20 soybean cultivars. *International Journal of Food Science & Technology* **2009**, *44* (11), 2127-2134.
155. Ueno, H.; Wang, J.; Kaji, N.; Tokeshi, M.; Baba, Y., Quantitative determination of amino acids in functional foods by microchip electrophoresis. *Journal of Separation Science* **2008**, *31* (5), 898-903.
156. Hoegger, D.; Morier, P.; Vollet, C.; Heini, D.; Reymond, F.; Rossier, J. S., Disposable microfluidic ELISA for the rapid determination of folic acid content in food products. *Analytical and bioanalytical chemistry* **2007**, *387* (1), 267-275.
157. Chu, Q.; Guan, Y.; Geng, C.; Ye, J., Miniaturized Capillary Electrophoresis with Amperometric Detection: Fast Separation and Detection of Bioactive Amines. *Analytical Letters* **2006**, *39* (4), 729-740.
158. Ávila, M.; González, M. C.; Zougagh, M.; Escarpa, A.; Ríos, Á., Rapid sample screening method for authenticity controlling vanilla flavors using a CE microchip approach with electrochemical detection. *ELECTROPHORESIS* **2007**, *28* (22), 4233-4239.
159. Blasco, A. J.; Crevillén, A. G.; de la Fuente, P.; González, M. C.; Escarpa, A., Electrochemical valveless flow microsystems for ultra fast and accurate analysis of total isoflavones with integrated calibration. *Analyst* **2007**, *132* (4), 323-329.
160. Kato, M.; Gyoten, Y.; Sakai-Kato, K.; Toyo'oka, T., Rapid analysis of amino acids in Japanese green tea by microchip electrophoresis using plastic microchip and fluorescence detection. *Journal of Chromatography A* **2003**, *1013* (1), 183-189.